

DISCRIMINATION AND MANIPULATION OF VIRTUAL OBJECTS
THROUGH RENDERING CONTACT LOCATION AND
COMPLIANCE INFORMATION

by

Seied Muhammad Yazdian

A dissertation submitted to the faculty of
The University of Utah
in partial fulfillment of the requirements for the degree of

Doctor of Philosophy

Department of Mechanical Engineering

The University of Utah

December 2015

Copyright © Seied Muhammad Yazdian 2015

All Rights Reserved

The University of Utah Graduate School

STATEMENT OF DISSERTATION APPROVAL

The dissertation of Seied Muhammad Yazdian
has been approved by the following supervisory committee members:

William Provancher , Chair 6/14/2015
Date Approved

Hong Tan , Member 6/19/2015
Date Approved

Jake Abbott , Member 6/19/2015
Date Approved

David Johnson , Member 6/3/2015
Date Approved

Bart Raeymaekers , Member 6/3/2015
Date Approved

and by Tim Ameel , Chair of
the Department of Mechanical Engineering

and by David B. Kieda, Dean of The Graduate School.

ABSTRACT

Virtual reality is becoming a common technology with applications in fields such as medical training, product development, and entertainment. Providing haptic (sense of touch) information along with visual and audio information can create an immersive virtual environment and enables intuitive interaction with objects in the environment. Haptic information is usually categorized into two modalities: kinesthetic (force) feedback and tactile (cutaneous) feedback. Compared to kinesthetic-force feedback, tactile feedback conveys high-resolution and low-level force information, which enables precise discrimination and dexterous manipulation of small or delicate objects.

The main drawback of the state-of-the-art tactile display devices is the lack of transparency and mobility since replicating a realistic tactile sensation on a fingerpad requires a high degree of freedom system. This dissertation presents the development of two separate haptic interfaces in which simplified tactile feedback for local contact geometry and compliance information are displayed on a user's fingerpad via a compact tactile display device.

The first interface is a two-degree-of-freedom contact location display device, which improved upon the capabilities of prior one-degree-of-freedom contact location display device designs. This device renders the location of contact between the user's fingerpad and three-dimensional virtual objects. The results of a virtual ball manipulation experiment showed that providing two-degree-of-freedom contact location information,

in addition to kinesthetic force feedback, helped participants to locate the ball easier and manipulate it more intuitively.

The second interface is a tilting-plate compliance display device, which replicates the compliance property of deformable and nondeformable virtual objects. This tactile display utilizes two tilting plates that create a first-order approximation of the concavity that is created when pressing on a compliant object. Despite its simple design and compact packaging, the compliance display device can provide a high-range of stiffness levels from 100 N/m up to rigid surfaces. The tilting-plate device is suitable for integration within devices such as robotic surgery consoles or cell phone touch screens.

TABLE OF CONTENTS

ABSTRACT.....	iii
LIST OF TABLES.....	viii
LIST OF FIGURES.....	ix
ACKNOWLEDGEMENTS.....	xiii
Chapters	
1. INTRODUCTION.....	1
1.1 Contributions.....	3
1.2 Chapter Overview.....	4
2. BACKGROUND.....	6
2.1 Overview.....	6
2.2 Tactile Feedback.....	6
2.3 Tactile Feedback Rendering of Local Contact Geometry Information.....	7
2.4 Tactile Feedback Rendering of Compliance Information.....	12
3. TWO-DEGREE-OF-FREEDOM CONTACT LOCATION DISPLAY.....	18
3.1 Overview.....	18
3.2 Device Description.....	18
3.3 Methods.....	24
3.4 Experimental Results and Discussion.....	29
3.5 Improved 2-DOF Contact Location Display Device.....	33
3.6 Conclusions.....	36
4. TILTING-PLATE TACTILE COMPLIANCE DISPLAY DEVICE.....	38

4.1 Overview.....	38
4.2 Tilting-plate Concept and Device Description	38
4.3 Tilt-displacement and Force-displacement Models	40
4.4 Methods: Tilting-plate plus Force Feedback vs. Force Feedback	41
4.5 Experimental Results and Discussion.....	46
4.6 Experiment Conclusions	51
5. PURE TILTING-PLATE FEEDBACK AS A SUBSTITUTE FOR KINESTHETIC COMPLIANCE INFORMATION	53
5.1 Overview.....	53
5.2 Device Description.....	53
5.3 Methods: Pure Tilting-plate Feedback vs. Pure Force Feedback	55
5.4 Experimental Results and Discussion.....	58
5.5 Experiment Conclusions	61
6. TILTING-PLATE FEEDBACK VS. REAL MATERIALS	62
6.1 Overview.....	62
6.2 Selection of Real Materials.....	62
6.3 Silicone Rubber Specimens	63
6.4 Device Description.....	65
6.5 Methods: Tilting-plate Feedback vs. Silicon Rubber Specimens	65
6.6 Experimental Results and Discussion.....	68
6.7 Experiment Conclusion.....	73
7. TILT-UP FEEDBACK VS. TILT-DOWN FEEDBACK.....	75
7.1 Overview.....	75
7.2 General Methods.....	75
7.3 Experiment 7.1: Preliminary Comparison between Tilt-up and Tilt-down Feedback	76
7.4 Experiment 7.2: Kinesthetic Stiffness of Tilt-up and Tilt-down Feedback	82
7.5 Experiment 7.3: Reducing the Kinesthetic Stiffness of Tilt-up Feedback.....	86
7.6 Experiment 7.4: Comparison between Perceived Compliance of Tilt-up and Tilt-down Feedback after Controlling for the Kinesthetic Stiffness.....	97
7.7 Experiment 7.5: Contact Width Spread Rate of Tilt-up and Tilt-down Feedback	105

7.8 Chapter Conclusions	111
8. TILTING-PLATE FEEDBACK FOR PINCH GRASP	113
8.1 Overview	113
8.2 Device Description.....	114
8.3 General Methods.....	115
8.4 Experiment 8.1: Index-finger-display Pinch Feedback vs. Index-finger-display Push Feedback	116
8.5 Experiment 8.2: Dual-display Pinch Feedback vs. Single-display Pinch Feedback.	122
8.6 Experiment 8.3: Thumb-display Pinch Feedback vs. Index-finger-display Pinch Feedback	126
8.7 Chapter Conclusions	129
9. CONCLUSION.....	132
9.1 Two-degree-of-freedom Contact Location Display Device	132
9.2 Tilting-plate Tactile Compliance Display Device	134
APPENDIX.....	140
REFERENCES	142

LIST OF TABLES

3.1	Tactile rendering conditions (C1-C5)	26
4.1	All reference and comparison stimuli	43
6.1	Kinesthetic stiffness of silicone rubber specimens	64
7.1	Estimated kinesthetic stiffness values for tilt-up and tilt-down feedback.....	85
7.2	Estimated spring stiffness for matching the kinesthetic stiffness of tilt-up and tilt-down feedback with 16 deg/N tilting ratio and 40-degree tilt range.....	89
A.1	Possible compliance perception tests using the tilting-plate device	140

LIST OF FIGURES

2.1	Concept of 2-DOF contact location display feedback	10
3.1	2-DOF contact location display device.....	19
3.2	Thimble of the 2-DOF contact location display device	20
3.3	Actuator box of the contact location display device.....	22
3.4	Proximal-distal backlash characterization and compensation of the device with and without a finger inserted.....	23
3.5	The virtual environment used for the ball manipulation experiment.....	25
3.6	Illustration of haptic rendering conditions C1-C5	26
3.7	The setup of the experiment.....	28
3.8	Mean speed of ball manipulation for different tactile conditions	30
3.9	Mean number of ball-maze contacts	30
3.10	Mean of number of requested helps.....	31
3.11	Results of subjective survey.....	32
3.12	The prototype of modified 2-DOF CLD.....	34
3.13	Dual loop control scheme for reducing backlash.....	34
3.14	Backlash characterization of the revised 2-DOF CLD	34
3.15	Contact location display device prototype with an active making and breaking contact system.....	35
4.1	Tilting-plate compliance display device: (left) concept, (middle) actuation mechanism, and (right) the prototyped device.....	39
4.2	Tilting-plate compliance display device integrated with a force-feedback device (modified Haptic Paddle).....	39

4.3	Experiment setup	44
4.4	A participant’s psychometric curves for reference stimuli with the kinesthetic stiffness of 60 deg/N and the tilting ratios of 8.33, 16.67, and 33.33 deg/N	47
4.5	The average of mean PSEs for all participants of each reference kinesthetic stiffness group.....	48
4.6	Very strong negative linear correlation between kinesthetic stiffness PSE and tilting ratio of reference stimuli with 60 N/m kinesthetic stiffness (dotted line).....	49
4.7	Strong negative linear correlation between kinesthetic stiffness PSE and tilting ratio of reference stimuli with 400 N/m kinesthetic stiffness (dotted line). The dashed curves indicate 95% confidence intervals.....	50
4.8	Strong negative linear correlation between kinesthetic stiffness PSE and tilting ratio of reference stimuli with 1600 N/m kinesthetic stiffness (dotted line). The dashed curves indicate 95% confidence intervals.....	51
5.1	A standalone tilting-plate compliance display device	54
5.2	Experiment Setup. A participant is comparing the compliance of tilting-plate feedback with the compliance of pure kinesthetic feedback	56
5.3	An example for a participant’s response through ascending and descending runs at different reference kinesthetic stiffness levels	58
5.4	The means and 95% confidence intervals of tilting ratio PSEs at different reference kinesthetic stiffness and hand-device configurations.....	59
5.5	Correlation between tilting ratio and perceived kinesthetic stiffness for different hand-device configurations	60
6.1	Dimensions of the silicone rubber specimens cast in a muffin tray	63
6.2	Force-displacement characteristic of the silicone rubber specimens.....	64
6.3	Experiment setup	66
6.4	The means and 95% confidence intervals of tilting ratio PSEs of all participants for different silicone rubber (SR) specimens and hand-device configurations.....	68
6.5	Linear correlations between the tilting ratio PSE and the kinesthetic stiffness of the silicone rubber specimens for each hand-device configurations	69
6.6	An example of contact force profile for an ascending run: (Top) all trials of the entire run and (bottom) inset area for the few first trials	70

6.7	Means and 95% confidence intervals of maximum applied force on silicone rubber (SR) and titling-plate (TP) surfaces.....	71
7.1	Sequential motion of the plates for rendering reference (tilt-up) and comparison (tilt-down) stimuli	77
7.2	Percentage of the time tilt-up feedback was perceived as more compliant than tilt-down feedback with the same tilting ratio	79
7.3	Mean and 95% confidence interval of maximum force applied to tilt-up and tilt-down surfaces at different levels of tilting ratios and tilt ranges	80
7.4	A non-contact finger displacement measurement system. The image processing program (OpenCV) tracks the position of the blue marker (right) captured by the camera (left)	83
7.5	An example of force-displacement characteristic curves for tilt-up and tilt-down feedback	84
7.6	The surface with tilt-up feedback is mounted on a linear spring (right) to match its kinesthetic stiffness with that of tilt-down feedback (left).....	87
7.7	Matching the average kinesthetic stiffness of tilt-up and tilt-down feedback using a virtual spring for data points above 1 N force	88
7.8	Sum of squares of error vs. spring stiffness	89
7.9	The tilting-plate device mounted on a spring-loaded lever arm	91
7.10	Force-displacement characteristic curves of tilt-up (TU), tilt-down (TD), and tilt-up plus 1000 Nm/ spring (TU+S) feedback	93
7.11	Force-displacement characteristic curves of tilt-up (TU), tilt-down (TD), and tilt-up plus 3000 N/m spring (TU+S) feedback.....	93
7.12	Equivalent kinesthetic stiffness of tilt-up (TU), tilt-down (TD) feedback, and tilt-up plus spring feedback with 1000 N/m stiffness (TU+S).....	94
7.13	Equivalent kinesthetic stiffness of tilt-up (TU), tilt-down (TD) feedback, and tilt-up plus spring feedback with 3000 N/m stiffness (TU+S).....	95
7.14	Setup of the experiment	98
7.15	Upper and lower tilt-down PSEs vs. tilt-up tilting ratios. Error bars are 95% confidence intervals	100
7.16	The effect of width of index finger distal phalanx on relative perceived compliance of tilt-down and tilt-up plus spring feedback	103

7.17	The effect of finger width on kinesthetic stiffness of tilt-down feedback	104
7.18	Fingerprint contact areas different contact force levels for tilt-up feedback with 16 deg/N tilting ratio and 40-degree tilt range	107
7.19	Net contact width for tilt-up (TU) and tilt-down (TD) feedback as a function of applied force (top) and tilt angle (bottom) under different conditions	109
7.20	Net contact width vs. applied force generated using a rigid finger model	110
8.1	Back-to-back tilting-plate device for two-finger pinch grasp	114
8.2	Three different operation configurations of the back-to-back tilting-plate device	114
8.3	The experimental setup	117
8.4	Means and 95% confidence intervals of tilting ratio PSEs of the index-finger- display pinch (comparison) stimuli at different tilting ratio levels of the index- finger-display push (reference) stimuli	119
8.5	Very strong correlation between tilting ratios of tilting index-finger-display pinch stimuli (comparison PSE) and index-finger push (reference) stimuli	120
8.6	Average of maximum applied force on reference and comparison stimuli for all participants	121
8.7	PSE tilting ratios of dual-finger, dual-display, (comparison) stimuli at different tilting ratios of dual-finger, single-display, (reference) stimuli	125
8.8	The mean tilting ratio PSEs of thumb-display pinch (comparison) stimuli at different tilting ratios of index-finger-display pinch (reference) stimuli across all participants	129

ACKNOWLEDGEMENTS

The Lord, I would like to express my deepest gratitude to you for creating me and helping me to learn what I did not know. Indeed, you are the only one who made all aspects possible so I could finish this research. I would like to thank my father whose nurturing guidance encouraged me to always believe in myself, follow my passion, and keep going. My mother, I thank you for your unconditional support and endless patience. You taught me the meaning of life.

Special thanks to my advisor, Dr. William Provancher, who taught me to be an independent researcher. He always allocated time to discuss challenges that I had never anticipated. Most importantly, he taught me how to think simply and effectively. Accomplishing this research would not have been possible without his kind support and many valuable insights. I would like to thank Hong Tan, David Johnson, Andrew Doxon, and Jaeyoung Park for their continuous guidance on conducting human-subject experiments and their feedback on interpreting experiment results. I will never forget those extensive online meetings you sacrificed your family time for. I also thank my committee members, Jake Abbott and Bart Raeymaekers, for their critical reviews and suggestions to investigate unforeseen aspects of tilting-plate feedback. Thanks to Patrick Hadley for proofreading this dissertation.

Thanks to Andrew Petruska and Josh Schmeisner for their brainstorming and help on the development of the two-degree-of-freedom contact location display device. Thanks to

ME Office staff and Tom Slowik, who facilitated all conditions for me to purchase and fabricate the devices used in this research. Special thanks to all of you who participated in my experiments and trusted me to connect your fingers to electro-mechanical devices you could not see!

I would like to thank my friends and lab mates Markus, Nathan, Ashley, Hamid, and Mark for their support in and out of the lab. It was so much fun hanging out with you. Thanks to my family who encouraged me to move forward in difficult times. Lastly, I would like to thank the National Science Foundation for their research funding under award IIS-0904456.

CHAPTER 1

INTRODUCTION

The sense of touch (haptics) is one of the most important sensations that we use to explore, identify, and manipulate many different objects in daily life. For instance, we rely on haptic feedback when searching for objects in our pockets and/or taking them out. Similarly, providing haptic feedback, along with visual and audio information, is necessary for creating an immersive virtual environment with intuitive physical interaction capabilities. Providing haptic feedback is usually critical in applications such as laparoscopic and telerobotic surgeries, medical training, product development prior to manufacturing, and entertainment.

Full haptic feedback usually requires rendering both kinesthetic (force) and tactile (cutaneous) information [Frisoli et al. 2008; Lederman and Klatzky 1990; Lederman and Klatzky 1999]. Kinesthetic information is perceived through human body joint angles and muscle activities, which enables gross manipulations such as lifting a load or changing the gear shift of a vehicle. Tactile information, however, usually pertains to the local properties of contact on skin and assists us in performing delicate tasks such as typing on a keyboard or tying a knot.

Studies show that providing tactile feedback, in addition to kinesthetic feedback, enhances human performance when interacting with real or virtual objects [Frisoli et al.

2008; Lederman and Klatzky 1990; Lederman and Klatzky 1999]. More importantly, tactile feedback is the only reliable and intuitive information for dexterous manipulation of virtual objects or delicate telerobotic surgery operations where kinesthetic force or visual information might not be deployed as a substitution [Culmer et al. 2012; Okamura 2009; Schostek, Schurr, and Buess 2009].

Despite successful progress in displaying kinesthetic information, providing intuitive tactile information is still a challenge and tactile feedback is usually disregarded in virtual or teleoperation haptic interactions. This challenge is merely because of the high degree of freedom and small package requirements of tactile display devices. Unfortunately, the large size and/or complexity of state-of-the-art tactile display devices usually prevent them from being integrated with kinesthetic force-feedback systems, or being utilized in mobile devices. This dissertation presents the development of two compact haptic interfaces that provide *simplified* tactile feedback for rendering contact location and compliance information. These devices, instead of providing the actual and realistic tactile feedback, only render approximated contact properties. The compact size of these interfaces enables them to be integrated with kinesthetic-force-feedback devices and to be used as standalone devices for handheld applications.

For the first interface, a two-degree-of-freedom (2-DOF) contact location display (CLD) device was developed to extend the device workspace and also eliminate the restricted finger motion of the previous 1-DOF CLD devices [Doxon et al. 2010; Provancher et al. 2005]. The 2-DOF CLD renders the center of contact between the user's fingerpad and a three-dimensional (3-D) virtual object. The CLD was integrated with a force-feedback device to provide both kinesthetic and tactile feedback simultaneously for dexterous and intuitive manipulation of virtual objects.

One of the drawbacks of the CLD devices is that their rigid tactile element cannot replicate surface deformation or compliance information of virtual objects. For the second interface, a simple method of rendering compliance through tactile tilting-plate feedback was introduced. The tilting-plate interface reproduces approximated surface deformation by tilting two small rigid plates around the finger. The simple and compact design of this compliance display device enables it to be embedded in mobile and handheld devices.

1.1 Contributions

The main research contributions of this research in haptic technology are outlined as follows:

1. Developed 2-DOF contact location display device

A 2-DOF contact location display device was designed and developed based on the prior 1-DOF CLD designs. Using the 2-DOF CLD device, a user can perceive consistent kinesthetic and tactile feedback when interacting with 3-D virtual objects.

2. Developed tilting-plate tactile compliance display device

A simple tilting-plate concept was developed for rendering compliance information through tactile feedback. The most important benefits of the tilting-plate concept compared to the state-of-the-art compliance display devices are its compact package, low power conception, and capability of rendering a wide range of compliance levels. Further investigations on the performance of the tilting-plate device revealed that pure tilting-plate feedback can substitute for kinesthetic compliance information. This

important feature opens many potential uses of the tilting-plate device for rendering compliance information on mobile and handheld devices with small package size.

3. Evaluated tilting-plate feedback for rendering compliance of real materials

To provide realistic compliance rendering, the perceived compliance of tilting-plate feedback was compared against the perceived compliance of real materials. The results of the experiments show that tilting-plate feedback can significantly replicate the compliance of silicone rubber specimens with kinesthetic stiffness values between ~450 to ~1500 N/m.

4. Investigated the effect of tilt direction on perceived compliance

It was found that there is a positive correlation between tilting ratio and perceived compliance for both tilt-up and tilt-down modes of the tilting-plate feedback. Tilt-down feedback is perceived as more compliant than tilt-up feedback, likely because the tilt-up feedback has higher initial contact spread rate.

5. Utilized tilting-plate feedback for rendering compliance in pinch grasp

Lastly, the performance of the tilting-plate device was tested in different pinch grasp configurations that might potentially be used in handheld devices. The experimental results showed that the perceived compliance of dual tilting-plate display is higher than that of a single tilting-plate display.

1.2 Chapter Overview

This dissertation is organized in nine chapters as outlined below:

Chapter 2 presents background and reviews relevant methods for rendering tactile

feedback regarding local geometry and compliance information.

Chapter 3 introduces development and evaluation of the 2-DOF contact location display (CLD) device for manipulating virtual objects. Different types of tactile rendering conditions were selected for human-subject experiments to assess the benefit of providing CLD information in addition to kinesthetic-force feedback. Although no significant beneficial effect of CLD information on participants' performance was found, participants significantly preferred to receive CLD feedback, and reported that the haptic interaction in the presence of CLD feedback was more realistic compared to pure force feedback.

Chapters 4-8 provide the concept, development, and evaluation of a compliance tactile display device for different interaction configurations. The effect of superimposing tilting-plate feedback with kinesthetically rendered surfaces is presented in Chapter 4. The comparison between the perceived compliance of pure tilting-plate feedback and pure kinesthetic feedback are investigated in Chapter 5. Chapter 6 provides the comparison between the perceived compliance of tilting-plate feedback and the compliance of real materials. In Chapter 7, a dual-display tilting-plate device is introduced for pinch-grasp applications. The comparison between the perceived compliance of tilt-up and tilt-down feedback is presented in Chapter 8.

Chapter 9 concludes with the main results obtained from this research and presents possible future work.

CHAPTER 2

BACKGROUND

2.1 Overview

Many different methods of rendering haptic feedback can be found in the literature. The advance of haptic technology led to successful commercial force-feedback systems, such as Geomagic's Phantom or Force Dimension's Omega force-feedback devices. In these systems, the interaction forces or torques are applied to a user's finger or hand through interfaces such as a thimble, stylus, or handle. Despite their remarkable capabilities in providing gross haptic interactions, the rigid interface of force-feedback devices is not capable of displaying fine tactile information to the user. In recent decades, rendering tactile information has received more attention. This chapter summarizes the methods of rendering tactile feedback, especially regarding local contact geometry and compliance information, and discusses the advantages and disadvantages of each method in the scope of this research.

2.2 Tactile Feedback

Tactile feedback is important for identifying detailed features on the surface of an object or dexterously manipulating it. Studies show that providing tactile feedback in conjunction with kinesthetic-force feedback can enhance participants' performance in

exploration and manipulation of virtual objects [Frisoli et al. 2008; Lederman and Klatzky 1990; Lederman and Klatzky 1999]. Tactile feedback conveys different types of properties, such as temperature, texture, local contact geometry, and compliance [Lederman and Klatzky 1990]. Consequently, many different types of tactile display devices have been developed. The following sections review relevant studies regarding local contact geometry and compliance information.

2.3 Tactile Feedback Rendering of Local

Contact Geometry Information

The most common method for displaying local contact geometry is a pin array. Similar to a Braille machine [Linville and Bliss 1966], a pin-array device controls the height of a series of pins to recreate approximated local contact geometry of a virtual surface. For example, Wagner et al. developed a benchtop 6×6 pin array, in which 36 servomotors actuate the pins individually [Wagner, Lederman, and Howe 2004]. Another example is the compact pin-array device developed by Caldwell et al., wherein pneumatic actuators move the mechanical pins both vertically and laterally [Caldwell et al. 1999]. This device is capable of rendering edges, corners, and friction through stimulating corresponding mechanoreceptors in a fingerpad. Wellman et al. presented a 1×10 pin array for palpation in remote surgery [Wellman et al. 1998]. They utilized shape-memory-alloy actuators to provide a high level of force and stiffness. However, they reported that their system was difficult to control and unreliable due to the complex and nonlinear behavior of the actuators [Howe 2004]. Sarakoglou et al. developed a compact 4×4 pin-array device integrated with an Omega7 feedback device for remote three-dimensional contour-following task [Sarakoglou et al. 2012]. The results of their

experiment indicated that participants had significantly better performance when tactile information was provided in addition to kinesthetic information. Despite their promising capabilities in providing local contact geometry information, pin arrays usually suffer from the two main drawbacks — that they tend to be bench-top apparatuses, and that they are mostly used in passive touch interactions. Due to the high pin density requirement (arrays with less than 1 mm pin spacing [Moy et al. 2000]), the state-of-the-art pin-array devices usually have many active degrees of freedom, require complex controllers and suffer from low force capabilities.

Rendering *simplified* tactile information is an alternative approach to reduce the number of required independent actuators. Some researchers studied the effect of only rendering the direction of surface normal [Dostmohamed and Hayward 2005, Frisoli et al. 2008] or the direction of contact force [Chinello et al. 2012; Pacchierotti et al. 2012; Prattichizzo, Pacchierotti, and Rosati 2012] at the point of contact. Dostmohamed and Hayward designed a tactile display device in which a small plate reproduces the orientation of a tangent plane at the point of contact between finger and a virtual surface [Dostmohamed and Hayward 2005]. Their experimental results indicated that participants had a similar level of performance in distinguishing between the curvature of virtual and real surfaces. In another study, Frisoli et al. improved this concept by developing a finger-mounted device capable of providing the sensation of making and breaking contact [Frisoli et al. 2008]. They showed that providing tactile information, in addition to kinesthetic information, significantly improves the curvature discrimination ability of participants.

Chinello et al. developed a miniaturized wearable tactile device that pushes a small plate against the finger to render direction and magnitude of contact force [Chinello et al.

2012]. They reported that the tactile force information, in conjunction with graphically provided contact location information, enables participants to perceive curvature of virtual spheres with reasonable accuracy. Prattichizzo et al. extended this concept to display tactile information to both the thumb and the index finger [Prattichizzo, Pacchierotti, and Rosati 2012]. They found that pure tactile information can substitute for the combined tactile and kinesthetic information. Using a similar tactile device, the same finding was reported by Pacchierotti et al. for a peg-in-hole task [Pacchierotti et al. 2012]. These findings suggest that compact, mobile, and low-power multifinger haptic display devices can be obtained through sensory substitution.

Most of the devices introduced above suffer from the drawback of always being in contact with the user's finger. Providing the sensation of making and breaking contact between the finger and a virtual object can create a more intuitive haptic interaction. An encounter-type haptic device enables the user to perceive where on the finger a contact is made or broken. For example, the encounter-type device developed by Yoshikawa and Nagura used a series of optical sensors to actively position an oversized thimble around the user's finger without making contact with it [Yoshikawa and Nagura 1999]. To render an intuitive contact sensation, the device holds the thimble stationary and the finger can come into contact with the inside of the thimble. Despite its active positioning for providing realistic contact sensation, the complexity and difficulty of integration with commercial feedback devices is the main practical limitation of this system. Later, Kuchenbecker et al. developed a passive encounter-type device called the Touch Thimble [Kuchenbecker et al. 2008]. The Touch Thimble is similar to the thimble of a Geomagic Phantom force-feedback device except that it is slightly oversized and utilizes a few radial springs to connect the thimble to the base of the finger. When a contact is made

with an object in a virtual environment, reaction force deforms the spring and the user's finger comes into contact with the inside of the thimble. However, the results of their 3-D shape recognition experiment revealed that the Touch Thimble significantly reduced participants' completion speed compared to using a conventional thimble. They reported that this deficiency might be due to the delay between the perceived force and perceived contact or inadvertent contact in free space [Kuchenbecker et al. 2008].

2.3.1 Contact Location Display

A contact location display (CLD) device provides simplified tactile information by rendering the location of the center of contact between the finger and a virtual object (Figure 2.1). Provancher et al. developed the first CLD device, which has only one active degree of freedom [Provancher 2003]. The 1-DOF CLD device controls the position of a small roller (contactor) along the proximal-distal direction of the fingerpad to render the location of contact. Two sheathed push-pull wires driven by a remote actuator box control the location of the roller with respect to a small thimble worn on the finger. The actuator box is mounted on the user's forearm to reduce size and mass of the device at the finger as well as relocate any undesirable mechanical vibrations of the actuator. The compact size of thimble enables the system to be integrated with conventional kinesthetic force-feedback devices. In the current CLD device, the axis of the roller is directly

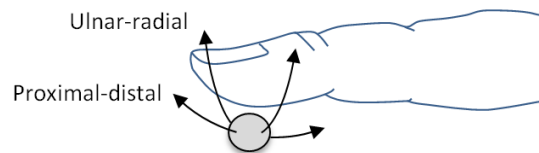


Figure 2.1. Concept of 2-DOF contact location display feedback. A spherical tactile element underneath the fingerpad moves in ulnar-radial and proximal-distal directions to display the location of contact.

attached to the end of a Geomagic Phantom Premium 1.5. There is no contact between the user's finger and the roller when the finger moves in free space. In this phase, the roller is prepositioned to the anticipated location of collision in the virtual environment. When a contact is detected, the force-feedback device prevents the motion of the roller in the direction of the penetration. Consequently, the applied force by the finger bends the push-pull wires slightly and the finger comes into contact with the roller (similar to passive encounter-type devices [Kuchenbecker et al. 2008]).

Many studies using the 1-DOF CLD device showed that providing contact location information can be beneficial for haptic interaction in virtual environments. Provancher et al. investigated the effect of the 1-DOF CLD on the perception of curvature and object motion [Provancher et al. 2005]. They found that participants could discriminate the curvature of virtual planar surfaces with the same level of performance when they interacted with real physical objects. They also addressed the benefit of the CLD information in distinguishing between pivoted and anchored virtual objects. Kuchenbecker et al. evaluated the effect of the CLD in a contour following task [Kuchenbecker et al. 2004]. They reported that the contact location display helped participants to accomplish the task faster and more accurately compared to using a conventional force-feedback device. Doxon et al. developed a haptic shading algorithm to render CLD information when interacting with general polygonal virtual objects [Doxon et al. 2011]. In their human-subject experiment, participants could identify the edges of polygonal objects easier when the CLD information was available. Park et al. investigated the effect of CLD on perception of sharpness of virtual edges [Park et al. 2012]. They found that providing CLD information, in addition to kinesthetic information, did not improve or worsen participants' ability to discriminate sharp edges.

They found that the kinesthetic information is the dominant cue in discrimination of virtual edges regardless of the size of the roller.

State-of-the-art contact location display devices still have limitations. For example, the 1-DOF CLD only provides contact location in the proximal-distal direction of the finger. Furthermore, the passive degree of freedom induces false breaking-and-making-contact sensation when the user's fingertip or fingernail interacts with the virtual object. Also, Doxon et al. emphasized that the restricted finger motion prevents using the CLD for exploration of 3-D virtual objects [Doxon et al. 2011]. For these reasons, the CLD device was mostly used for the exploration of planar surfaces. The 1-DOF contact location display can be improved by providing ulnar-radial motion of the contactor in addition to proximal-distal motion, which will be addressed in Chapter 3.

2.4 Tactile Feedback Rendering of Compliance Information

In addition to perceiving local contact geometry information, perceiving mechanical properties, such as compliance, is also important for identification and discrimination of objects [Klatzky and Lederman 2002]. For example, in daily life we use compliance information to select ripe fruit [Greer 2009] or to check the pressure of a bicycle tire [Bergmann Tiest and Kappers 2009]. More importantly, in medical procedures, doctors rely on compliance information to diagnose symptoms of some diseases [Klaesner et al. 2002] or to identify malignant tumors from healthy tissue [Barton, Harris, and Fletcher 1999]. Unfortunately, in laparoscopic or robotic surgeries, the rigid-handled instruments prevent surgeons from perceiving any tactile information [Bicchi et al. 1996; Culmer et al. 2012; Schostek, Schurr, and Buess 2009]. In these circumstances, surgeons rely mostly on visual or limited kinesthetic information [Schostek, Schurr, and Buess 2009].

The visual feedback displayed by two-dimensional screens may provide false cues due to the misalignment between the camera and monitor coordinate frames [Haveran et al. 2007] or may not convey compliance information sufficiently. Unlike geometry, perception of compliance depends more on haptic information than visual information [Gurari, Kuchenbecker, and Okamura 2009; Klatzky, Lederman, and Matula 1993]. Currently, in robotic surgery, surgeons may combine visual and kinesthetic information to estimate the compliance of a tissue [Tavakoli et al. 2006; Tholey, Desai, and Castellanos 2005]. It has been reported that this combined information helped doctors to estimate the mechanical properties of tissue more precisely, compared to relying either on pure visual information or on pure kinesthetic information. For this reason, it is essential to design medical instruments capable of displaying useful kinesthetic [Culmer et al. 2012; Okamura 2009] or tactile [Kuebler, Seibold, and Hirzinger 2005; Schostek, Schurr, and Buess 2009] feedback to surgeons in real-time and in an intuitive fashion.

Ideal reproduction of compliance information requires considering many different phenomena, such as nonlinear [Johnson 1985] and viscoelastic [Pawluk and Howe 1999] behaviors of the remote or virtual objects. This research only focuses on simplified techniques for rendering compliance.

Studies show that both kinesthetic and tactile feedback contribute in the perception of compliance [Bergmann Tiest and Kappers 2008; Scilingo et al. 2010; Srinivasan and LaMotte 1995]. One of the feedback modalities can be the dominant source of information, depending on the characteristics of the compliant surface. Compliant surfaces are usually categorized into two groups: (1) deformable compliant surfaces (e.g., an inflated balloon) and (2) nondeformable compliant surfaces (e.g., a piano key). The relationship between applied force and rigid displacement (force-displacement

characteristics) of a nondeformable compliant surface is conveyed through the kinesthetic modality [Bergmann Tiest and Kappers 2008; Scilingo et al. 2010], whereas the relationship between the applied force and contact area (force-area characteristics) of a deformable compliant surface is perceived via tactile information [Bianchi et al. 2010; Fujita and Ohmori 2001; Kimura, Yamamoto, and Higuchi 2010; Scilingo et al. 2010].

Srinivasan and LaMotte reported the importance of tactile information in the perception of compliance [Srinivasan and LaMotte 1995]. They found that participants could discriminate nondeformable specimens less accurately compared to deformable specimens. Furthermore, they reported that anesthetizing the fingerpad dramatically reduced participants' ability in discrimination of deformable compliant specimens. It was also found that participants could not discriminate between nondeformable compliant specimens in a passive touch task. However, participants could discriminate the compliance of deformable specimens in the passive touch task. This difference is related to the stimulation of tactile information when interacting with deformable specimens [Srinivasan and LaMotte 1995]. These findings suggest that rendering tactile information is important in the discrimination of compliant objects.

Furthermore, Bergmann Tiest et al. qualified the contribution of each modality in the compliance perception of deformable surfaces [Bergmann Tiest and Kappers 2009]. They estimated the contribution of tactile and kinesthetic information to be ~90% and ~10% respectively. This is in agreement with the finding in Srinivasan and LaMotte [1995] and suggests that compliance is mostly perceived through the tactile modality. Despite the dominant role of the tactile information, Scilingo et al. addressed the idea that rendering kinesthetic information may also be essential for discriminating "unimodal ambiguous" objects [Scilingo et al. 2010]. Such an object may have the same force-area

characteristics while having different force-displacement characteristics.

In the literature, there are different examples of tactile display devices for rendering compliance information. One of the most common concepts is controlling the contact area between the finger and the device. For example, Bicchi et al. created a contact area spread rate (CASR) display using a set of rigid telescoping cylinders [Bicchi, Scilingo, and De Rossi 2000]. Using this device, participants could distinguish the compliance of virtual surfaces with roughly the same level of performance they discriminated the compliance of physical specimens in direct finger contact. Fujita and Ohmori also developed a display device in which the contact area is controlled by the fluid pressure beneath a flexible rubber sheet [Fujita and Ohmori 2001]. This device only provides tactile (force-area) information, and the kinesthetic (force-displacement) information is masked by preventing the rigid displacement of the finger. Later, Bianchi et al. developed a device in which the compliance is controlled by the amount of tension in a fabric surface [Bianchi et al. 2010]. The flexible interfaces in Bianchi et al. [2010] and Fujita and Ohmori [2001] have some advantages over the rigid interface of the CASR display. These flexible interfaces are initially flat and can render changes in the contact area with higher resolution compared to the CASR display. Recently, Scilingo et al. integrated a CASR display with a force-feedback device in order to study the contribution of tactile and kinesthetic information in the compliance perception of “unimodal objects” [Scilingo et al. 2010]. Their human-subject experiments revealed that providing kinesthetic information, in addition to tactile information, only slightly improves the perception of compliance.

Porquis et al. also developed a tactile display device, called TAKO-Pen, to render the compliance of kinesthetic surfaces [Porquis et al. 2014]. Instead of controlling the contact

area, the compliance is artificially rendered by modulating air pressure on the fingerpad of thumb and index finger. They found that superimposing suction pressure on the fingerpads decreases the perceived compliance of kinesthetic surfaces.

One of the recent techniques for rendering compliance is the concept of displaying the contact width between the finger and the virtual object. Instead of rendering uniform surface deformation [Bianchi et al. 2010; Bicchi; Scilingo, and De Rossi 2000; Fujita and Ohmori 2001; Scilingo et al. 2010], this concept only renders approximated surface deformation. Kimura et al. designed a tactile display device in which a flexible surface wraps around the user's finger and controls the contact width to render artificial compliance information [Kimura, Yamamoto, and Higuchi 2009]. They evaluated the capabilities of the contact width display in a remote task. A force sensor measures the user's finger force and commands a linear actuator to push a contact width sensor against the surface of the remote object. The contact width measured by the sensor is feedback to the tactile display to recreate compliance information. The result of this experiment indicated that participants could discriminate compliance of remote objects using this system [Kimura, Yamamoto, and Higuchi 2009]. In another study, Kimura et al. extended this concept by rendering asymmetric contact by 2-DOF actuation of the surface [Kimura, Yamamoto, and Higuchi 2010]. They reported that the simplified but non-uniform surface deformation provided by such a device can be used to locate tumor lumps underneath a compliant tissue. However, one of the main drawbacks of the system is the rolling of the user's finger when the device surface actuated asymmetrically.

The state-of-the-art compliance display devices are usually large, heavy, and complicated. They are mostly benchtop systems and cannot embed in handheld devices such as laparoscopic instruments or game controllers. This dissertation introduces a

simple concept for rendering compliance using a tilting-plate tactile display (see Chapters 4-8). This concept can be used to develop compact and low-cost compliance display devices that can be easily integrated with other systems.

CHAPTER 3

TWO-DEGREE-OF-FREEDOM CONTACT LOCATION DISPLAY

3.1 Overview

This chapter describes the concept, fabrication, and experimental evaluation of a 2-DOF contact location display (CLD) device. Using this device, participants manipulated a virtual ball through a maze in three-dimensional space without visual information. The objective and subjective results under different haptic conditions showed that providing 2-DOF CLD information in addition to kinesthetic force-feedback information enhanced participants' fine manipulation performance and enabled a more intuitive interaction with the virtual object.

3.2 Device Description

The concept of 2-DOF contact location display (CLD) is shown in Figure 2.1. A spherical contactor (tactile element) displays the location of contact between the finger and a virtual object. The contactor position underneath the fingerpad is determined by two coordinates along ulnar-radial and proximal-distal directions. Figure 3.1 shows the prototype of the 2-DOF contact location display (CLD) device mounted on a kinesthetic force-feedback apparatus with capabilities similar to a Geomagic Phantom Premium 1.5. The 2-DOF contact location display device consists of two main units: (1) a thimble and

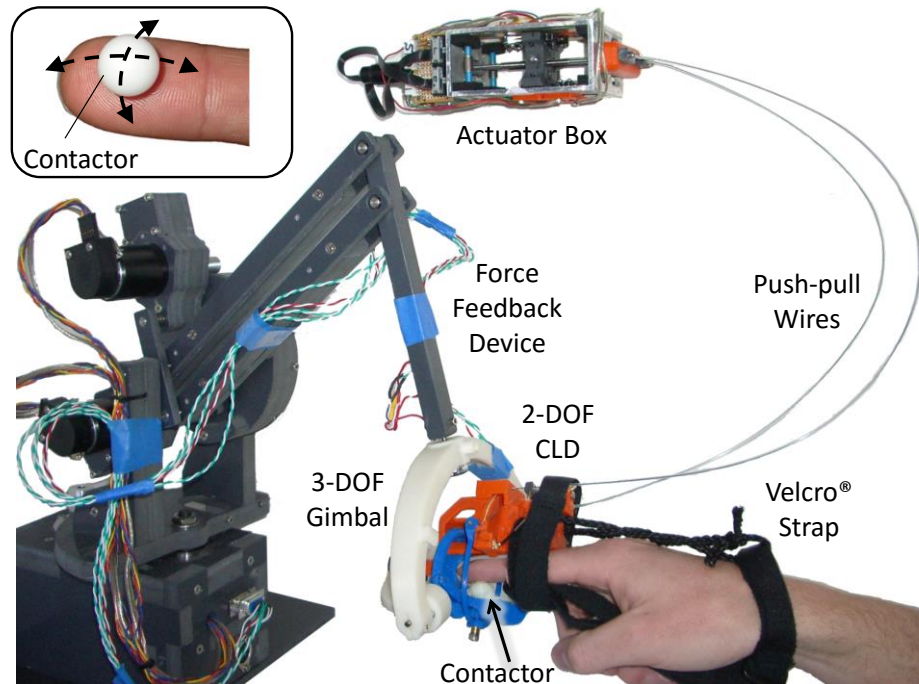


Figure 3.1. 2-DOF contact location display device attached to a 6-DOF force-feedback device with a passive gimbal. The actuator box is mounted on a neighboring structure (see Figure 3.7) next to the device such that the push-pull wires form a U-shaped profile. Images were taken with permission from Yazdian et al. [2013] © 2013 IEEE.

(2) an actuator box. The detail specifications of each unit are described in the following sections.

3.2.1 Thimble and Spherical Mechanism

The thimble consists of a spring loaded contactor, a 5-bar mechanism, and finger restraint (Figure 3.2). The contactor is a ~ 9.5 mm diameter Delrin plastic sphere and can freely rotate inside a hemispherical cup. A spring-loaded arm brings the contactor into contact with the fingerpad with a contact force of ~ 0.3 N at an equivalent spring stiffness of less than 0.1 N/mm. Using this spring loaded arm, the contactor is always in contact with the finger regardless of difference in the curvature of finger or difference in the finger sizes of users. The contactor can move in the ulnar-radial and proximal-distal

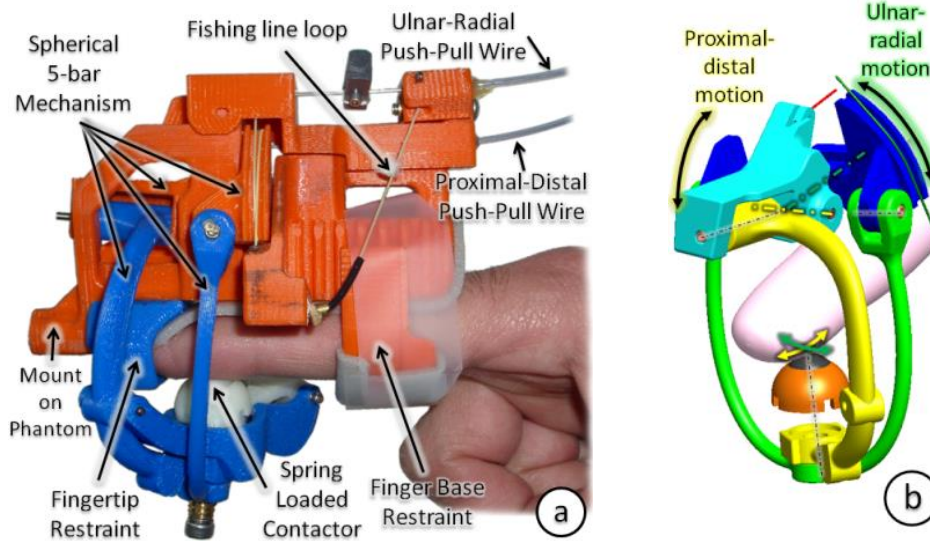


Figure 3.2. Thimble of the 2-DOF contact location display device: (a) worn on a user's index finger, (b) 5-bar spherical mechanism. Images were taken with permission from Yazdian et al. [2013] © 2013 IEEE.

directions within a $\sim 12 \times \sim 12$ mm workspace underneath the fingerpad.

The spring-loaded arm is driven by the spherical 5-bar parallel mechanism mounted on the thimble. Examples of this mechanism can be found in several haptic devices such as the kinesthetic force-feedback Immersion Impulse Engine 2000 joystick and the tactile feedback display devices presented in Frisoli et al. [2008] and Dostmohamed and Hayward [2005]. The parallel configuration of the mechanism provides higher structural stiffness and lower backlash compared to a serial mechanism configuration. Another important feature of the 5-bar mechanism is that the motions of the contactor in the proximal-distal and ulnar-radial directions are decoupled and can be achieved independently, which simplifies the algorithm for position control.

The thimble is worn securely on the user's index finger. Two finger restraints located at the tip and base of the finger prevent relative displacement of the finger in radial direction (i.e., normal to the finger center axis). In addition, a Velcro strap prevents the

finger displacement along the finger. The thimble and the 5-bar mechanism were fabricated using fused deposition modeling (FDM) of ABS plastic material. The thimble dimensions are $\sim 85 \times 80 \times 60$ mm and weighs ~ 100 grams. Contrary to the previous 1-DOF CLD design [Provancher et al. 2005], the 2-DOF CLD thimble is directly attached to the kinesthetic force-feedback device to properly render axial and lateral forces.

3.2.2 Actuator Box and Push-Pull Wires

A remote actuator box drives the 5-bar mechanism through two push-pull wires. This configuration reduces the effective mass and inertia of the system on the user's finger. One of the push-pull wires is directly attached to the 5-bar mechanism and controls the proximal-distal motion. The other push-pull wire controls the ulnar-radial motion via a loop of low-stretch fishing line (Figure 3.2). Both push-pull wires enter the thimble adjacent and parallel to each other and are deformed into a U-shape to enable unrestricted finger motion of the thimble in 6-DOF (see Figure 3.1).

The push-pull wires are ~ 640 mm long and made from 0.61 mm diameter spring steel wires. They passed through flexible Teflon (PTFE) sheathes with inner and outer diameters of 0.79 and 1.59 mm, respectively. Although the sheathing is flexible, its high axial stiffness (2700 N/m) and low inner surface friction make it suitable for a reasonably accurate position control when combined with a push-pull wire of proper diameter.

The motion of push-pull wires is controlled by corresponding linear motion carriages, which are driven by 3.18 mm pitch lead screws (Figure 3.3). The lead screws are connected to two Maxon RE16 motors with 4.4:1 planetary gearboxes through helical couplers. Motor encoders determine the position of each push-pull wire with a resolution of ~ 0.01 mm at the linear motion carriage. The actuator box is mounted on a stationary

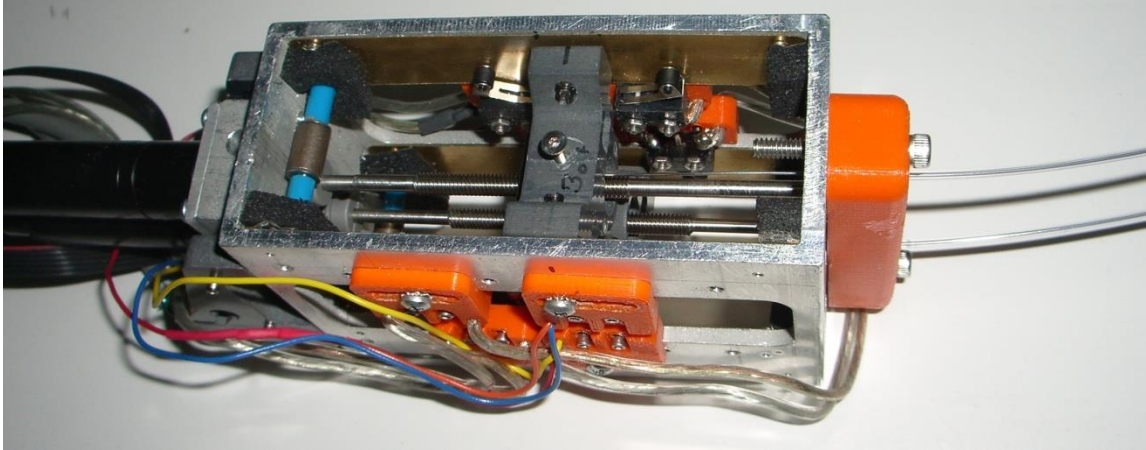


Figure 3.3. Actuator box of the 2-DOF contact location display device. The range of motion of the push-pull wires are limited by the micro switches.

frame (Figure 3.1) instead of on the user's forearm as in the previous design [Provancher et al. 2005]. This setup simplifies the application and removal of the apparatus.

3.2.3 Device Characterization and Backlash Compensation

To evaluate the performance of the device, the difference (backlash) between the commanded position and true position of the contactor was analyzed. The contactor's true position was measured via two orthogonal linear optical encoders (PE-500-2-I-S-L) with a resolution 12 μm . For contactor motions similar to those seen in normal manipulation, the uncompensated backlash for the proximal-distal and ulnar-radial directions was ~ 5.2 mm and 6.1 mm, respectively (see Figure 3.4 for example). Conducting a study using 1-DOF CLD, Doxon et al. reported that participants could detect backlash of more than 0.46 mm along their fingerpad during active exploration of low-curvature surfaces [Doxon et al. 2013].

The backlash was compensated for in software by adding/subtracting a fixed offset value to the desired position of the contactor upon its reversal motions. The offset value

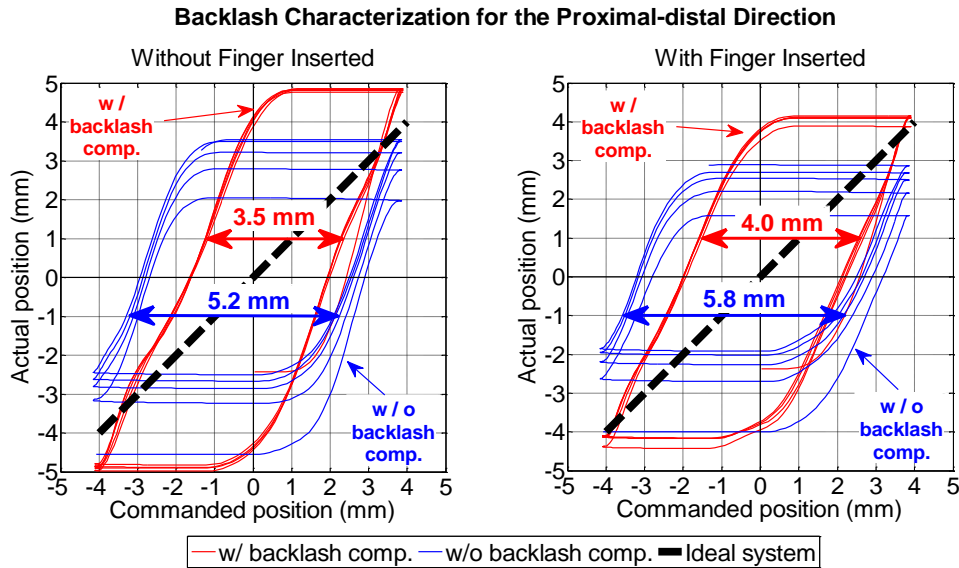


Figure 3.4. Proximal-distal backlash characterization and compensation of the device with and without a finger inserted. The dashed black line shows an ideal system. The horizontal spans of the loops indicate overall backlash values. Images were taken with permission from Yazdian et al. [2013] © 2013 IEEE.

was selected to be less than the full backlash to prevent any unrealistic sudden jump in the contactor position. Compensated, the backlash for the proximal-distal and ulnar-radial directions was reduced to 3.5 mm and 3.1 mm, respectively. When a finger was inserted into the device the backlash levels slightly increased by ~ 0.5 mm. To reduce the backlash further, more sophisticated techniques such as ‘standard’ or ‘improved dual-loop’ backlash compensation schemes [Tal 1999] may be implemented. These techniques require additional position sensors in the contactor side and may make the thimble slightly larger and more difficult to package (Section 3.5). Pilot studies showed that the current device can provide consistent tactile information without any confusion for the ball manipulation in the experiment task.

3.3 Methods

It is hypothesized that providing 2-DOF contact location information, in addition to kinesthetic force-feedback information, can enhance users' performance and provide a more intuitive interaction when exploring and manipulating 3-D virtual objects. To test this hypothesis, a virtual ball manipulation experiment was conducted.

3.3.1 Participants

Eight naïve volunteers (1 female, 1 left-handed) aged from 18 to 35 years (mean 27 years old) participated in the experiment. The participants had no known abnormalities in their index fingers. Before the experiment, they were informed about the experiment procedures and signed informed consent forms in accordance with the University of Utah's Institutional Review Board (IRB) policy.

3.3.2 Virtual Environment

The virtual environment consisted of three elements: a virtual ball, a virtual finger, and a virtual maze.

The virtual finger was modeled as a sphere with a 13 mm diameter, approximating the tip of a human finger. The diameter of the virtual ball was 16 mm (slightly larger than the physical contactor) to enable ease of manipulation under all tactile and kinesthetic rendering conditions. A maze with a rectangular perimeter was selected to force the participants to perceive both proximal-distal and ulnar-radial motions of the contactor (Figure 3.5). The perimeter dimensions were 105×180 mm. A channel with a 25 mm width and 10 mm height and 560 mm length was built around the maze. The channel width and height were selected based on the results of a pilot study to create a maze with



Figure 3.5. The virtual environment used for the ball manipulation experiment. For the experiment only the top view of the maze was visible and the virtual finger and ball were invisible. A wall between the start and end points prevented participants from moving the ball in the opposite direction. Image was taken with permission from Yazdian et al. [2013] © 2013 IEEE.

a reasonable level of difficulty for the experiment task.

A perfect rolling (no slip) contact mechanism was considered assumed between the ball and the finger/maze. This no-slip condition prevented participants from simply pushing/sliding the ball along a maze wall and forced them to use the contact location information during manipulation. The ball was rendered through CLD and kinesthetic-force feedback, as appropriate for the respective rendering condition. However, the maze walls were rendered only through kinesthetic-force feedback since the current CLD device cannot render multipoint contacts. Friction was rendered between the ball and maze wall to slow the participants' progress as a penalty for pushing the ball against the wall. This frictional feedback also informed participants about the contact since no visual information was provided during the experiment.

Using a pilot study, the difficulty of the ball manipulation task was tested in different environments: (1) no visual feedback, (2) diminished visual feedback, and (3) vibration feedback where superimposed sinusoidal vibration onto kinesthetic feedback warned participants that the finger or the ball contacts with the wall of the maze. The preliminary results show that the participants could accomplish the task reasonably well without

vibration and visual feedback. The next sections focus only on this environmental condition, with fewer independent variables affecting the participants' performance.

3.3.3 Stimuli

Two general haptic conditions – kinesthetic-force feedback and 2-DOF CLD plus kinesthetic-force feedback – were used in this experiment. In the current 2-DOF CLD device, the contactor is always in contact with the user's finger; thus, it cannot replicate the sensation of making and breaking contact through tactile feedback and may cause unintuitive interaction. To address this issue, four different prepositioning feedback conditions were considered for the contactor. Table 3.1 and Figure 3.6 summarize all haptic conditions used in this experiment. In condition C1 (no CLD), only force-feedback information is rendered and the contactor is held in its centered position under the user's finger. In condition C2 (kinesthetic feedback plus CLD with no prepositioning), the

Table 3.1. Tactile rendering conditions (C1-C5)

	Feedback Conditions
C1	Kinesthetic feedback only (no CLD)
C2	Kinesthetic feedback + CLD with no prepositioning
C3	Kinesthetic feedback + CLD with 30 mm prepositioning
C4	Kinesthetic feedback + CLD with 30 mm hybrid prepositioning
C5	Kinesthetic feedback + CLD with prepositioning always

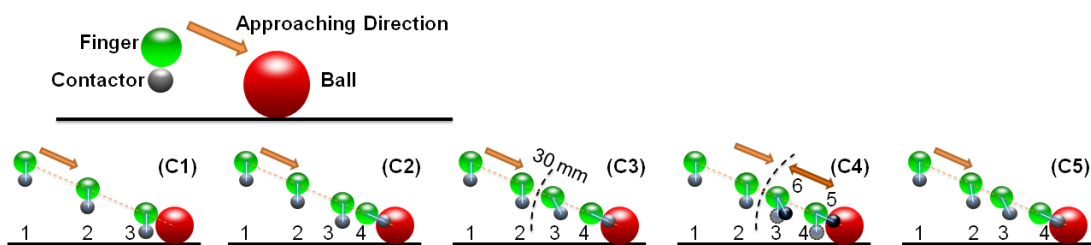


Figure 3.6. Illustration of haptic rendering conditions C1-C5. For C4, the contactor does not move until contact is made with the virtual ball, and then it acts like C3 until the user exceeds 30 mm from the virtual ball.

contactor suddenly moves from the center of the finger to the contact location upon a contact in the virtual environment and suddenly moves back to the center position upon breaking contact with that environment. This quick displacement of the contactor may distract participants and cause an unintuitive interaction. In condition C3 (kinesthetic feedback plus CLD with 30 mm prepositioning), the contactor stays at the center position if it is 30 mm away from the expected contact point. For distances less than 30 mm, the contactor is prepositioned to the weighted average location of the expected contact point and the center of the fingerpad. Thus for zero distance, the contactor is at the contact location. In a pilot study, the 30 mm threshold used in C3 was found to be slightly larger than the average distance between the ball and finger during manipulation. Condition C4 (CLD with 30 mm hybrid prepositioning) is rendered similarly to condition C3 with the exception that once the distance between the finger and the virtual surface exceeds 30 mm, the contactor position will remain centered until a new contact has been made with the surface again (similar to C2). This hybrid mode reduces the distraction of contactor prepositioning in free space while providing the benefit of contactor prepositioning during active manipulation through directional localization cues. Lastly, during condition C5 (always prepositioning) the contactor is continuously prepositioning regardless of distance from the surface of the ball.

3.3.4 Procedures

The participants manipulated the ball through the maze under two main haptic conditions: (1) force feedback only and (2) force feedback plus 2-DOF CLD information. The participants sat next to the apparatus and wore the thimble on their right index finger (Figure 3.7). The apparatus and their hands were covered by a cloth to block visual cues.

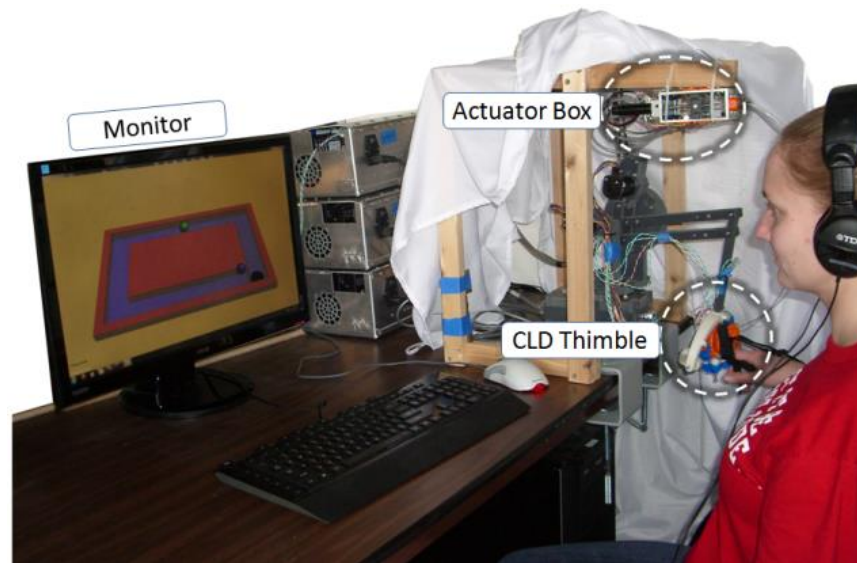


Figure 3.7. The setup of the experiment. A participant is manipulating a virtual ball using the 2-DOF contact location display integrated with the kinesthetic-force feedback apparatus. Image taken with permission from Yazdian et al. [2013] © 2013 IEEE.

Participants wore headphones, which played white noise to block any audio cues from the apparatus as well as distraction from background noise. The instructions for the experiment were displayed on the computer screen.

The participant's task in the experiment was to roll the ball through the maze in less than 60 seconds and with the smallest number of contacts between the ball and maze walls. The experiment was divided into two 60-minute sessions with a short break in between to reduce muscle fatigue. In each session, the participants accomplished the experiment task under all five tactile rendering conditions (C1-C5 in Table 3.1). The conditions were presented based on 5×5 Latin Squares for each participant to reduce the number of condition permutations required in a balanced experiment design.

The starting position and desired manipulation direction were chosen randomly from a list of eight possible combinations to reduce possible learning effects (e.g., muscle memory) caused by repeated motions.

Without any form of visual feedback, it is possible one could lose track of the ball and spend too much time locating the ball instead of manipulating it. To overcome this issue and reduce variation in completion time, a temporary ‘help’ option was provided. By pressing spacebar on the keyboard, the participants could visually locate the finger and the ball. After contact was made with the ball, both ball and finger became invisible again. To prevent the participants from cheating, they were informed that requesting ‘help’ would negatively affect their task completion score. Total completion time, travel distance (for incomplete trials), and number of requested helps were recorded for each trial.

After the experiment, participants filled out a survey regarding the preference and realism of each tactile rendering condition. During the survey, participants were asked to manipulate the ball back and forth at a corner of the maze and switch between the conditions to help them judge the conditions. No visual feedback was provided in the session. The survey consisted of questions with 5-point Likert scale (‘strongly disagree’ to ‘strongly agree’). Survey questions were randomized and designed with both positive and negative phrases to avoid biasing effect.

3.4 Experimental Results and Discussion

3.4.1 Objective Results

Participants’ performance was analyzed by three objective metrics: (1) the average speed of ball manipulation, (2) the number of times the ball contacted the maze, and (3) the number of times that help was requested.

The average speed is defined as the distance the ball traveled along the center-line of the maze per completion time. Figure 3.8 shows the mean and 95% confidence interval of

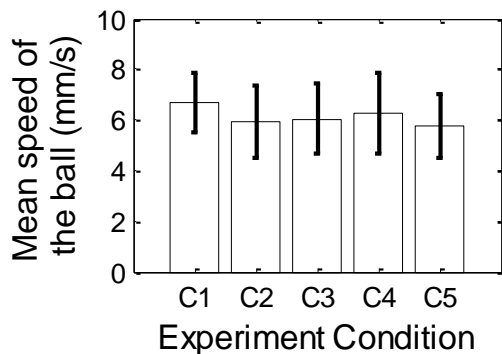


Figure 3.8. Mean speed of ball manipulation for different tactile rendering conditions (see Table 3.1). Error bars show 95% confidence intervals.

the average speed of the ball under tactile rendering conditions C1-C5 for all participants. The average speed is ~ 6 mm/s regardless of tactile rendering condition. A within-subjects one-way ANOVA (analysis of variance) shows no statistical differences among the conditions [$F(4,75) = 0.22$, $p = 0.92$].

Figure 3.9 shows the mean and 95% confidence intervals of the number of contacts between the ball and maze wall for each rendering condition. The average number of contacts is between 80 to 100 contacts and no statistical difference was found among the rendering conditions [$F(4,75) = 0.46$, $p = 0.76$]. The kinesthetic-feedback-only condition (C1) seems to have the least number of contacts. This suggests that 2-DOF CLD

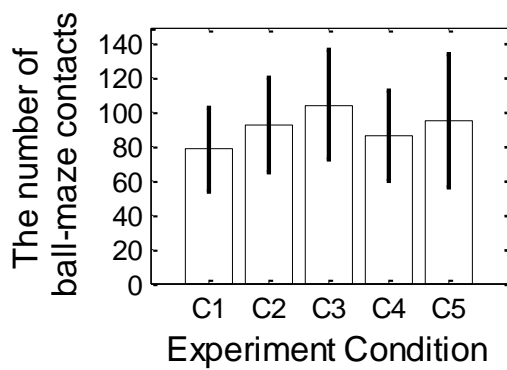


Figure 3.9. Mean number of ball-maze contacts. Error bars show 95% confidence intervals.

information could not help the participants prevent the ball from contacting the maze wall. Lederman and Klatzky also found that participants with anesthetized fingertips (i.e., with no local tactile sensation) had reasonable shape recognition performance [Lederman and Klatzky 1999]. They hypothesized that kinesthetic feedback provided enough information for the shape recognition task.

The minimum and maximum numbers of requested ‘help’ to temporarily locate the missing ball belong to 30 mm hybrid prepositioning (C4) and kinesthetic feedback only (C1) conditions, respectively (Figure 3.10). Although there is no significant difference among all five conditions [$F(4,75) = 0.92$, $p = 0.46$], the data indicates participants lost the ball less using 2-DOF CLD compared to force feedback only. This suggests that CLD feedback provides useful information to keep track of the ball or locate the ball in the absence of visual feedback.

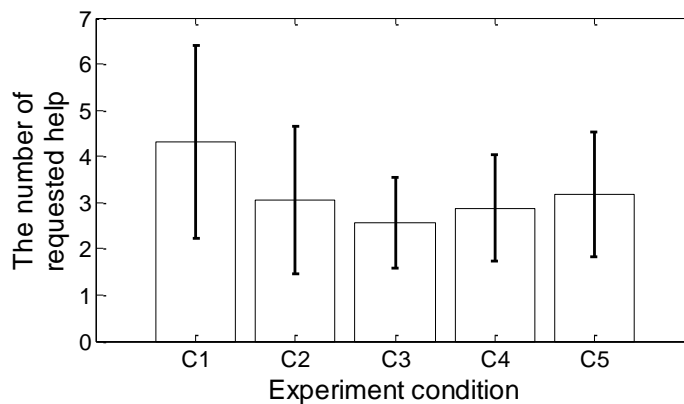


Figure 3.10. Mean of number of times participants requested help. Error bars are 95% confidence intervals. Participants lose track of the ball under kinesthetic feedback only more compared to the other CLD conditions.

3.4.2 Subjective Results

Figure 3.11 shows the average subjective ratings for preference of use and realism of the tactile conditions. Likert scale data were visualized using net stacked distribution graph with a central base [Becker 2012]. This visualization technique shows the skewness, non-neutrality, and intensity of responses in an easily read manner. It seems that the CLD has a nearly significant effect on participants' preference of use [Kruskal-Wallis test, $H(4) = 9.42$, $p = 0.051$]. The most preferred rendering condition was the CLD

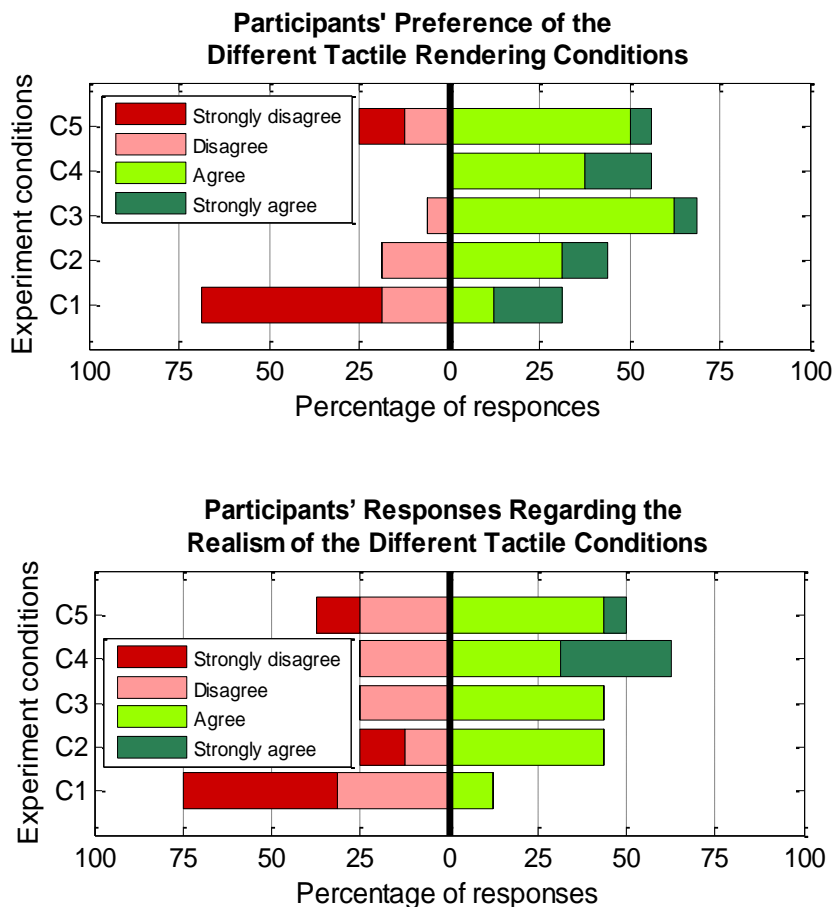


Figure 3.11. Results of subjective survey: average of participants' preference of use for different tactile rendering conditions (top) and their average responses regarding the realism of the conditions (bottom). The bars on the right (left) side of the center line show positive (negative) responses. The neutral responses are not shown. Each section represents the percentage of responses of a specific Likert item for all participants [Yazdian et al. 2013].

under the 30 mm hybrid prepositioning condition (C4) and the least preferred rendering condition was kinesthetic feedback only (C1). The second least preferred condition was CLD with no prepositioning condition (C2), which might be due to the distracting sudden motions of the contactor in this condition.

The level of realism is statistically significantly different among rendering conditions C1-C5, with mean ranks of 21.56, 41.88, 43.75, 53.19, and 42.13, respectively [Kruskal-Wallis test, $H(4) = 16.98$, $p = 0.002$]. The results suggest that the CLD conditions are subjectively assessed to provide a more realistic interaction than the kinesthetic-feedback-only condition. Post-hoc paired comparisons [Langley 1970] revealed that only conditions C1 and C4 are significantly different in terms of realism [$K = 7.89$, $K_{critical} = 5.60$]. The 30 mm hybrid prepositioning (C4) and the kinesthetic feedback only (C1) conditions provide the most and the least realistic interactions, respectively. The hybrid condition (C4) might be more realistic compared to the other condition since the contactor position only updates when the participants made a first contact with the ball and stayed close to the ball for an interactive manipulation.

3.5 Improved 2-DOF Contact Location Display Device

The current 2-DOF CLD device was improved by reducing its backlash and adding making-and-breaking-contact functionality to the contactor. Figure 3.12 shows the prototype of the revised 2-DOF CLD. Two small position sensors (potentiometers from a S3114 analog Futaba RC servomotor) were embedded inside the thimble to measure the position angle or the proximal-distal and ulnar-radial arms directly. The device backlash was reduced by implementing a ‘dual loop’ control scheme [Tal 1999] (Figure 3.13). The amount of backlash for the new 2-DOF CLD was measured less than 1 mm (Figure 3.14),

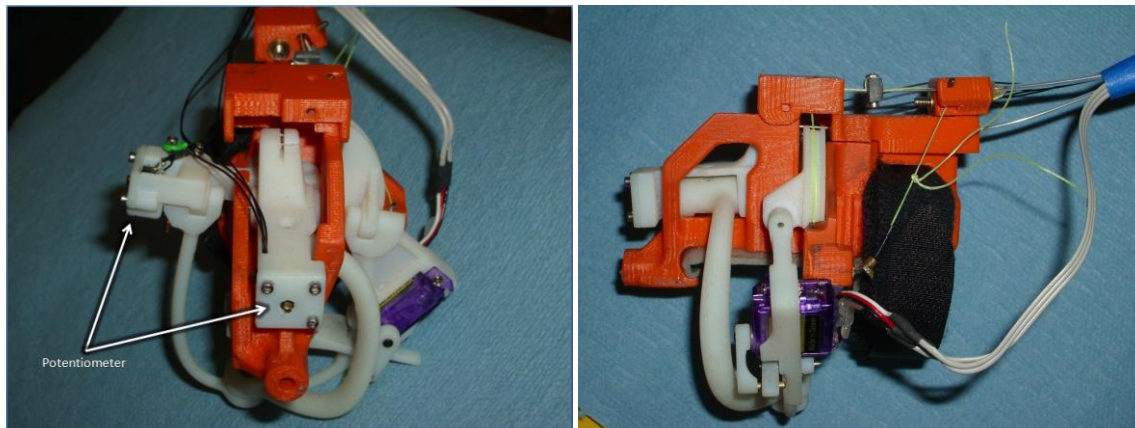


Figure 3.12. The prototype of modified 2-DOF CLD equipped with two small potentiometer sensors measuring the position of the contactor directly.

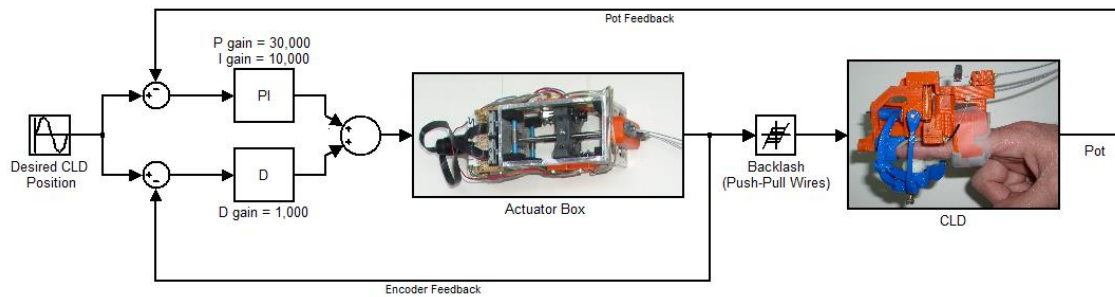


Figure 3.13. Dual loop control scheme for reducing backlash

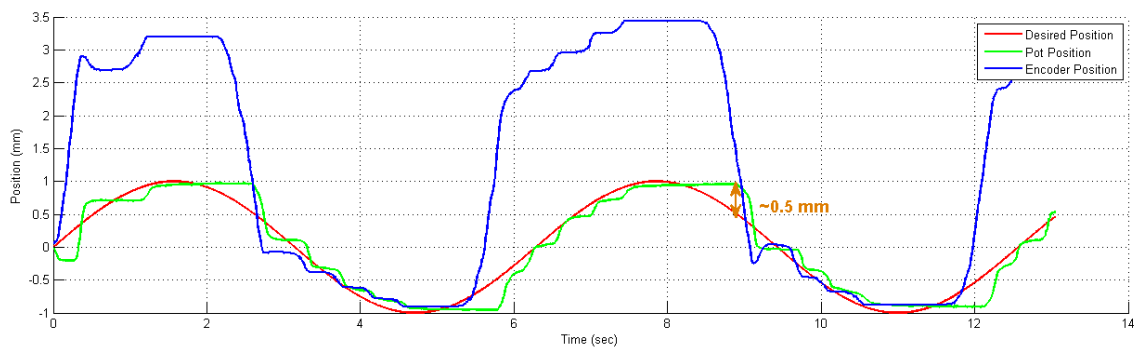
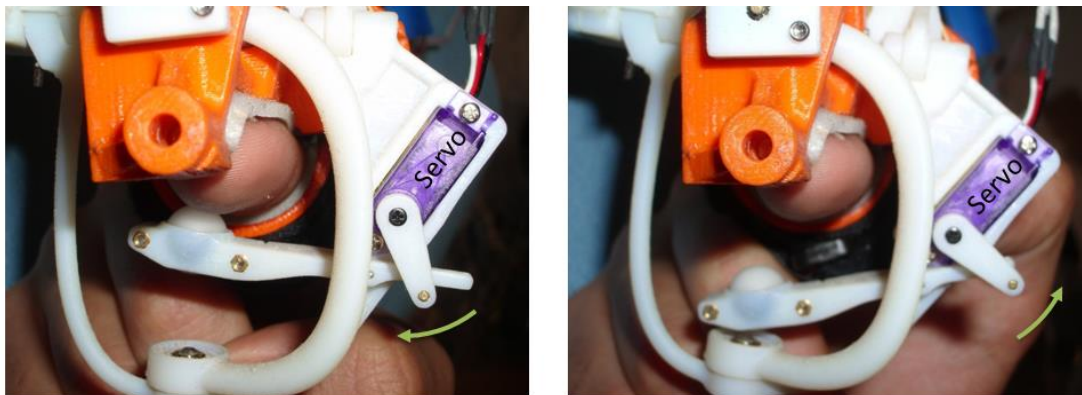


Figure 3.14. Backlash characterization of the revised 2-DOF CLD for ulnar-radial direction. The maximum backlash was measured less than 1 mm.

which is slightly above a human's backlash detection threshold (i.e., 0.4 mm [Doxon et al. 2013]).

To provide a sensation of making-and-breaking-contact, a spring-loaded contactor with an active degree of freedom was prototyped (Figure 3.15). The spring provides a gentle contact force when the finger is in contact with a virtual surface (similar to the contact force explained in Section 3.2.1). Upon breaking contact, a small RC servomotor (Blue Bird's BMS-303) separates the contactor from the user's fingerpad. The servomotor generates undesirable mechanical vibratory cues when idling. To eliminate vibration, the servomotor power is kept off unless a change in contact status is detected.

While this revised 2-DOF CLD device was prototyped and improved upon the performance of the prior version, further experiments were not conducted, as my research interests took me in a different direction.



Making contact
The contactor is spring loaded.

Breaking contact
The mechanism stays in breaking-contact configuration even when the servomotor is off.

Figure 3.15. Contact location display device prototype with an active making-and-breaking-contact system.

3.6 Conclusions

A two-degree of freedom (2-DOF) contact location display (CLD) device was designed, fabricated, and evaluated. The 2-DOF CLD device provides fine tactile feedback through rendering the location of contact between the user's finger and 3-D virtual objects. Due to its compact size and low weight, this device can be mounted onto a kinesthetic feedback device and simultaneously provides both kinesthetic and tactile information for exploring and manipulating 3-D virtual or remote objects. The backlash of the device was characterized and partially compensated for by software.

A ball manipulation experiment was conducted to assess the performance of the 2-DOF CLD device at five different tactile rendering conditions in the absence of visual feedback. No statistically significant difference was found between the kinesthetic-feedback-only and kinesthetic-feedback-plus-CLD information conditions in terms of the speed or the number of contacts between the ball and the maze.

However, providing CLD information with 30 mm hybrid prepositioning condition (C4), in addition to kinesthetic-force feedback, seems to help the participants in the active manipulation of the ball since the participants requested 'help' fewer times compared to the pure kinesthetic feedback condition (C1). In the 30 mm hybrid prepositioning, the contactor stayed at the center of the fingerpad until the virtual finger touched the ball. Then, the contactor was prepositioned continuously for an active manipulation where the distance between the finger and the ball was less than 30 mm. For distances of more than 30 mm, the contactor stayed at the center of the fingerpad.

The result of the subjective survey revealed the difference between the tactile rendering conditions. The 30 mm hybrid prepositioning condition (C4) and the kinesthetic feedback only condition (C1) were reported as the most and the least

preferred/realistic rendering conditions, respectively. The results of the subjective survey indicate that while the current 2-DOF CLD device could not improve the participant's manipulation performance, it provides a more realistic and intuitive interaction for manipulation of a virtual ball.

CHAPTER 4

TILTING-PLATE TACTILE COMPLIANCE DISPLAY DEVICE

4.1 Overview

This chapter presents the concept, prototype design, and evaluation of a simple tilting-plate tactile compliance display device. Instead of rendering full surface deformation of a compliant surface, the tilting-plate device only provides approximated surface deformation. The compact size of this compliance display device enables it to be integrated with systems such as the human interfaces of robotic surgery consoles, game controllers, or mobile devices. To evaluate the effect of tilting-plate feedback on perceived compliance a human-subject experiment was conducted. Experimental results showed that the superimposing tilting-plate feedback on a kinesthetically rendered surface reduced the perceived compliance of the rendered surface.

4.2 Tilting-plate Concept and Device Description

The concept and prototype of the tilting-plate compliance display device are shown in Figure 4.1. The tilting-plate device consists of two adjacent rigid plates that pivot around a common axis (i.e., point A in Figure 4.1). Each plate has a dimension of $20 \times 10 \times 2$ mm. Prior to contact, the plates are horizontal and provide a flat interface with 20×20 mm workspace. As a user applies force on the plates, they wrap around the user's

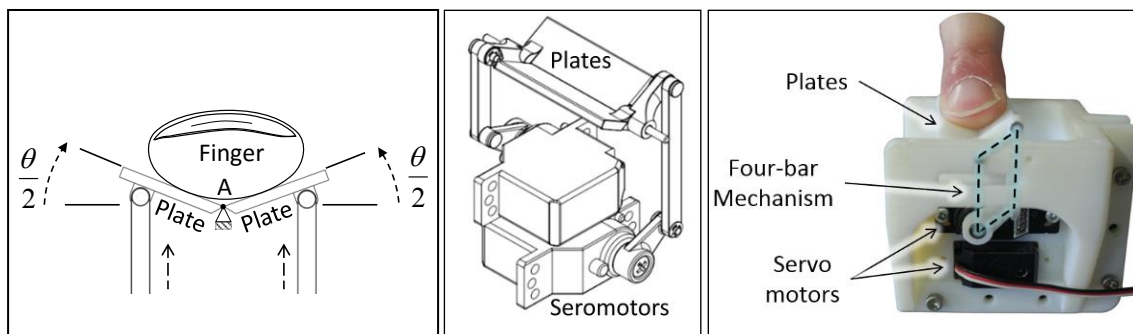


Figure 4.1. Tilting-plate compliance display device: (left) concept, (middle) actuation mechanism, and (right) the prototyped device.

fingerpad and form a shallow V-shaped groove beneath his/her finger. The V-shaped groove approximates the surface deformation of a deformable compliant object in a virtual/remote environment. We refer to this type of tactile compliance information as tilting-plate feedback.

To provide both kinesthetic and tactile information, the tilting-plate device was mounted on a Haptic Paddle force-feedback device [Provancher and Doxon 2009] via an extended rotational arm (Figure 4.2). An optical encoder (HEDS-5540 A02) on the

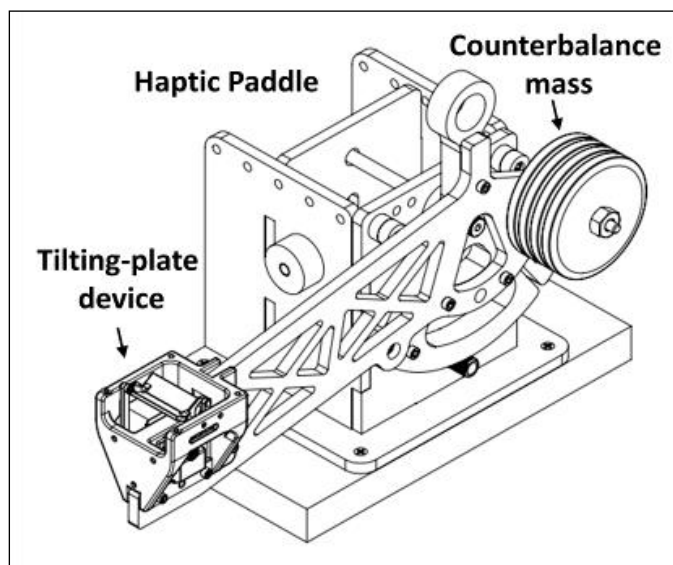


Figure 4.2. Tilting-plate compliance display device integrated with a force-feedback device (modified Haptic Paddle).

Haptic Paddle measures the finger's displacement with a resolution of ~ 0.04 mm. A microcontroller (Microchip dsPIC 33EP256MU806) analyzes the finger displacement and commands two servomotors (Futaba S3156) to tilt the plates via two parallelogram four-bar mechanisms with a tilt angle resolution of less than 0.1 degrees of each plate at an update rate of 500 Hz.

Kinesthetic-force feedback is generated by a DC motor (Maxon RE25) and is transmitted to the rotational arm through a capstan pulley mechanism. The resolution of rendered kinesthetic force at the center of the tilting-plate interface is ~ 1 mN. The relatively long rotational arm (200 mm) limits the lateral displacement of the device interface (~ 0.025 mm per 1.0 mm vertical displacement of the center of the interface). To prevent the Haptic Paddle's arm from sagging, especially at low kinesthetic force levels, a counterweight on the other side of the rotational arm was implemented.

The plates, four-bar mechanisms, and the supporting frame of the tilting-plate device were prototyped using PolyJet technology on a Stratasys's Objet 3-D printer. The current prototype weighs less than 55 grams. The weight of the device can be reduced further by using only one servomotor to actuate the two plates symmetrically. However, the current system uses two servomotors to compensate for the undesired tilt due to the rotation of the Haptic Paddle's arm. The current device is capable of rendering asymmetrical deformation, similar to that in Kimura, Yamamoto, and Higuchi [2010]; however, this dissertation only focuses on rendering symmetric tilting-plate feedback.

4.3 Tilt-displacement and Force-displacement Models

For rendering simplified tactile feedback, it was assumed that the amount of tilt is a linear function of the device's rigid displacement; i.e.,

$$\theta = RF \quad (4.1)$$

where θ is the relative angle change between the plates in degrees (e.g., zero degree means a flat interface), R is the tilting ratio in deg/N, and F is the contact force in Newtons. To render materials with different compliance levels, different levels of R are used.

The contact force rendered by the force-feedback device was computed using a simple linear spring model, representing the linear kinesthetic stiffness of a virtual object:

$$F = \frac{Kd}{100}, \quad (4.2)$$

where F is the rendered kinesthetic force in Newtons and K is the kinesthetic stiffness of the virtual object in N/m, and d is the vertical displacement of the center of the device surface in cm.

4.4 Methods: Tilting-plate plus Force

Feedback vs. Force Feedback

We hypothesized that the perceived compliance of a surface with combined tilting-plate and kinesthetic-force feedback is higher than the perceived compliance of a surface with the same kinesthetic-force feedback. A compliance discrimination experiment using the method of constant stimuli was conducted to test this hypothesis.

4.4.1 Participants

A total of 30 participants (11 female, 3 left-handed) aged 19 to 37 years old (mean 26 years old) took part in this experiment. The participants had no known abnormalities in their index fingers. Before the experiment, they were informed about the experiment procedures and signed informed consent forms in accordance with the University of Utah's Institutional Review Board (IRB) policy.

4.4.2 Stimuli

Two types of stimuli were used in this experiment: reference and comparison stimuli. The reference stimuli provided both kinesthetic and tilting-plate feedback simultaneously. A total of 9 reference stimuli were considered (3 kinesthetic stiffness levels \times 3 tilting ratio levels). A wide range of kinesthetic stiffness levels (60, 400, and 1600 N/m) were considered for these stimuli. The integrated device is not capable of rendering proper kinesthetic stiffness below ~ 20 N/m or above ~ 1800 N/m because of the Haptic Paddle's friction and dynamic instability, respectively. These minimum and maximum kinesthetic stiffness levels were used for the comparison stimuli. At the 60 N/m kinesthetic stiffness level, the reference tilting ratios were 8.33, 16.67, and 33.33 deg/N. These values were initially selected in terms of displacement-tilt relationship (i.e., 5, 10, 20 deg/cm). At 400 and 1600 N/m kinesthetic stiffness level, the tilting ratios were 4, 8, and 16 deg/N. In contrast, the comparison stimuli were purely kinesthetic surfaces with zero tilting ratios (, flat surface). For each of the 9 reference stimuli, 9 different kinesthetic stiffness levels between 20 and 1800 N/m were selected (see Table 4.1). All the kinesthetic stiffness and tilting ratio levels were obtained through a pilot study.

Table 4.1. All reference and comparison stimuli.

Reference Stimuli		Comparison Stimuli
Kinesthetic Stiffness (N/m)	Tilting Ratio (deg/N)	Kinesthetic Stiffness (N/m)
60	8.33	20, 30, 40, 50, 60, 70, 80, 90, and 100
	16.33	20, 30, 40, 50, 60, 70, 80, 90, and 100
	33.33	20, 30, 40, 50, 60, 70, 80, 90, and 100
400	4.00	125, 160, 200, 250, 300, 350, 400, 475, and 550
	8.00	108, 180, 200, 250, 300, 350, 400, 475, and 550
	16.00	75, 150, 200, 250, 300, 350, 400, 475, and 550
1600	4.00	1212, 1290, 1333, 1379, 1428, 1481, 1538, 1600, and 1739
	8.00	714, 833, 1000, 1111, 1250, 1428, 1538, 1632, and 1739
	16.00	333, 500, 667, 833 1000, 1176, 1428, 1666, and 1739

4.4.3 Procedures

4.4.3.1 Training

In a short training session before the experiment, the participants compared and sorted the perceived compliance of three easily distinguishable physical foam blocks with relatively high, medium, and low compliance levels. Correct-answer feedback was presented to the participants after they accomplished the task. The goal of this training session was to prevent the participants from confusing softness (compliance) with stiffness (the inverse of compliance) or with roughness (surface texture). In addition, the participants were advised to consider both surface deformation and displacement in their compliance judgments to prevent them from disregarding or biasing toward either kinesthetic or tilting-plate feedback.

The foam blocks were cylindrical with a diameter of ~7.5 cm and a height of ~4 cm. The high, medium, and low compliance foam blocks had kinesthetic stiffness values of ~260, 1000, and 2000 N/m, and contact area spread rates (surface deformation characteristics) of ~45, 130, and 150 mm²/N, respectively. These measurements were obtained by indenting the foam blocks with a 15 mm in diameter semi-spherical rigid

probe (close to the size of a human finger) and at 1 N contact force. The kinesthetic compliance levels of the low- and medium-compliant blocks were roughly the same; however, their contact area spread rates were reasonably different.

4.4.3.2 Experiment Setup

Participants placed their right arm on a wrist support and perceived the compliance of the stimuli using their index fingers (Figure 4.3). During the experiment, the participants' hands and the entire device were covered with a cloth screen to prevent any visual cues from affecting their compliance judgment. The participants wore noise cancelling headphones to mask audio cues from the device. Before each trial, a proctor aligned the position of the participant's finger with the center of the tilting-plate interface for proper symmetrical tactile feedback.

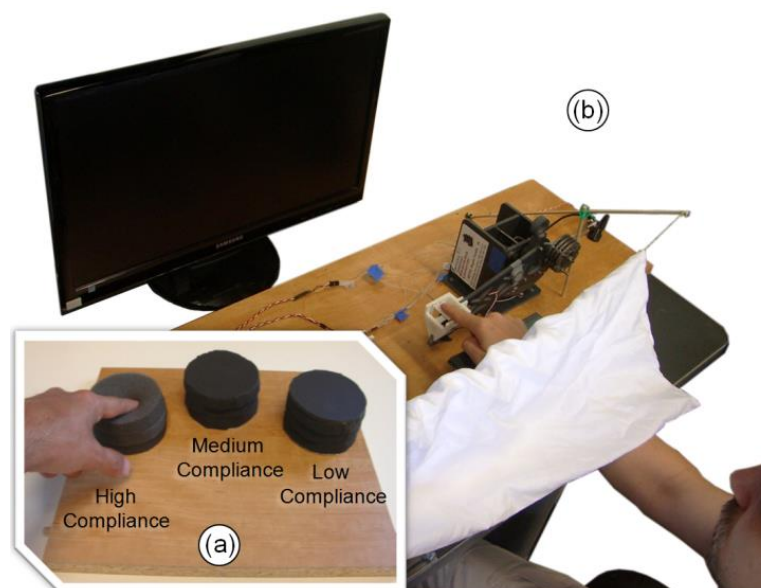


Figure 4.3. Experiment setup: (a) Training session using three foam blocks with high, medium, and low compliance levels. (b) A participant compares the compliance of a pure kinesthetic stimulus with the compliance of a kinesthetic plus tilting-plate stimulus using his right index finger. Image taken with permission from Yazdian et al. [2014] © 2014 IEEE.

4.4.3.3 Experiment Task

The participant's task was to compare the perceived compliance of pairs of reference and comparison stimuli (kinesthetic plus tilting-plate feedback vs. kinesthetic feedback only). The 2-alternative forced-choice experiment design, along with the method of constant stimuli [Gescheider 1997], was utilized to quantify the effect of tilting-plate feedback on perceived compliance.

The experiment was divided into three subexperiments, each conducted at a different level of reference kinesthetic stiffness (i.e., 60, 400, and 1600 deg/N). The participants were divided into three groups of 10 individuals and each group was assigned to a subexperiment. In each subexperiment, the participants compared the compliance of each of the three reference stimuli with the compliance of all nine corresponding comparison stimuli (see Table 4.1). Each comparison pair repeated 20 times, resulting in 540 total trials per subexperiment. The order of presenting all 540 trials was random and was the same for all the participants within a group.

In each trial, the participants perceived the compliance of two surfaces in sequence and identified whether the first or the second stimulus was perceived more compliant. The order of presenting reference and comparison stimuli was random but balanced. No information regarding the type of stimulus was released to the participants and they were not informed about the correctness of their responses. The participants were not allowed to retest previous stimuli.

The participants had to completely break contact with the device interface before a new stimulus was presented to them. There were two reasons for this: (1) all stimuli started at the same initial height and (2) the potential biasing or distracting haptic cues, caused by sudden changes in either kinesthetic stiffness or tilting ratio, were eliminated.

To inform the participants when a stimulus was presented, visual and audio cues were provided.

On average, each participant spent about two hours completing the subexperiment. The subexperiments were broken into two identical sessions conducted on two different days to reduce the potential effect of muscle fatigue. During the test, participants could take a short break at any time.

4.5 Experimental Results and Discussion

4.5.1 Psychometric Curve Function and Point of Subjective Equality

For each participant, the percentage of the time a comparison stimulus was perceived more compliant than a reference stimulus was computed. The percentages were plotted against the kinesthetic stiffness of the comparison stimuli. Using Probit regression analysis in SAS, three cumulative Gaussian psychometric functions [Gescheider 1997] were fit to data points to create psychometric curves for each participant. For example, Figure 4.4 shows a participant's psychometric curves for reference stimuli with the kinesthetic stiffness of 60 deg/N and the tilting ratios of 8.33, 16.67, and 33.33 deg/N. For this participant, the comparison stimulus with 20 N/m kinesthetic stiffness was perceived as more compliant than all three reference stimuli more than 90% of the time. However, the comparison stimuli with kinesthetic stiffness levels above 80 N/m were perceived to be less compliant than the reference stimuli all the time.

The kinesthetic stiffness corresponding to the 50% response level estimates the Point of Subjective Equality (PSE) between the compliance of reference and comparison stimuli. For the example curves of one participant in Figure 4.4, the PSEs for tilting ratios of 8.33, 16.67, and 33.33 deg/N are ~53, 47, and 33 N/m, respectively. This means that

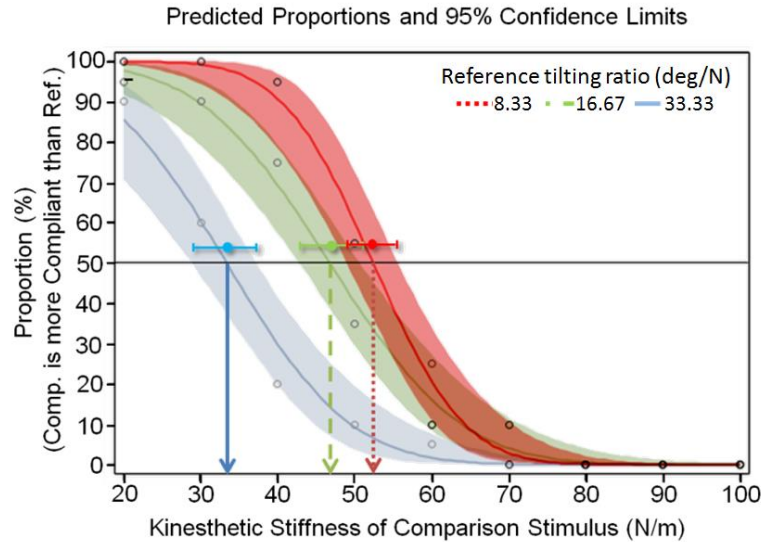


Figure 4.4. A participant's psychometric curves for reference stimuli with the kinesthetic stiffness of 60 deg/N and the tilting ratios of 8.33, 16.67, and 33.33 deg/N (i.e., 5, 10, 20 deg/cm). Image taken with permission from Yazdian et al. [2014] © 2014 IEEE.

tilting-plate feedback reduces the perceived compliance. For example, the perceived compliance of a surface with 8.33 deg/N tilting ratio and 60 N/m kinesthetic stiffness would be the same as the perceived compliance of a pure kinesthetic surface with 53 N/m kinesthetic stiffness.

The mean and 95% confidence intervals of PSEs of all participants for all 9 reference stimuli conditions (3 tilting ratios \times 3 kinesthetic stiffness levels) were obtained (Figure 4.5). All mean PSEs are significantly lower than the kinesthetic stiffness of their corresponding reference stimuli (t-tests [$t(9) > 27.26$, $p < 0.001$]). In addition, as tilting ratio increases the perceived compliance of surface increases. At the 60 N/m reference kinesthetic stiffness, the mean PSEs (across all participants) are 57, 51, and 43 N/m for tilting ratios of 8.33, 16.67, and 33.33 deg/N, respectively. At the 400 N/m reference kinesthetic stiffness, the mean PSEs are 306, 260, and 211 N/m for tilting ratios of 4, 8, and 16 deg/N, respectively. At the 1600 N/m reference kinesthetic stiffness, the mean

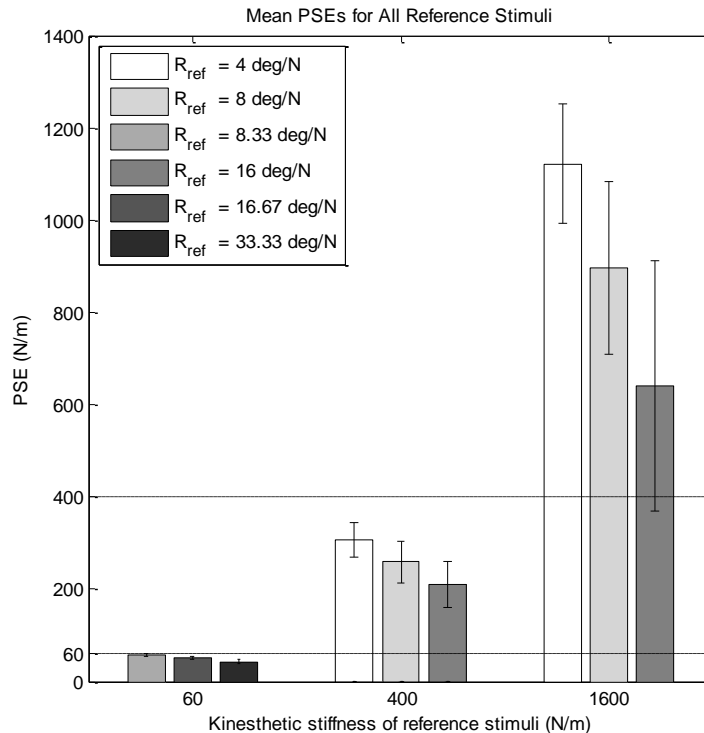


Figure 4.5. The average of mean PSEs for all participants of each reference kinesthetic stiffness group. The same tilting rates were used with the references at 400 and 1600 N/m. Error bars indicate 95% confident intervals. All PSEs are significantly lower than the kinesthetic stiffness of their corresponding reference stimuli—i.e., tilting-plate feedback decreases perceived stiffness. The amount of reduction in stiffness is greater at higher reference kinesthetic stiffness level.

PSEs are 1122, 896, and 641 N/m for tilting ratios of 4, 8, and 16 deg/N, respectively.

4.5.2 Linear Regression Models

Linear regression models were used to estimate the perceived stiffness of tilting-plate feedback at tilting ratios other than those used for the reference stimuli. At 60 N/m reference kinesthetic stiffness, there is a very strong negative and significant linear correlation between the tilting ratio and the PSEs [Pearson $R^2 = 0.67$, $F(1, 28) = 53.78$, $p < 0.0001$] (Figure 4.6). The kinesthetic stiffness of a surface with a tilting ratio between 8.33 and 33.33 deg/N can be estimated by Equation (4.3). At 60 N/m reference

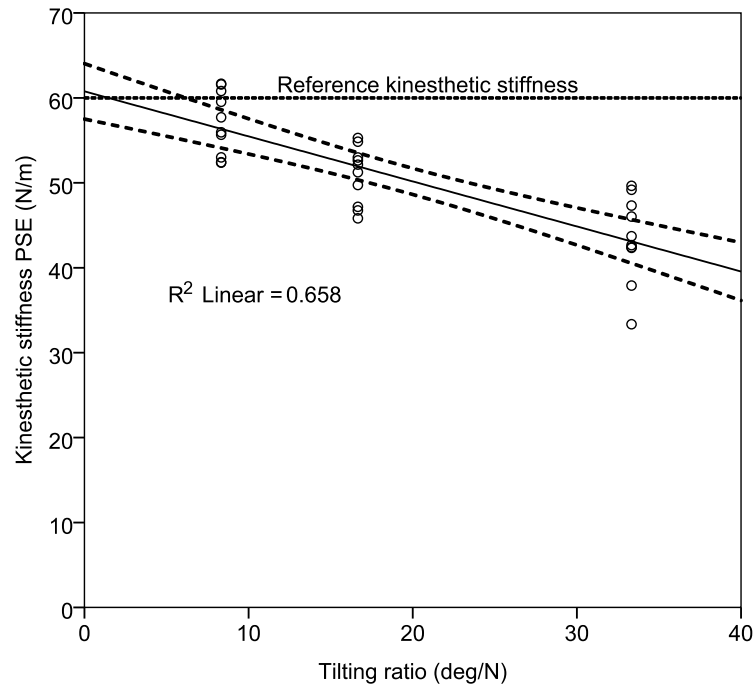


Figure 4.6. Very strong negative linear correlation between kinesthetic stiffness PSE and tilting ratio of reference stimuli with 60 N/m kinesthetic stiffness (dotted line). The dashed curves indicate 95% confidence intervals.

kinesthetic stiffness, there is ~ 0.53 N/m reduction in the perceived stiffness per unit change in tilting ratio.

$$\widehat{PSE} = -0.53 R + 60.77 \quad (4.3)$$

At 400 N/m reference kinesthetic stiffness, there is a strong negative and significant linear correlation between the tilting ratio and the PSEs [Pearson $R^2 = 0.41$, $F(1, 28) = 19.69$, $p < 0.0001$] (Figure 4.7). The kinesthetic compliance of a surface with tilting ratio between 4 and 16 deg/N can be estimated by Equation (4.4). At 400 N/m reference kinesthetic stiffness level, there is ~ 7.87 N/m reductions in the perceived stiffness per unit change in tilting ratio.

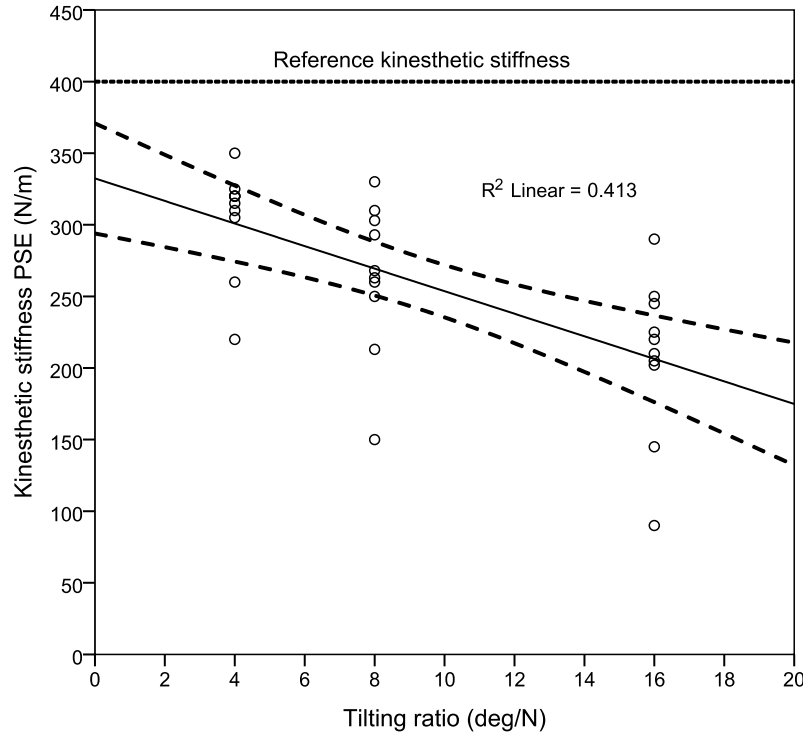


Figure 4.7. Strong negative linear correlation between kinesthetic stiffness PSE and tilting ratio of reference stimuli with 400 N/m kinesthetic stiffness (dotted line). The dashed curves indicate 95% confidence intervals.

$$\widehat{PSE} = -7.87 R + 332.40 \quad (4.4)$$

At 1600 N/m reference kinesthetic stiffness, there is a strong negative and significant linear correlation between the tilting ratio and the PSEs [Pearson $R^2 = 0.43$, $F(1, 22) = 16.35$, $p = 0.001$] (Figure 4.8). The kinesthetic compliance of a surface with a tilting ratio between 4 and 16 deg/N can be estimated by Equation (4.5). At 1600 N/m reference kinesthetic stiffness, there is ~ 38.94 N/m reduction in the perceived stiffness per unit change in tilting ratio in terms of deg/N.

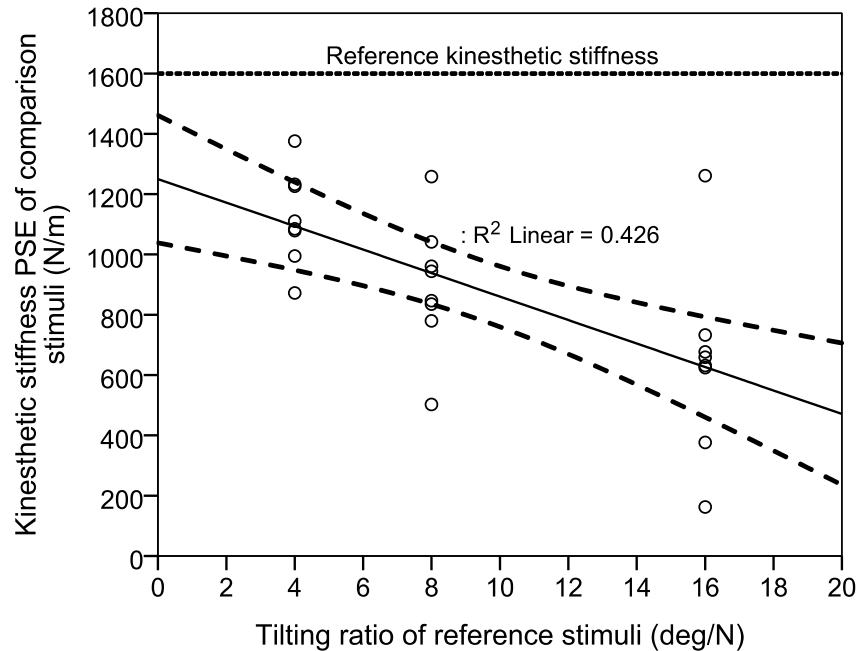


Figure 4.8. Strong negative linear correlation between kinesthetic stiffness PSE and tilting ratio of reference stimuli with 1600 N/m kinesthetic stiffness (dotted line). The dashed curves indicate 95% confidence intervals.

$$\widehat{SE} = -38.94 R + 1249.72 \quad (4.5)$$

Comparing the correlation coefficients across different reference kinesthetic stiffness levels shows that tilting-plate feedback has higher softening effect at higher reference kinesthetic stiffness levels.

4.6 Experiment Conclusions

A simple and compact tactile compliance display device using the tilting-plate concept was developed. The device was integrated with a force-feedback system to provide both kinesthetic and tactile information for replicating the softness sensation of both deformable and nondeformable objects. In this chapter, the capability of the tilting-plate feedback in modulating perceived compliance of kinesthetically rendered surfaces

was investigated.

In the compliance discrimination experiment, the participants compared the compliance of pure kinesthetic feedback with the compliance of kinesthetic plus tilting-plate feedback. The results of the experiment support the stated hypothesis: increasing tilting ratio decreases perceived stiffness. This correlation was very strong and significant at different levels of the reference kinesthetic stiffness (60, 400, and 1600 N/m). On average at 60, 400, and 1600 N/m reference kinesthetic stiffness, there are ~ 0.53 , 7.87, and 38.94 N/m reductions in the perceived stiffness per unit change in tilting ratio in terms of deg/N, respectively.

The following chapters further investigate the capabilities of tilting-plate feedback for substituting for kinesthetic-force feedback (Chapter 5) and real deformable compliant objects (Chapter 6), the difference between tilt-up and tilt-down feedback (Chapter 7), and the effect of tilting-plate feedback in pinch grasp (Chapter 8). A list of all possible experiments along with their benefits and drawbacks is provided in the Appendix.

CHAPTER 5

PURE TILTING-PLATE FEEDBACK AS A SUBSTITUTE FOR KINESTHETIC COMPLIANCE INFORMATION

5.1 Overview

Compared to kinesthetic-force feedback, tactile feedback has more contribution in perception of compliance [Bergmann Tiest and Kappers 2008; Scilingo et al. 2010; Srinivasan and LaMotte 1995]. This chapter investigates whether pure tactile information provided by a standalone tilting-plate device can substitute for compliance information of a pure kinesthetic surface. A human-subject experiment was conducted to test this feedback substitution. The results of the experiment revealed a negative linear correlation between the tilting ratio and perceived kinesthetic stiffness. Having this correlation, one can substitute a compact, simple, and low-power-consumption tilting-plate device for a large and high-power kinesthetic-force-feedback system for rendering compliance information.

5.2 Device Description

The integrated compliance display device introduced in Section 4.2 displays both tactile and kinesthetic information at the same time. To disregard kinesthetic information and render pure tilting-plate feedback, a similar tilting-plate unit was fabricated and

mounted on a force sensor (Omega LCAE-2KG) instead of the Haptic Paddle arm. Figure 5.1 shows the standalone tilting-plate compliance display device. The force sensor measures finger force while gross displacement of the finger is prevented by the rigid structure of the system. The force signal is amplified by an instrumentation amplifier (Analog Devices Inc. AD623AN) and is sent to the microcontroller (Microchip dsPIC 33EP256MU806). The microcontroller commands the servomotors (Futaba S3156) to tilt the plates based on contact force and desired tilting ratio (Equation (4.1)). Each plate is positioned with a tilt angle resolution of less than 0.1 degrees at an update rate of 500 Hz. This standalone tilting-plate device can measure up to 22 N of force with a resolution of 8.85 mN.

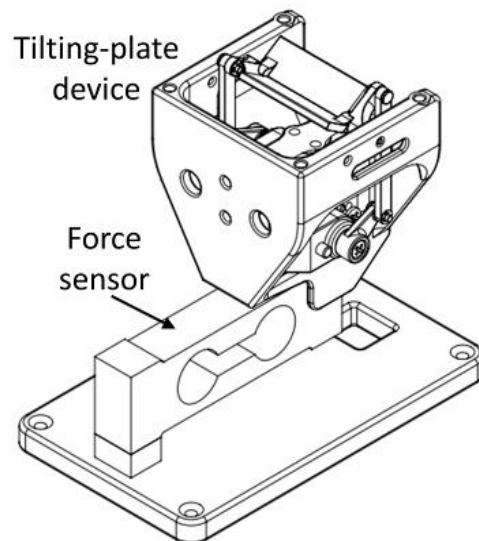


Figure 5.1. A standalone tilting-plate compliance display device.

5.3 Methods: Pure Tilting-plate Feedback vs. Pure Force Feedback

5.3.1 Participants

A total of 12 participants (3 females, 2 left-handed) aged from 22 to 34 years (mean 26 years old) were recruited for this experiment. The participants had no known abnormalities in their index fingers. Before the experiment, they were informed about the experiment procedures and signed informed consent forms in accordance with the University of Utah's Institutional Review Board (IRB) policy.

5.3.2 Stimuli

Reference stimuli were pure kinesthetic surfaces with kinesthetic stiffness levels of 200, 400, 800, and 1600 N/m (between 0.625 and 5 mm/N in terms of compliance). The integrated compliance display device (described in Section 4.2) with zero tilting ratio was used to render reference kinesthetic stimuli. This was done so that participants would be pressing on the same tilting plate surface on both devices. The result of a pilot study showed that kinesthetic stiffness values lower than 120 N/m cannot be rendered by the standalone tilting plate-device because of unrealistic surface deformations at high tilting ratios (> 45 deg/N). As such, comparison stimuli during the experiment were rendered by the pure tilting-plate device with tilting ratios between zero and 20 deg/N. Furthermore, the maximum relative tilt between the plates was limited to 45 degrees.

5.3.3 Procedures

The 1-up 1-down adaptive staircase method [Levitt 1971] was used to find the tilting ratio (PSE) at which the compliance of pure tilting-plate feedback (comparison stimulus)

was perceived as equal to the compliance of a pure kinesthetic surface (reference stimulus).

The experiment was split into two sessions, each with different hand-device configuration and conducted on a different day. The participants sat in front of the test apparatus (Figure 5.2). Their right and left hands were placed on two adjustable wrist supports. Their right and left index fingers were placed above the haptic devices. To eliminate the effect of handedness, the position of the devices was swapped in the second session.

Each session was divided into four conditions, each presenting a different reference kinesthetic stiffness. A 4×4 Latin Square was used to present different reference stimuli in a different order across all participants. Each session was accomplished in two runs: one ascending run and one descending run. In the ascending runs, the tilting ratio of comparison stimuli was set to zero, well below estimated PSE. In the descending runs,

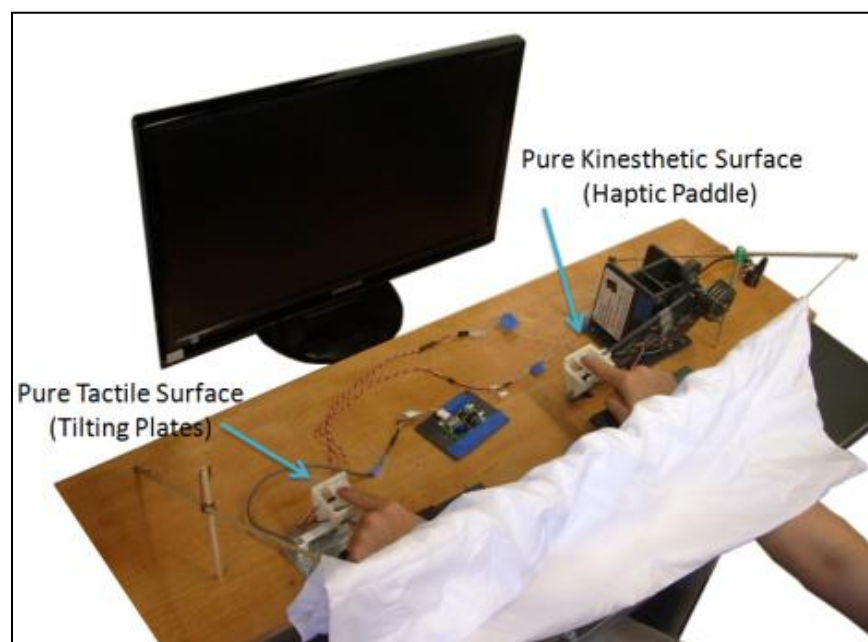


Figure 5.2. Experiment Setup. A participant is comparing the compliance of tilting-plate feedback with the compliance of pure kinesthetic feedback.

the tilting ratio of comparison stimuli was set to a high value; i.e., 35, 30, 15, and 10 deg/N for reference kinesthetic stiffness values of 200, 400, 800, and 1600 deg/N, respectively. The presentation order of ascending and descending runs was balanced both within and between participants.

In each trial, the participants compared the compliance of a reference stimulus using the index finger of one hand with the compliance of a comparison stimulus using the index finger of the contralateral hand. Using two foot pedals, they indicated which surface was perceived as the more compliant surface. If the participants selected the comparison stimulus as the more compliant (or less compliant) surface, its tilting ratio was decreased (or increased) by a specific step size to make the task more difficult to discriminate in the next trial comparison. The initial tilting ratio step size was 5 deg/N and was reduced to 2.5 and then to 0.5 deg/N after the first and the fourth reversals.

The experiment terminated after 10 total reversals. The arithmetic mean of comparison tilting ratios in the six last reversals of each run was considered as the PSE of that run. Four PSEs (2 ascending and descending runs \times 2 hand-device configurations) were averaged to compute the PSE for each condition.

During the experiment, the participants' hands and the test apparatus were covered with a cloth screen to prevent any visual cues from affecting their compliance judgment. The participants wore noise cancelling headphones to mask audio cues from the device. Before each trial, a proctor aligned the position of their fingers with the center of the tilting-plate interfaces, guaranteeing proper symmetrical tactile feedback. Before the experiment, a short training using foam blocks was provided for the participant (see Section 4.4.3.1).

5.4 Experimental Results and Discussion

Figure 5.3 shows a participant's typical responses through ascending and descending runs. At higher reference kinesthetic stiffness, lower tilting ratio was required to match the compliance of the two stimuli type. For each participant, the total PSE at each condition is computed based on the average of ascending and descending PSEs of both hand-device configurations.

Figure 5.4 shows the means and 95% confidence intervals of PSEs at a different reference kinesthetic stiffness and hand-device configuration across all participants. A two-way repeated measured analysis of variance (ANOVA) revealed significant effects of (1) reference kinesthetic stiffness [$F(3, 19) = 13.10, p < 0.01$]; (2) hand-device

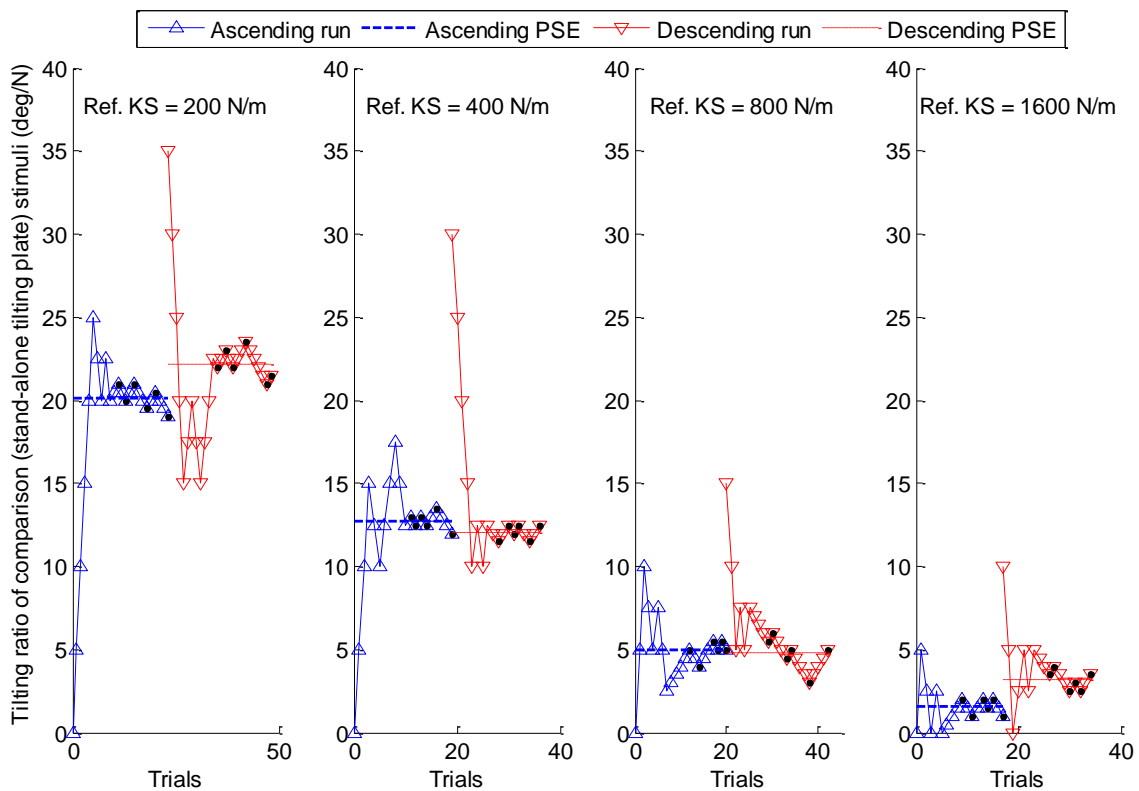


Figure 5.3. An example of a participant's response through ascending and descending runs at different reference kinesthetic stiffness levels. The small dots indicate the last six reversals.

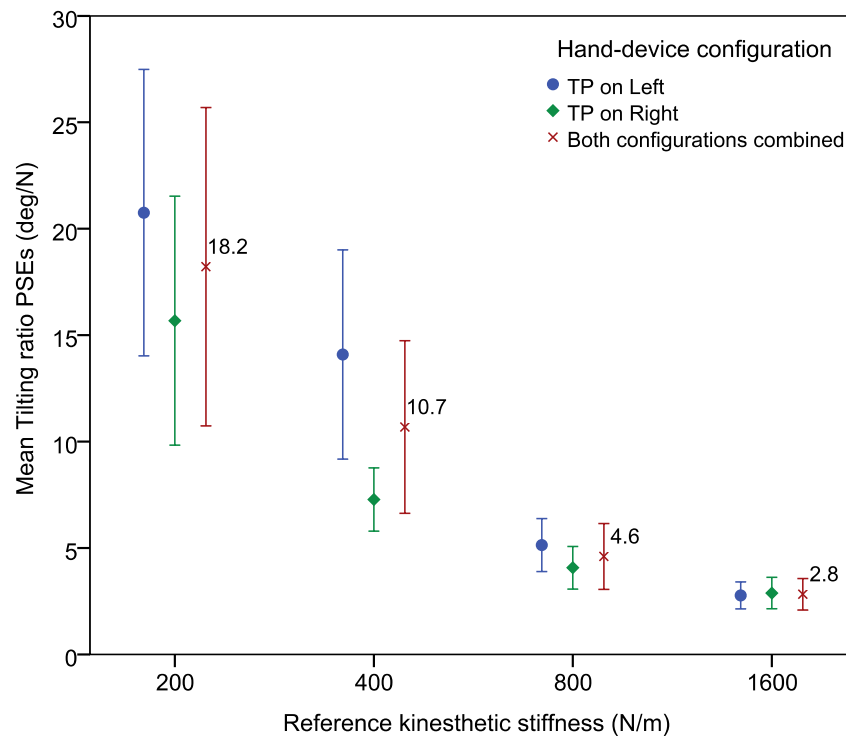


Figure 5.4. The means and 95% confidence intervals of tilting ratio PSEs at different reference kinesthetic stiffness and hand–device configurations.

configuration [$F(1, 21) = 8.68, p < 0.01$]; and (3) interaction between kinesthetic stiffness and hand-device configurations [$F(3, 19) = 5.52, p < 0.01$] on the PSE.

The mean PSEs for reference kinesthetic stiffness of 200, 400, 800, and 1600 N/m are 18.2, 10.7, 4.6, 2.8 deg/N, respectively. Post-hoc comparisons using Bonferroni's method indicated that each pairwise difference among these PSE means was significant [$p < 0.01$]. This suggests that as the tilting ratio of a standalone tilting-plate device decreases, its equivalent perceived kinesthetic stiffness increases.

Comparing the mean PSEs between the hand-device configurations, the PSE for tilting-plate feedback on the right index finger is lower than the PSE for tilting-plate feedback on the left index finger. Although this effect is not statistically significant, it suggests that the same tilting-plate feedback is likely perceived as more compliant on the right index finger than on the left index finger (Figure 5.5). It was found that this trend

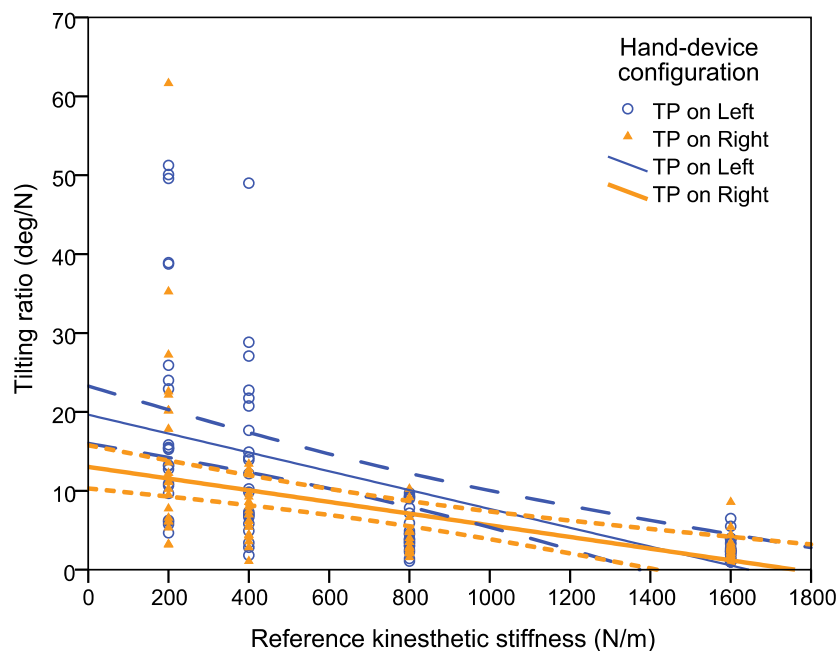


Figure 5.5. Correlation between tilting ratio and perceived kinesthetic stiffness for different hand-device configurations. Dashed lines indicate 95% confidence intervals.

holds for ~58% of the right-handed participants and 50% (one individual) of the left-handed participants. An opposite trend was found for ~16% of the right-handed participants and 50% of left-handed participants. No specific trend was found for 25% of the right-handed participants.

The lower PSE for tilting-plate feedback on the right index finger might be because of (1) the better force and/or motion control of the right index finger compared to the left index finger due to more interactively dexterous skills of the right index finger for right handed individuals (cortical plasticity), or (2) richer tactile information provided by mechanoreceptors of the right index finger.

The linear correlations between tilting ratio and perceived kinesthetic stiffness (Equations (5.1) and (5.2)) were significant for both hand-device configurations [Pearson $R^2 = 0.30$, $F(1, 86) = 36.25$, $p < 0.001$ for tilting-plate feedback on the left index finger configuration and Pearson $R^2 = 0.22$, $F(1, 86) = 24.51$, $p < 0.001$ for tilting-plate

feedback on the left index finger configuration].

$$\widehat{PSE} = -0.012 K + 19.64 \text{ (TP on left)} \quad (5.1)$$

$$\widehat{PSE} = -0.007 K + 13.03 \text{ (TP on right)} \quad (5.2)$$

5.5 Experiment Conclusions

The result of the compliance discrimination experiment indicated that the standalone tilting-plate device can be used as a substitute for large kinesthetic-force-feedback devices for rendering compliance information. A strong and significant linear correlation between tilting ratio and perceived kinesthetic stiffness was found. As the tilting ratio increases, the perceived kinesthetic stiffness decreases. For example, the tilting ratios of 2.8 and 18.2 deg/N are mapped to kinesthetic stiffness levels of ~1600 and ~200 deg/N, respectively.

The comparison between the PSEs of both hand-device configurations showed that tilting-plate feedback on right index finger was likely perceived as more compliant than the same tilting-plate feedback on left index finger. The result of regression models suggest that there are ~83 and ~143 N/m reduction in perceived kinesthetic stiffness per unit change of tilting ratio when tilting-plate feedback is provided to left and right index finger, respectively.

CHAPTER 6

TILTING-PLATE FEEDBACK VS. REAL MATERIALS

6.1 Overview

This chapter investigates whether pure tilting-plate feedback can reproduce the compliance of real materials. A compliance discrimination experiment was conducted to quantify the relation between tilting ratio and perceived compliance of silicone rubber specimens as real materials.

6.2 Selection of Real Materials

Many different options can be considered for use as real materials for this experiment; however, the criteria dictated by the experiment design narrow down the selection. A suitable real material should (1) have quantifiable properties for direct comparison with future studies, (2) provide a wide range of compliance levels similar to those of biological tissues (one of the assumed best use-cases for the developed tactile display), (3) possess low hysteresis, and (4) possess homogenous properties. For example, standard biological tissue phantoms, which are widely used in medical training, are an ideal but expensive option. An inflated membrane with variable air pressure is another option that can provide continuous compliance levels. However, the main drawback of this option is that the membrane would have different surface curvature at

different air pressure levels. For the conducted experiment, it was decided to cast silicone rubber specimens. Further explanation is provided in the following section.

6.3 Silicone Rubber Specimens

For the compliance discrimination experiment, three different silicone rubber specimens (SR1, SR2, and SR3) were cast using Smooth-on's EcoFlex 10, EcoFlex 30, and Dragon Skin 10 materials. Each specimen was cast with 50 grams of Part A and 50 grams of Part B in a muffin tray. The specimens had the same geometry with height, base diameter, and face diameter of ~28, 70, and 52 mm, respectively (Figure 6.1).

The force-displacement characteristics of specimens were obtained using a spherical probe 15 mm in diameter seven days after the silicone specimens were cast (Figure 6.2). The probe was attached to the extended arm of the Haptic Paddle to measure displacement through the encoder of the Haptic Paddle, and the specimens were placed on a force sensor to measure applied force. The average kinesthetic stiffness values of the specimens are 540, 940, and 1514 N/m (Table 6.1).

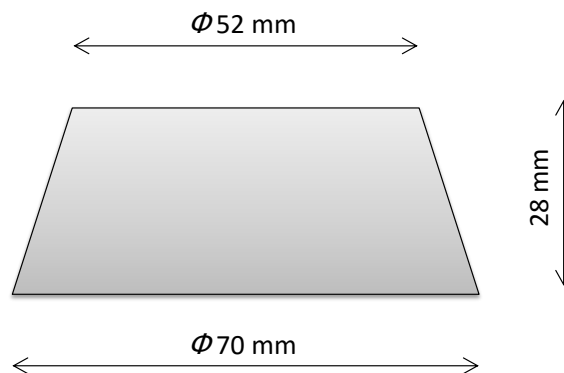


Figure 6.1. Dimensions of the silicone rubber specimens cast in a conical muffin tray.

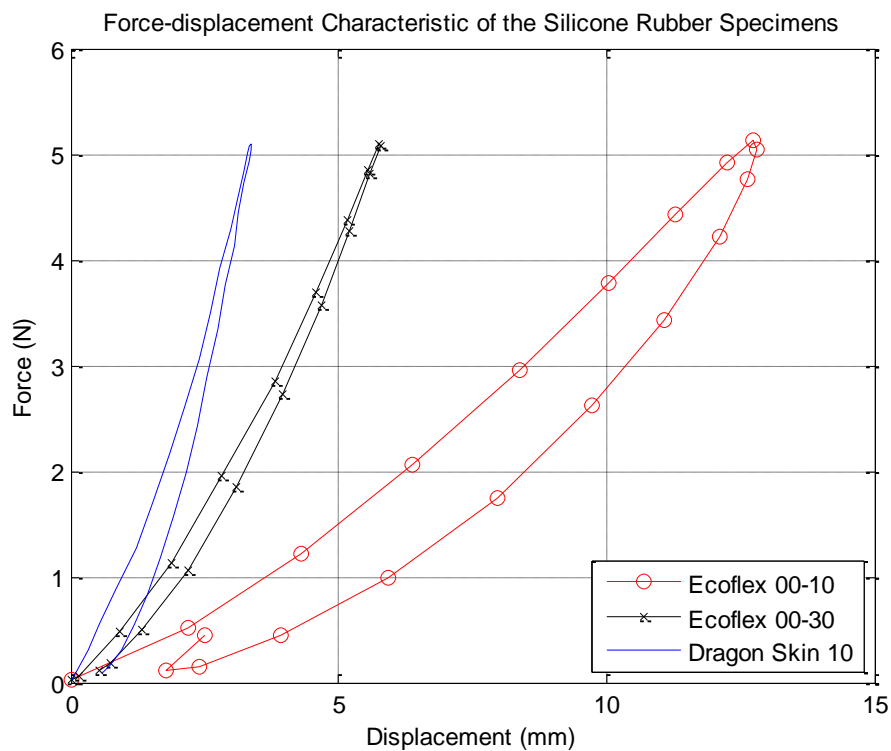


Figure 6.2. Force-displacement characteristics of the silicone rubber specimens.

Table 6.1. Kinesthetic stiffness of silicone rubber specimens.

Specimen	Material	Average Kinesthetic Stiffness (N/m)
SR1	Ecoflex 0010	540
SR2	Ecoflex 0030	940
SR3	Dragon Skin 10	1514

6.4 Device Description

The standalone tilting-plate device was used to display the compliance of a virtual surface (see Section 5.2 for more details). For each trial of the experiment, a silicone rubber specimen was placed on a force sensor (Omega LCAE-2KG) to measure the contact force.

6.5 Methods: Tilting-plate Feedback vs.

Silicon Rubber Specimens

6.5.1 Participants

A total of 10 participants (5 female, all right-handed) aged from 19 to 30 years (mean 25 years old) were recruited for this experiment. The participants had no known abnormalities in their index fingers. Before the experiment, they were informed about the experiment procedures and signed informed consent forms in accordance with the University of Utah's Institutional Review Board (IRB) policy.

6.5.2 Stimuli

Silicone rubber specimens with three different compliance levels of 540, 940, and 1514 N/m (Table 6.1) were selected as reference stimuli. Pure tilting-plate feedback with tilting ratios between zero and 20 deg/N were chosen as comparison stimuli. To match the texture and thermal property of all surfaces, the surfaces of the specimens as well as the tilting-plate device were covered by a ~0.15 m-thick cloth.

6.5.3 Procedures

Figure 6.3 shows the setup of the experiment. The participants' hands were placed on two wrist supports and their index fingers were positioned above the interface of the tilting-plate device and the top face of a given silicone rubber specimen. The entire test apparatus and the participants' hands were covered by a cloth to prevent any visual cues from affecting their compliance judgment. The participants wore noise cancelling headphones which blocked background noise and played audio cues indicating when a stimulus was ready to be examined.

Using an adaptive 1-up 1-down staircase method [Levitt 1971], the participants compared the compliance of pairs of reference-comparison stimuli. The experiment was split into two sessions on different days, each with a different hand-device configuration: (1) tilting-plate device on left index finger and (2) tilting-plate device on right index

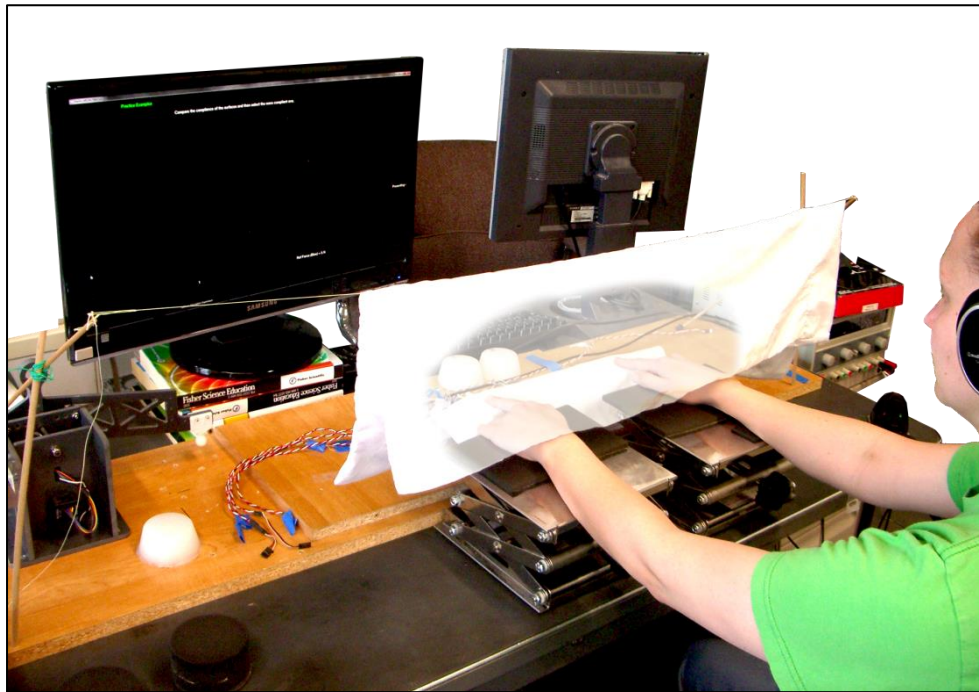


Figure 6.3. Experiment setup: a participant compares the compliance of a silicone rubber specimen and tilting-plate feedback.

finger. The order of presenting hand-device configurations was balanced across all participants. The experiment was divided into three conditions, each deploying a different silicone rubber specimen. A 3×3 Latin Square was used to present different specimens in different orders across all participants. Each condition was accomplished in two runs: one ascending run and one descending run. In the ascending runs, the tilting ratio of comparison stimuli was set to zero, well below estimated PSE. In the descending runs, the tilting ratio of comparison stimuli was set to a high value (i.e., 10, 8, and 6 deg/N for reference stimuli with 540, 940, and 1514 deg/N kinesthetic stiffness, respectively). The presentation order of ascending and descending runs was balanced both within and between participants.

In each trial, the participants perceived the compliance of a reference and a comparison stimulus at the same time. Using two foot pedals, they indicated whether the left or right stimulus was perceived to be more compliant. If the participants selected the comparison stimulus as the more compliant (or less compliant) surface, its tilting ratio was decreased (or increased) by a specific step size to make the task more difficult for the next trial comparison. The initial tilting ratio step size was 0.5, 0.5, and 1.0 deg/N for SR1 (softest), SR2, and SR3 (stiffest) specimens, respectively. After the first and the fourth reversals the step size was reduced by half each time. The experiment terminated after 10 total reversals and the PSEs were computed based on the average of tilt-down tilting ratios in the last six reversals. There were four PSEs per condition.

Participants were asked to break contact with the specimen and the device interface before responding with their answers and proceeding to the next trial. A minimum contact force of 0.25 N was required to ensure that participants made contact with a surface before entering their answers. A warning feedback message on the screen

informed participants to reduce their applied forces on both surfaces when either tilt angle exceeded 75% of maximum allowable tilt range or contact force exceeded 5.0 N.

Prior to the actual experiment, a short practice session helped participants become familiar with the experiment procedure (see Section 4.4.3.1).

6.6 Experimental Results and Discussion

Figure 6.4 shows the means and 95% confidence intervals of PSE for different silicone rubber specimens and hand-device configurations across all participants. For example, for tilting-plate feedback on right index finger, the mean PSEs for SR1, SR2, and SR3 are 5.87, 3.06, and 1.28 deg/N, respectively.

The comparison between the PSEs of both hand-device configurations showed that tilting-plate feedback on the right index finger was likely perceived as more compliant

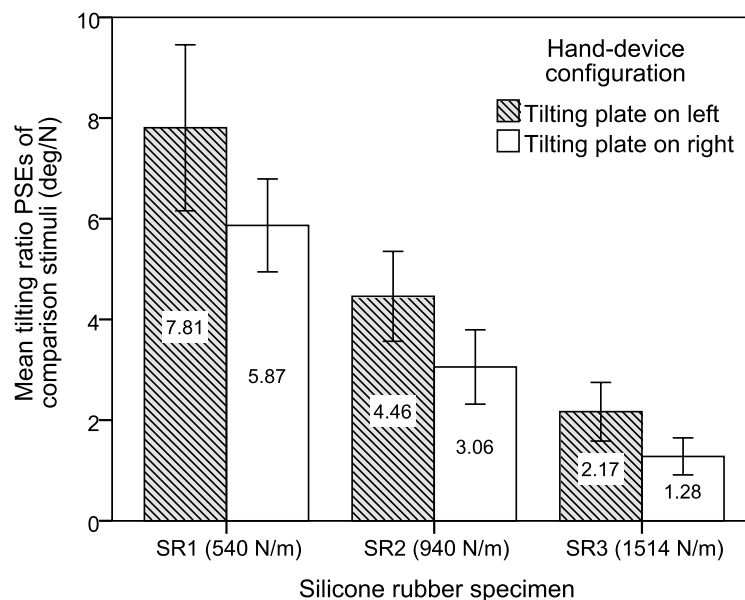


Figure 6.4. The means and 95% confidence intervals of tilting ratio PSEs of all participants for different silicone rubber (SR) specimens and hand-device configurations. The higher the kinesthetic stiffness of the silicone rubber, the lower the mean PSE of tilting-plate feedback. A higher tilting ratio on left index finger than right index finger is required to reproduce the compliance of a real object.

than the same tilting-plate feedback on the left index finger (Figure 6.5). This is in agreement with the observations in the prior experiment (see Section 5.4). The linear correlations between tilting ratio and the kinesthetic stiffness of silicone rubbers (Equations (6.1) and (6.2)) were significant for both hand-device configurations [Pearson $R^2 = 0.47$, $F(1, 58) = 51.20$, $p < 0.001$ for tilting-plate feedback on the left index finger configuration and Pearson $R^2 = 0.58$, $F(1, 58) = 81.64$, $p < 0.001$ for tilting-plate feedback on the right index finger configuration]. This hand-device effect is consistent with the results obtained in Section 5.4.

$$\widehat{PSE} = -0.006 K + 10.64 \text{ (TP on left)} \quad (6.1)$$

$$\widehat{PSE} = -0.005 K + 7.99 \text{ (TP on right)} \quad (6.2)$$

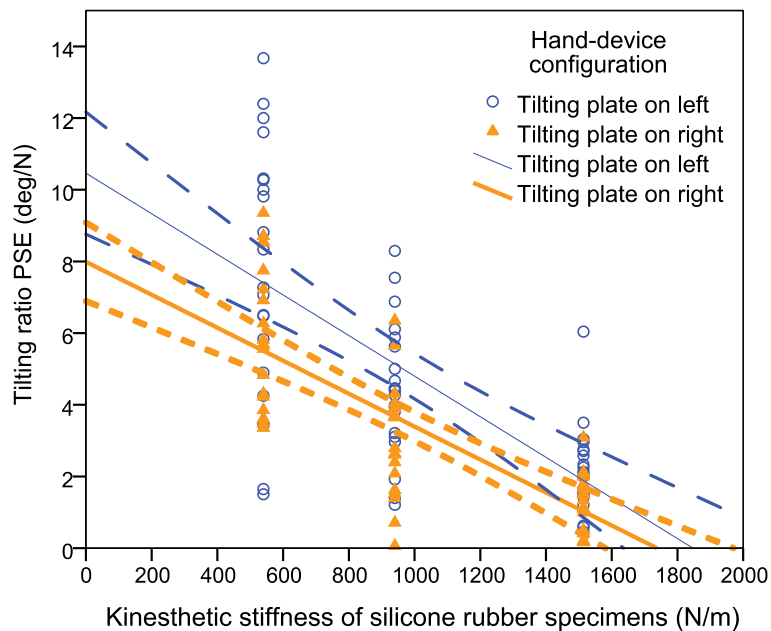


Figure 6.5. Linear correlations between the tilting ratio PSE and the kinesthetic stiffness of the silicone rubber specimens for each hand-device configurations. At the same tilting ratio, tilting-plate feedback represents the compliance of a softer silicone rubber when it is provided to the right index finger than the left index finger.

Whether there were differences in the manner in which participants explored the “real” vs. the simulated tilting-plate stimuli was also investigated. Although there are similarities, the analysis below shows subtle differences. Figure 6.6 shows the profile of contact forces that a participant applied on both the tilting-plate device and SR1 (silicone rubber specimen with 540 N/m kinesthetic stiffness) in an ascending run. It seems that the contact forces of the participant decreased over time on both surfaces. This reduction in applied force might be because of reduction in the compliance of tilting-plate feedback through time. In the first few trials, the tilting ratio of tilting-plate feedback was close to zero and in the last few trials the ratio was close to the participants’ PSE.

Comparing the force profile across participants revealed that they had different

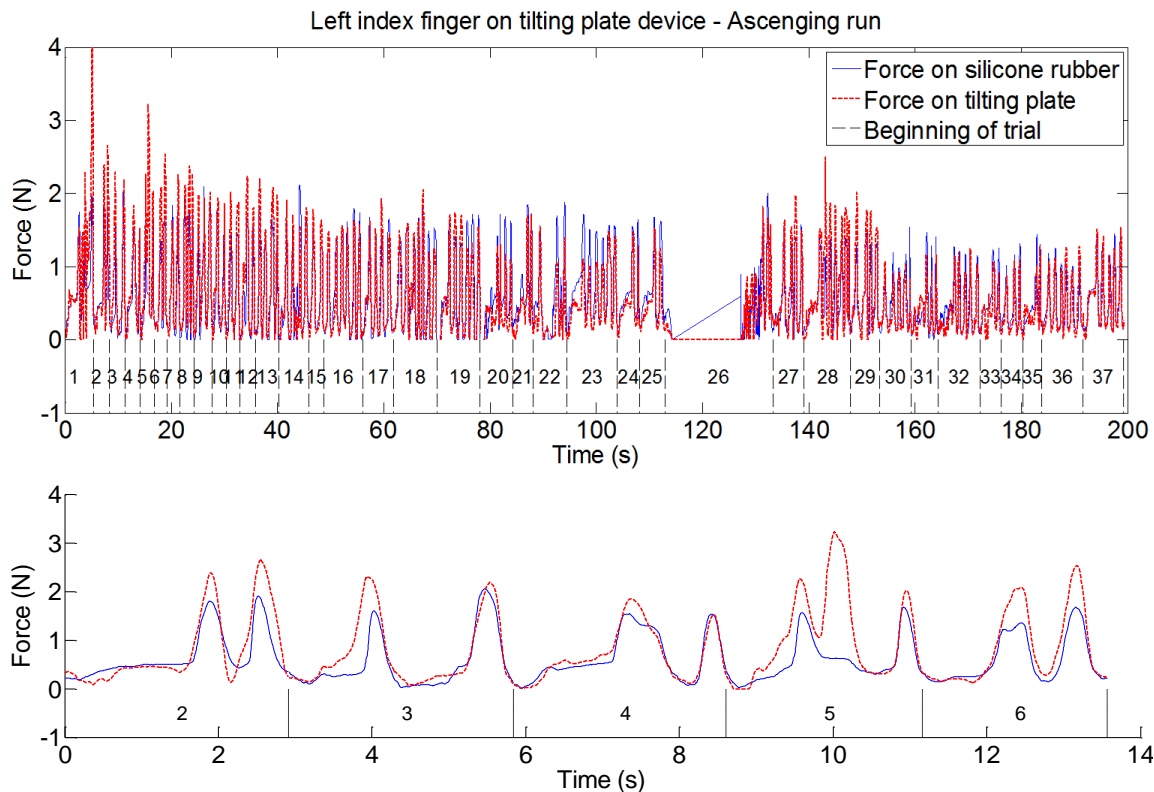


Figure 6.6. An example of contact force profile for an ascending run: (Top) all trials of the entire run and (bottom) inset area for the few first trials.

approaches for comparing the compliance of given surfaces. Some participants tended to apply synchronized forces on both surface types whereas others applied forces to the two stimuli almost 180 out of phase (Figure 6.6 bottom).

Figure 6.7 shows the mean of maximum applied force of participants for different hand-device configurations, ascending/descending runs, and kinesthetic stiffness levels of the silicone rubber specimens. The results of a multiway ANOVA show that the kinesthetic stiffness of the silicone rubber specimens has a significant effect on the maximum applied force [$F(2, 4167) = 41.77, p < 0.01$]. When SR1 (softest), SR2, and SR3 (stiffest) were presented to the participants, they applied maximum forces of ~ 4.82 , 5.42 , and 5.37 N on both surface types regardless of hand-device configuration. Pairwise comparisons indicate that only the applied force on SR1 is significantly different from the

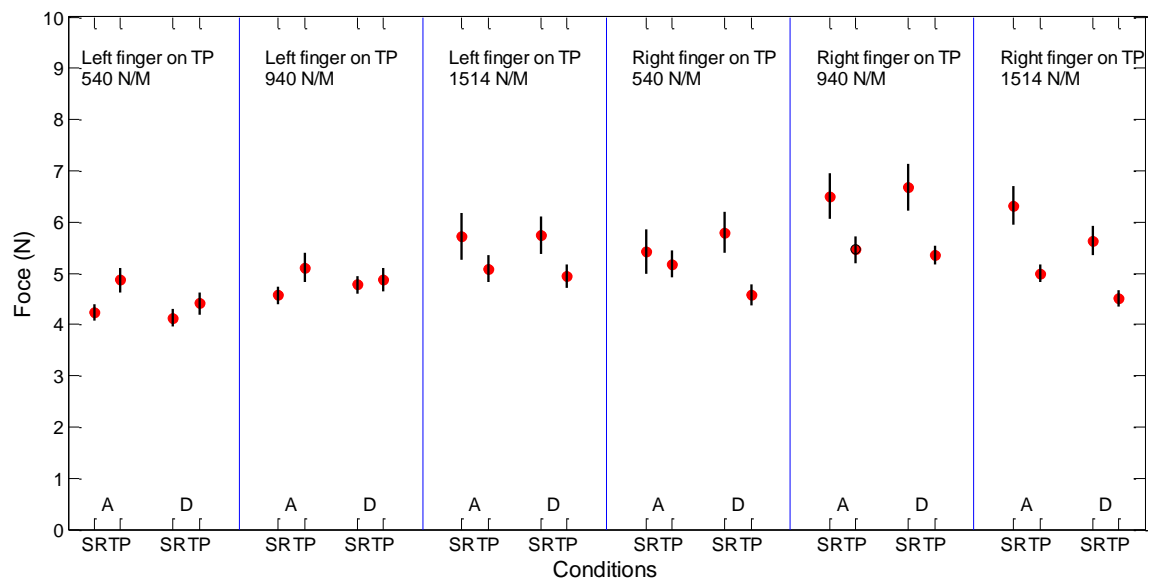


Figure 6.7. Means and 95% confidence intervals of maximum applied force on silicone rubber (SR) and tilting-plate (TP) surfaces for different hand-device configurations, ascending (A) and descending (D) runs, and different silicone rubber specimen with 540, 940, and 1514 N/m kinesthetic stiffness. The applied force on SR and TP surfaces are higher when a stiffer SR is presented. Also, more force is typically applied on both surfaces when TP surface is under the right index finger.

applied force on the other two. This suggests that the participants tended to apply more force on stiffer surfaces. The nonsignificant difference between the force applied to SR2 and SR3 might be because of two effects: (1) the ceiling effect due to the warning feedback presented to the participants when their applied force exceeded more than 5 N, or (2) the lower tilting ratio PSE SR3 (i.e., the plates move the finger up less, thus causing a lower interaction force (refer to Chapter 7 for more details)).

Additionally, hand-device configuration has a significant effect on the maximum applied force [$F(1, 4167) = 149.62, p < 0.01$]. When the tilting-plate feedback was presented to the left and right index fingers, the average maximum applied forces on both surface types were ~4.83 and 5.58 N, respectively. This difference may be due to more interactively dexterous skills of the index finger of the dominant hand in the compliance judgment of real materials (cortical plasticity) — i.e., the participants applied less force on the real specimens using their right index fingers than left index fingers and commanded roughly the same amount of force to their left index fingers on the tilting-plate device.

The result of ANOVA also showed that the surface type has a significant effect on maximum applied force [$F(1, 4167) = 52.42, p < 0.01$]. Regardless of hand-device configuration or silicone rubber kinesthetic stiffness, the participants applied a higher maximum force on the silicone rubber specimens (5.43 N) than the tilting-plate device (4.98 N).

The run type (ascending vs. descending) has a significant effect on maximum applied force [$F(1, 4167) = 5.18, p = 0.02$]. The average maximum applied force (regardless of other conditions) was 5.28 and 5.13 N in the ascending and descending runs, respectively. This is because the participants' tilting ratio PSEs in the ascending run were

generally lower (i.e., a stiffer surface) than the PSEs in the descending runs. Thus, the participants applied higher force on stiffer (lower tilting ratio) surfaces. However, this force difference is negligible (0.15 N), and it can be assumed that the participants applied relatively consistent maximum force on the surfaces with the same tilting-plate feedback regardless of the trial history of a run.

Further analysis shows that the interaction between the surface type and the hand-device configuration has a significant effect on the maximum applied force [$F(1, 4167) = 92.34, p < 0.01$]. Regardless of the kinesthetic stiffness of the silicone rubbers, the average maximum applied forces on the silicone rubber and tilting-plate surfaces were ~4.75 and 4.90 N when tilting-plate feedback was provided to the left finger and ~6.10 and 5.06 N when the tilting-plate feedback was rendered to the right index finger. These results indicate that the participants applied more force using their left index finger than their right index finger. In addition, this further supports the hypothesis that the right index finger has a better ability to judge the compliance information of tilting-plate feedback, such that the participants tended to less force on the device with their right index fingers than left index fingers.

6.7 Experiment Conclusion

This chapter investigated the capability of tilting-plate feedback in rendering the compliance information of real materials. Three homogenous silicone rubber specimens were cast as real materials. Through a human-subject experiment, a statistically significant linear correlation between the compliance of tilting-plate feedback and the silicone rubber specimens was obtained. Approximately for each unit increase in tilting-ratio, the equivalent kinesthetic stiffness of silicone rubber specimens decreases ~167

(~200 N/m) when tilting-plate surface is under to the left (right) index finger. The result of this experiment suggests that pure tilting-plate feedback may be used to portray the compliance of different real materials. For example, tilting-plate feedback could be utilized in robotic surgery applications to assist surgeons in distinguishing between the compliance of healthy biological tissues and tumors. However, more studies are required to assess the capability of the tilting-plate device in rendering the compliance of materials with nonlinear force-displacement and/or nonlinear force-area relationships.

CHAPTER 7

TILT-UP FEEDBACK VS. TILT-DOWN FEEDBACK

7.1 Overview

In the previous chapters, tilting-plate feedback was rendered using an upward tilting motion (tilt-up feedback). Experimental results showed that higher tilting ratios corresponded to more compliant surfaces (see Section 4.5, 5.4, and 6.6). This chapter investigates whether rendering a downward tilting motion (tilt-down feedback) may have the opposite effect and decrease the perceived compliance of the surface. To compare the compliance of tilt-up and tilt-down feedback, three main metrics were considered: the subjective perception of compliance, kinesthetic compliance, and contact area spread ratio.

7.2 General Methods

Five experiments (Experiments 7.1-7.5) were conducted to study the differences between tilt-up and tilt-down feedback. In Experiment 7.1, the perceived compliance of tilt-up feedback was compared to the perceived compliance of tilt-down feedback. In Experiment 7.2, kinesthetic force-displacement (stiffness) characteristic curves of these two feedback types were obtained. In Experiment 7.3, the equivalent kinesthetic stiffness

of tilt-up feedback in series with a spring was measured. Experiment 7.4 was conducted similarly to Experiment 7.1, except that the kinesthetic stiffness of the surface with tilt-up feedback was controlled to try to match or be less than that of tilt-down feedback. In Experiment 7.5, the contact widths (areas) of the two feedback types were characterized and a simple contact width spread ratio model was proposed for tilting-plate feedback.

7.3 Experiment 7.1: Preliminary Comparison between Tilt-up and Tilt-down Feedback

Since the compliance of a surface with tilt-up feedback increases as a function of tilting ratio, it was hypothesized that a surface with tilt-down feedback would be perceived as less compliant (stiffer) than a surface with tilt-up feedback when using the same tilting ratio magnitude. The goal of Experiment 7.1 was to test this hypothesis.

7.3.1 Participants

Eight participants (two females, one left handed) aged from 20 to 32 years (mean 27 years old) participated in this experiment. The participants had no known abnormalities in their index fingers. Before the experiment, they were informed about the experiment procedures and signed informed consent forms in accordance with the University of Utah's Institutional Review Board (IRB) policy.

7.3.2 Device

The device used in this experiment was identical to the tilting-plate device described in Section 5.2.

7.3.3 Stimuli

Two types of stimuli (reference and comparison stimuli) were used for this experiment. The reference stimuli rendered tilt-up feedback and the comparison stimuli rendered tilt-down feedback (see Figure 7.1). Prior to contact, the device interface was flat for tilt-up and V-shaped for tilt-down feedback. At the end of tilt motion, the device interface was V-shaped for tilt-up (this angle was limited to be 140 degrees maximum, as measured between the plates) and flat for tilt-down feedback (though the tilt-down mode only reached the flat configuration when participants applied 2.5—10 N or more during the experiment, correlating to the highest and lowest compliance reference conditions, respectively). The initial configuration of tilt-up feedback was the same as the final configuration of tilt-down feedback and vice versa. The final flat configuration of the plates for tilt-down feedback prevented rendering a sharp edge, which might have been a biasing cue.

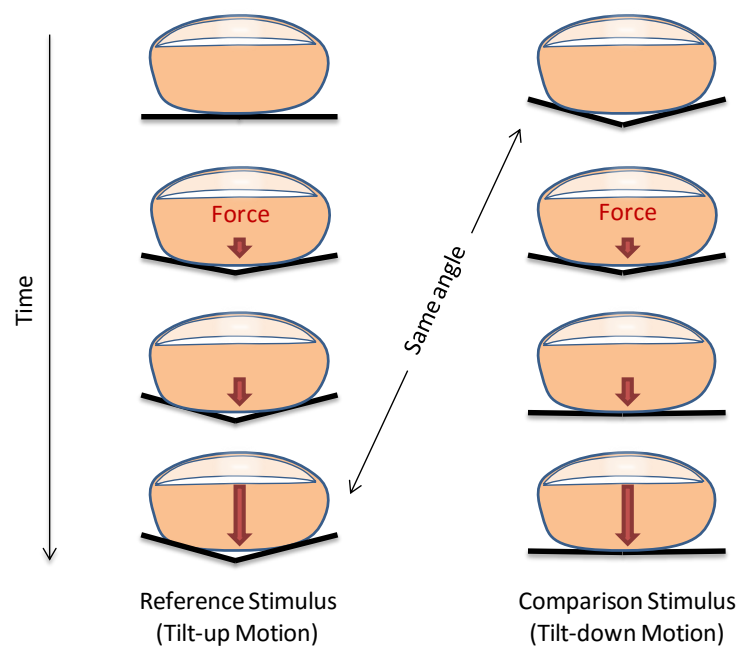


Figure 7.1. Sequential motion of the plates for rendering reference (tilt-up) and comparison (tilt-down) stimuli.

7.3.4 Procedures

The participants compared the compliance of pairs of reference-comparison stimuli under six different conditions (3 levels of tilting ratios \times 2 levels of tilt range). The tilting ratio of each reference-comparison pair was the same but in opposite directions (i.e., tilt-up vs. tilt-down feedback). The reference-comparison stimuli were presented in sequence with each other within each trial.

The participants sat in front of the tilting-plate device. Their right hands were placed on a wrist support and their right index finger was positioned above the device interface. The device and their hands were covered by a cloth to prevent any visual cues from affecting their compliance judgment. Participants wore noise cancelling headphones, which blocked background noise and played audio cues, indicating when a stimulus was ready to be examined.

The experiment was divided into two sessions: the first with a 20-degree tilt range and the second with a 40-degree tilt range. In each session, 30 pairs of reference-comparison stimuli were presented to the participants (10 repetitions per tilting ratio condition). These sessions were broken into 10 blocks, with each block consisting of one pair from each of the three tilting ratios. The presentation order of tilting ratios was randomized within each block. This randomized order was predetermined and was the same for all participants. The order of presenting reference and comparison stimuli was random but balanced between all trials.

A 2-alternative forced choice technique was used for this experiment. In each trial, participants perceived the compliance of a reference and a comparison stimulus. At the end of the trial, they indicated whether the first or the second stimulus was perceived to

be more compliant. Participants were asked to break contact with the device interface before proceeding to the second stimuli and when recording their responses. A minimum contact force of 0.25 N was required to ensure that participants made contact with the device interface before entering their answers. Prior to the actual experiment, a short practice session helped participants become familiar with the experiment procedure.

7.3.5 Experimental Results and Discussion

The percentage of the time that the tilt-up feedback (reference stimuli) was perceived to be more compliant than the tilt-down feedback (comparison stimuli) was computed for each participant. The mean and 95% confidence intervals of percentage values of all participants were reported for different tilting ratios and tilt ranges (Figure 7.2).

Regardless of the tilting ratio, mean percentages are ~50% and 30% for 20- and 40-

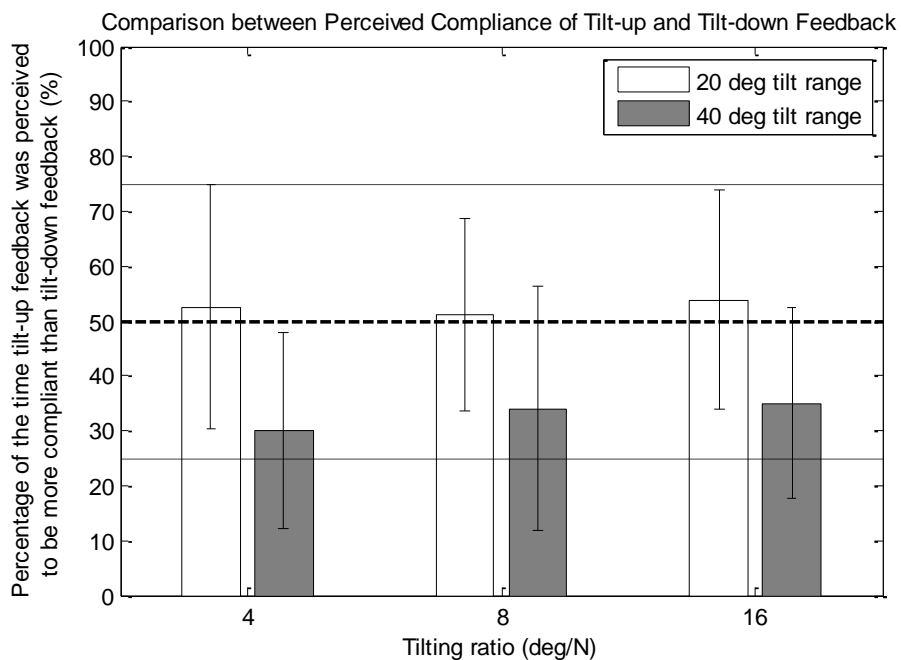


Figure 7.2. Percentage of the time tilt-up feedback was perceived as more compliant than tilt-down feedback with the same tilting ratio. The error bars are 95% confidence intervals.

degree tilt ranges, respectively. These results mean that for the 40-degree tilt range, tilt-down feedback was likely perceived as more compliant than tilt-up feedback. However, under the 20-degree tilt range, there is no significant difference between the perceived compliance of tilt-up and tilt-down feedback. For the 20-degree tilt range, the compliance of tilt-up and tilt-down feedback might be perceived as roughly the same. It seemed that under the 20-degree tilt range, the tilt motion quickly saturated and participants simply compared the compliance of two rigid surfaces.

Figure 7.3 shows the maximum applied force for all participants. The forces for tilt-up feedback are significantly higher than those for the tilt-down feedback in all six conditions (t-tests [$t(14) = 1.787$, $p < 0.05$]) except the condition with tilting ratio of 4 deg/N and tilt range of 40 degrees (the maximum force for this case is still greater for the reference). For example, at tilting ratio of 8 deg/N and tilt range of 40 degrees, the participants applied ~5.6 N and ~3.9 N of force on the tilt-up and tilt-down surfaces,

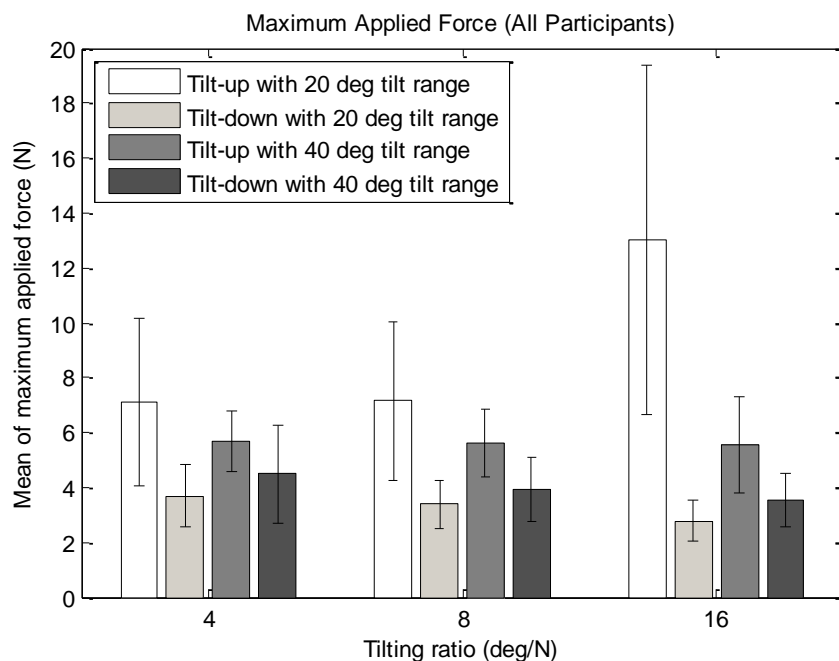


Figure 7.3. Mean and 95% confidence interval of maximum force applied to tilt-up and tilt-down surfaces at different levels of tilting ratios and tilt ranges.

respectively. There may be an interaction between the tilt range and the stimulus type since the tilt range has opposite effects on the applied force for tilt-up or tilt-down feedback. For example, the applied force in 4 deg/N tilt-up feedback drops from 7.1 N (under the 20-degree tilt range) to 5.6 N (under the 40-degree tilt range) while the applied force in 4 deg/N tilt-down feedback increases from 3.7 N to 4.5 N.

The comparison between the applied force shows that the participants tended to exert more force on the surfaces with tilt-up feedback rather than tilt-down feedback. Moreover, it was found that the applied force for tilt-up (tilt-down) feedback increases (decreases) as a function of tilting ratio. It was hypothesized that this difference in the level of applied force might be due to the difference in the kinesthetic stiffness of tilt-up and tilt-down feedback.

7.3.6 Experiment Conclusion

It was hypothesized that tilting-plate feedback with an opposite tilt direction (i.e., tilt-down feedback) would reduce the perceived compliance of the rendered surface (i.e., make it feel stiffer). However, the results of this preliminary experiment are in contrast with this hypothesis. There might be two reasons for this: (1) the kinesthetic information provided by tilt-down feedback causes the surface to be perceived as more compliant than tilt-up feedback, or (2) the contact area spread rate between the finger and the device with tilt-down feedback does not result in a lower perceived compliance. Both kinesthetic and tactile considerations for the above results have been investigated and will be discussed in the next sections.

7.4 Experiment 7.2: Kinesthetic Stiffness of Tilt-up and Tilt-down Feedback

The difference between perceived compliance of tilt-up and tilt-down feedback in Experiment 7.1 might be due to the difference in the kinesthetic feedback of the two feedback types. In this section, a pilot experiment was conducted to characterize the relationship between applied finger force and applied finger displacement for tilt-up and tilt-down feedback. Then corresponding equivalent kinesthetic stiffness values were obtained from measured force-displacement relationships. Only a small sample size of participants was considered to obtain representative force-displacement characteristics of the tilt-up and tilt-down displays.

7.4.1 Participants

Three experienced participants from Experiment 7.1 took part in this experiment. The participants had no known abnormalities in their index fingers. Before the experiment, they were informed about the experiment procedures and signed informed consent forms in accordance with the University of Utah's Institutional Review Board (IRB) policy.

7.4.2 Device

The haptic device used in this experiment was similar to the tilting-plate device described in Section 5.2. In addition, a non-contact finger tracking system was developed to measure finger displacements in real time (see Figure 7.4). A marker was attached to the participant's fingernail using a double-sided mini Glue Dot. A camera (Logitech Webcam C90) captured the marker position, and vertical displacements of the finger were computed using the OpenCV image processing program. The displacements were

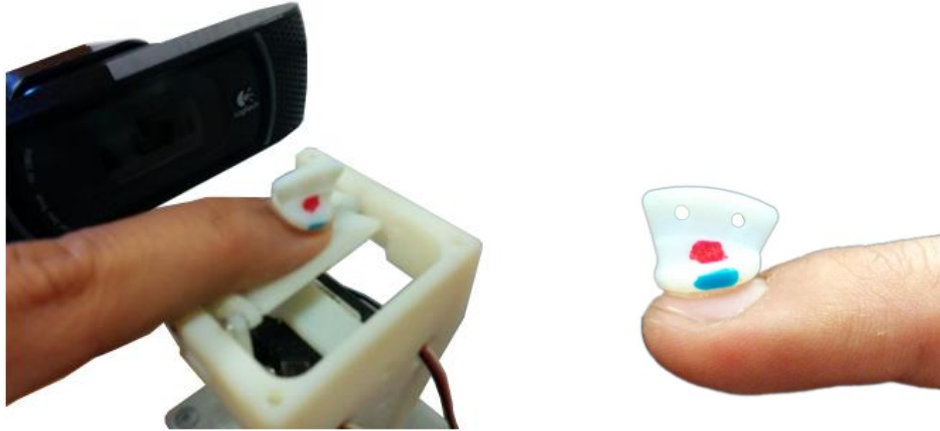


Figure 7.4. A non-contact finger displacement measurement system. The image processing program (OpenCV) tracks the position of the blue marker (right) captured by the camera (left).

recorded with a resolution of ~ 0.1 mm at a ~ 20 Hz sampling rate. This non-contact measurement technique enabled a natural interaction with the surface. Since the participant's finger is a part of the system, the measured displacements do not represent the exact displacements due to tilt-up or tilt-down feedback. However, these measurements can be used for relative comparison between the two feedback types.

7.4.3 Stimuli

The stimuli used in this pilot study were tilt-up and tilt-down feedback with a tilting ratio of 16 deg/N and a tilt range of 40 degrees.

7.4.4 Procedures

The tilt-up and tilt-down stimuli were presented to participants in two different trials. In each trial, the participants were asked to slowly push on the stimulus (with ~ 6 seconds pressing down). A timer on the computer screen helped them to keep track of the time. When the force exceeded 2.5 N, a 'stop' prompt on the screen informed the participants

to move up their fingers. The motion of the plates was saturated at 2.5 N. The participants were asked to move their fingers only in the vertical direction while accomplishing the task. The participants' hands were covered with a cloth during the entire experiment and they wore headphones playing white noise. The applied finger forces and applied finger displacements were recorded.

7.4.5 Experimental Results and Discussion

An example of force-displacement characteristic curves for tilt-up and tilt-down feedback is shown in Figure 7.5. The tilt-up feedback curve has a nonlinear characteristic whereas the curve for tilt-down feedback is almost linear ($R^2 = 0.95$). Similar trends

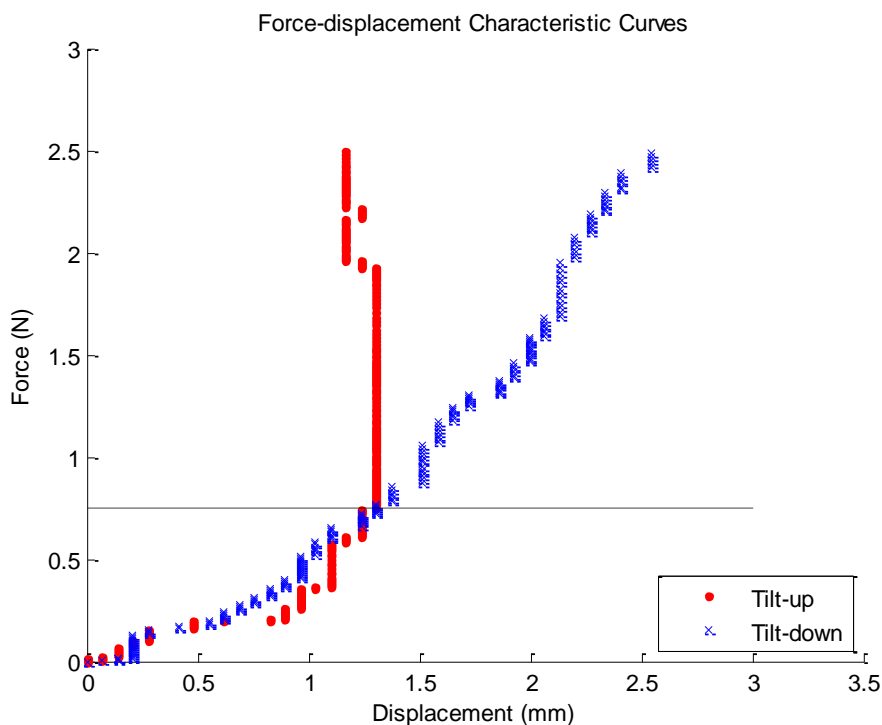


Figure 7.5. An example of force-displacement characteristic curves for tilt-up and tilt-down feedback. The tilt-up curve is nonlinear whereas the tilt-down curve is almost linear ($R^2 = 0.95$). All data points with forces greater than 2.5 N were excluded (tilt motion saturated at 40 degrees). The horizontal dashed line divides the plot into low- and high-level force regions.

were found for the other participants.

The tilt-up curve can be divided into low- and high-level force regions below and above 0.75 N, respectively. At low forces, the tilt-up curve matches the tilt-down curve. For this region, the average kinesthetic stiffness (the slope of the curve) is ~ 375 N/m, which is close to the measured stiffness of the human finger in Han and Kawamura [1999]. Thus, it is possible that the lower portion of the curves in Figure 7.5 mainly represents the compliance of the participant's fingerpad.

The stiffness (slope) of the tilt-up curve increased at higher levels of force and the finger was moved upward by the surface for forces above ~ 1.9 N. However, the tilt-down curve describes a linear spring model with kinesthetic stiffness of ~ 1489 N/m. Han and Kawamura found that the stiffness of the human fingerpad exponentially increases as a function of finger displacement [Han and Kawamura 1999]. Based on their results, the fingerpad stiffness is ~ 3000 N/m at 2.5 mm displacement. This means that under high levels of force, the displacement due to fingerpad deformation is negligible compared to the displacement due to tilting-plate feedback.

Table 7.1 summarizes the kinesthetic stiffness values based on the force-displacement measurements for tilt-up and tilt-down feedback for all three participants in low- and high-force regions. The stiffness deviation might be due to different finger sizes, different mechanical properties of the fingerpads, or difference in the interaction angle with the

Table 7.1. Estimated kinesthetic stiffness values for tilt-up and tilt-down feedback

Participant	Kinesthetic Stiffness (N/m)			
	Low Force		High Force	
	Tilt-up	Tilt-down	Tilt-up	Tilt-down
1	1170	1230	--	1085
2	360	390	--	1489
3	627	1200	--	1080

surfaces [Han and Kawamura 1999]. The second participant has the lowest (and highest) kinesthetic stiffness values at low-level (and high-level) force region. This might be because this participant has a more compliant layer of skin compared to the other participants.

7.4.6 Experiment Conclusion

The results of this pilot study indicate that *pure* tilting-plate feedback conveys both tactile and kinesthetic information. The participants' fingers moved slightly upward when they interacted with tilt-up feedback at contact forces more than 2 N. In contrast, their fingers moved downward when they pushed on the surface with tilt-down feedback. This means that the kinesthetic stiffness of tilt-down feedback is lower than that of tilt-up feedback. The lower kinesthetic stiffness of tilt-down feedback might be the main reason that it was perceived as more compliant compared to tilt-up feedback in the experiments in the previous section (Section 7.3.5). A method for reducing the kinesthetic stiffness of tilt-up feedback will be discussed in Section 7.5. Section 7.6 presents the comparison between the compliance of tilt-up and tilt-down feedback after controlling for the relative kinesthetic stiffness of these two methods to be approximately equal.

7.5 Experiment 7.3: Reducing the Kinesthetic

Stiffness of Tilt-up Feedback

By matching the kinesthetic feedback of tilt-up and tilt-down feedback, one can compare the pure effect of tilt direction in perceived compliance. Ideally, one would like to match the entire force-displacement characteristic curves of tilt-up and tilt-down feedback. However, this matching requires deploying a precise system to actively move

the tilting-plate device up and down based on collected force-displacement curves for each participant and each tilting condition. For simplicity, it was decided to use a passive spring as an alternative approach.

By adding a proper spring in series with tilt-up feedback, one can match the *average* kinesthetic stiffness of tilt-up and tilt-down feedback (see Figure 7.6). This spring is added to tilt-up feedback because the kinesthetic stiffness of tilt-up feedback is higher than that of tilt-down feedback and, in addition, the spring would enable a consistent causal downward finger motion for tilt-up feedback. In pure tilt-up feedback (without spring), the device moves the finger up when a user applies force to the surface (Figure 7.5). The total kinesthetic stiffness, k_t , of combined tilt-up feedback and the spring can be estimated by

$$\frac{1}{k_t} = \frac{1}{k_u} + \frac{1}{k_s}, \quad (7.1)$$

where k_u is the kinesthetic stiffness of tilt-up feedback and k_s is the stiffness of the spring.

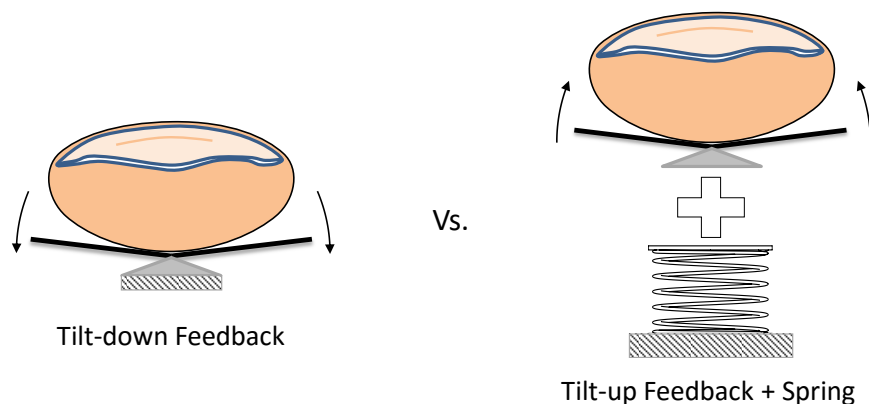


Figure 7.6. The surface with tilt-up feedback is mounted on a linear spring (right) to match its kinesthetic stiffness with that of tilt-down feedback (left).

7.5.1 Computing the Stiffness of an Optimized Spring

A virtual spring concept was used to compute proper spring stiffness matching the kinesthetic stiffness of tilt-up and tilt-down feedback. For a given stiffness of the virtual spring, a force-displacement curve for tilt-up feedback plus spring (Figure 7.7) can be obtained using Equation (4.2). Using a Least Squares optimization technique, the spring stiffness was obtained such that it minimized the difference between the slopes of tilt-down and tilt-up plus spring feedback in the high-level (above 1 N) force region. The low-level force region was disregarded since it mostly represents the stiffness of the fingerpad. An example of sum of squares of error vs. spring stiffness is depicted in

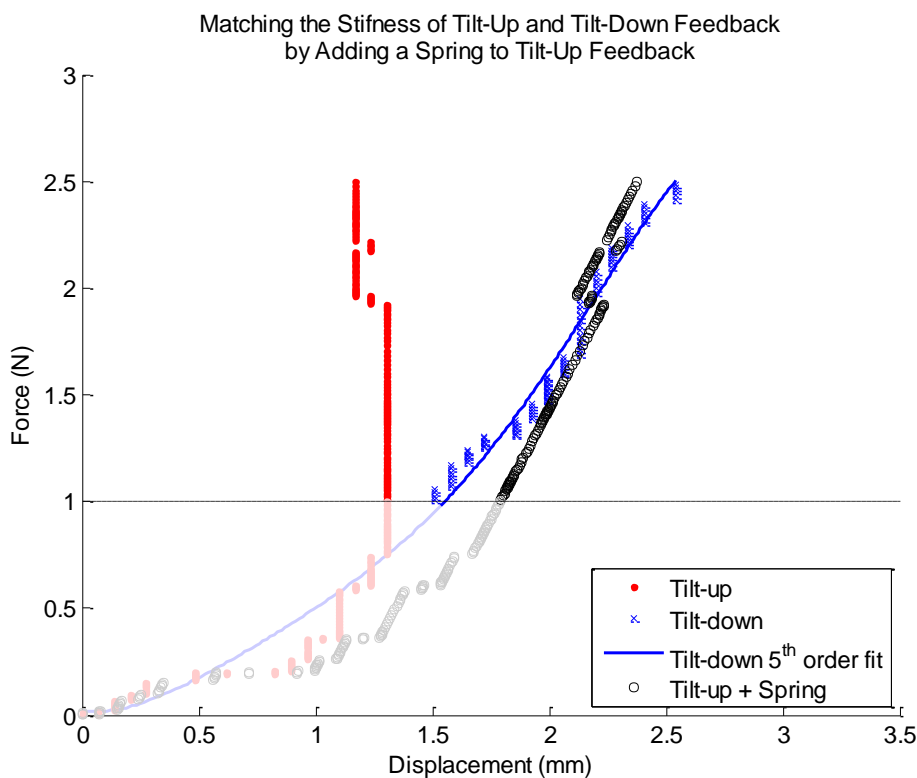


Figure 7.7. Matching the average kinesthetic stiffness of tilt-up and tilt-down feedback using a virtual spring for data points above 1 N force. By adding the spring, the tilt-up curve was transformed to the tilt-up plus spring curve. The tilt-down 5th order fit was used to interpolate corresponding data points needed for computing the least squares error.

Figure 7.8. For spring stiffness between 1500 and 1700 N/m, the sensitivity of the error (slope deviation) is relatively small. The error is more sensitive at low spring stiffness values than high stiffness values. Table 7.2 summarizes the optimal spring stiffness values under tilting ratio of 16 deg/N and tilt range of 40 degrees for all three participants in Experiment 7.2 (Section 7.4.5). Based on these results, different springs are required for different participants. The minimum, average, and maximum stiffness values of the spring are 1553, 1987, and 2445 N/m, respectively.

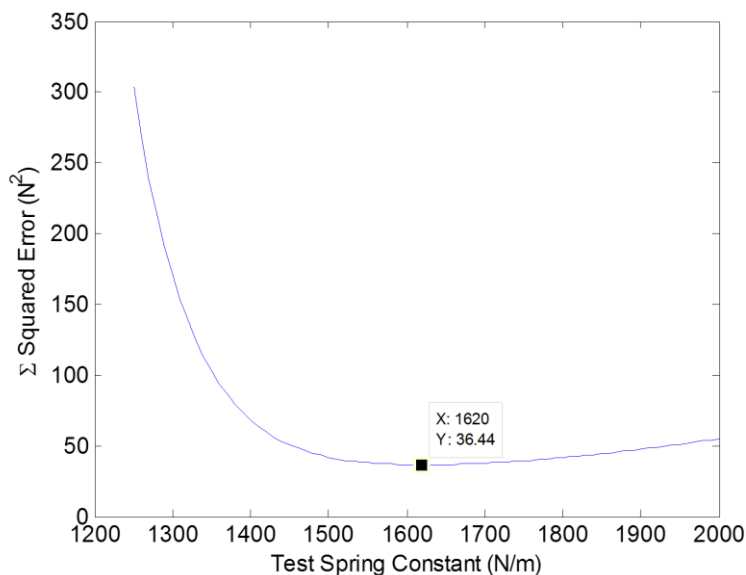


Figure 7.8. Sum of squares of error vs. spring stiffness. For spring stiffness between 1500 and 1700 N/m, error sensitivity is relatively small.

Table 7.2. Estimated spring stiffness for matching the kinesthetic stiffness of tilt-up and tilt-down feedback with 16 deg/N tilting ratio and 40-degree tilt range.

Participant	k_s (N/m)	
	Using all data points	Using data with $F > 1$ N
1	1620	1553
2	2054	1964
3	2675	2445
Average	2116	1987

Instead of modifying the kinesthetic stiffness of tilt-up feedback for each participant, two experiments were conducted with extreme spring stiffness values of 1000 and 3000 N/m (below and above the minimum and maximum estimated spring stiffness values obtained in the previous section). Although tilt-up and tilt-down feedback would not have the same kinesthetic stiffness, this approach has two advantages: (1) the experiment time and complexity of data analysis would be reduced and (2) the selected stiffness values provide a conservative test which would lead to conclusive results.

7.5.2 Participants

Ten right-handed participants (two female) with age range from 22 to 31 years (mean 26 years) were voluntarily recruited for this experiment. The participants had no known abnormalities in their index fingers. Before the experiment, they were informed about the experiment procedures and signed informed consent forms in accordance with the University of Utah's Institutional Review Board (IRB) policy.

7.5.3 Device

The tilting-plate device was mounted on a spring-loaded lever arm to reduce the kinesthetic stiffness of tilt-up feedback (see Figure 7.9). The position of the coil spring along the level arm was adjustable to render a desired kinesthetic stiffness (i.e., 1000 and 3000 N/m). The equivalent spring stiffness, k_s , at the device interface can be computed by

$$k_s = k_n \left(\frac{x}{l} \right)^2, \quad (7.2)$$

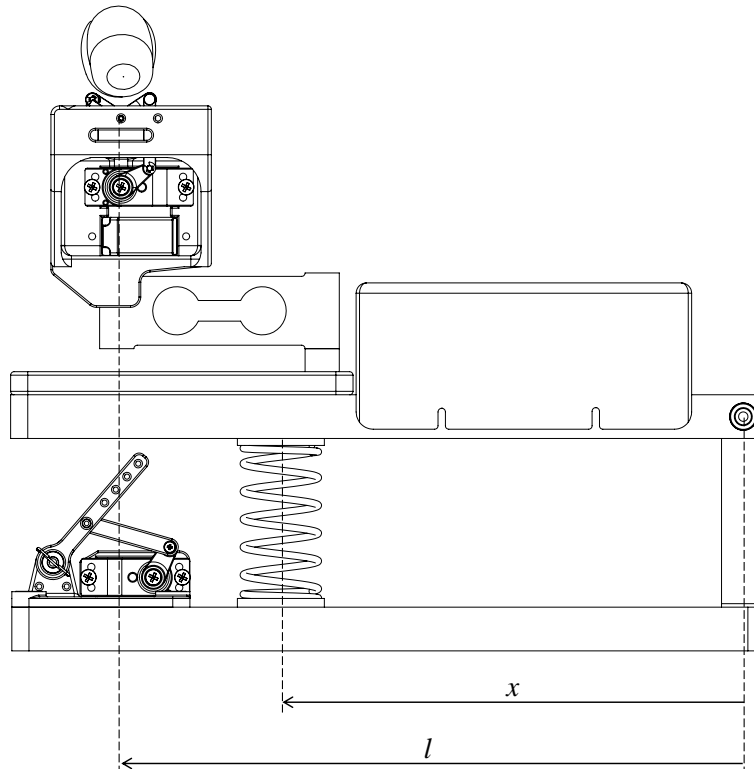


Figure 7.9. The tilting-plate device mounted on a spring-loaded lever arm. A mechanism next to the spring locks the lever arm when the tilt-down feedback is rendered.

where k_n is the nominal stiffness of the spring, x is the position of the spring with respect to the hinge of the lever arm, and l is the distance between the hinge and the center of the tilting-plate surface. Two different steel compression coil springs with stiffness values of 2747 and 8573 N/m were used (Associated Spring Raymond's MC0200063000 and McMaster's 9657K405). A mechanism locks the lever arm in place when tilt-down feedback is rendered. Similar to Experiment 7.2, the finger tracking system was used to measure finger displacements.

7.5.4 Stimuli

Three different types of stimuli were used in this experiment: 1) tilt-up feedback, 2) tilt-down feedback, and 3) tilt-up feedback plus physical spring. Two different levels of

spring stiffness values (1000 and 3000 N/m), two different levels of tilting ratios (4 and 16 deg/N) and two different levels of tilt range (20 and 40 degrees) were selected.

7.5.5 Procedures

The procedure for this experiment was similar to the procedure described in Section 7.4.4. In each trial, participants interacted with three types of stimuli. Their applied finger displacements and applied forces were recorded under eight different conditions (2 kinesthetic stiffness levels \times 2 tilting ratios \times 2 tilt ranges). Each condition was presented 5 times (120 total stimuli).

7.5.6 Experimental Results and Discussion

Figures 7.10 and 7.11 show examples of force-displacement characteristic curves for spring stiffness values of 1000 and 3000 N/m, respectively. At the same amount of applied force, tilt-up, tilt-down, and tilt-up plus spring curves have different slopes. The average slope of each curve was computed for high-level force region with applied forces above 1.0 N.

Means and confidence intervals of kinesthetic stiffness values across all participants are shown in Figures 7.12 and 7.13 for spring stiffness values of 1000 and 3000 N/m, respectively. It should be mentioned that the absolute value of kinesthetic stiffness was used to compute the means since the slopes of tilt-up curves were negative. The kinesthetic stiffness of tilt-up feedback is significantly higher than the kinesthetic stiffness of tilt-down feedback for all tilting ratio and tilt range levels [t-tests; e.g., $t(32) = 3.56$, $p < 0.05$]. However, by adding the spring with stiffness of 1000 N/m, the

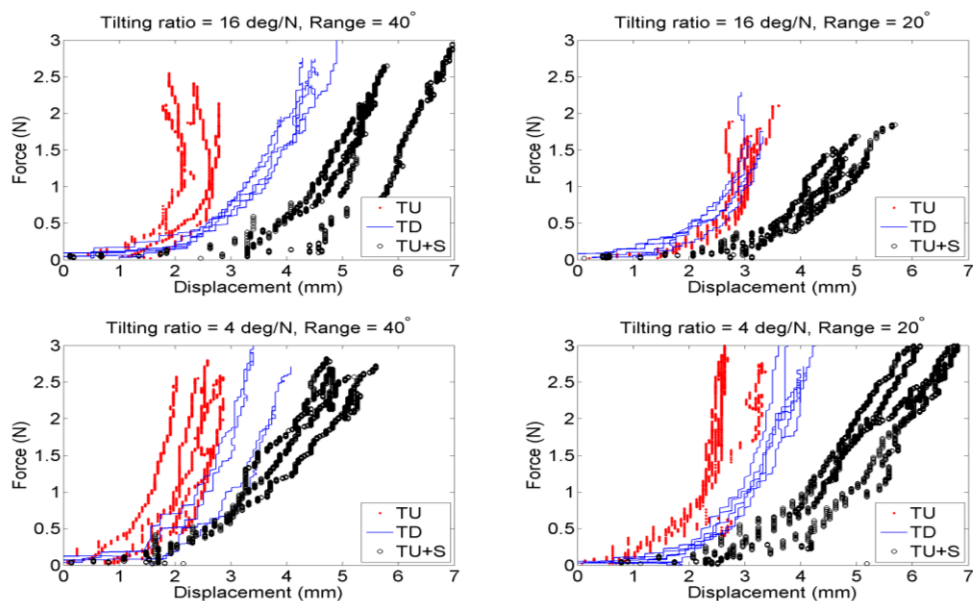


Figure 7.10. Force-displacement characteristic curves of tilt-up (TU), tilt-down (TD), and tilt-up plus 1000 N/m spring (TU+S) feedback. Adding the spring reduced the slopes of TU+S curves lower than the slope of TD curves.

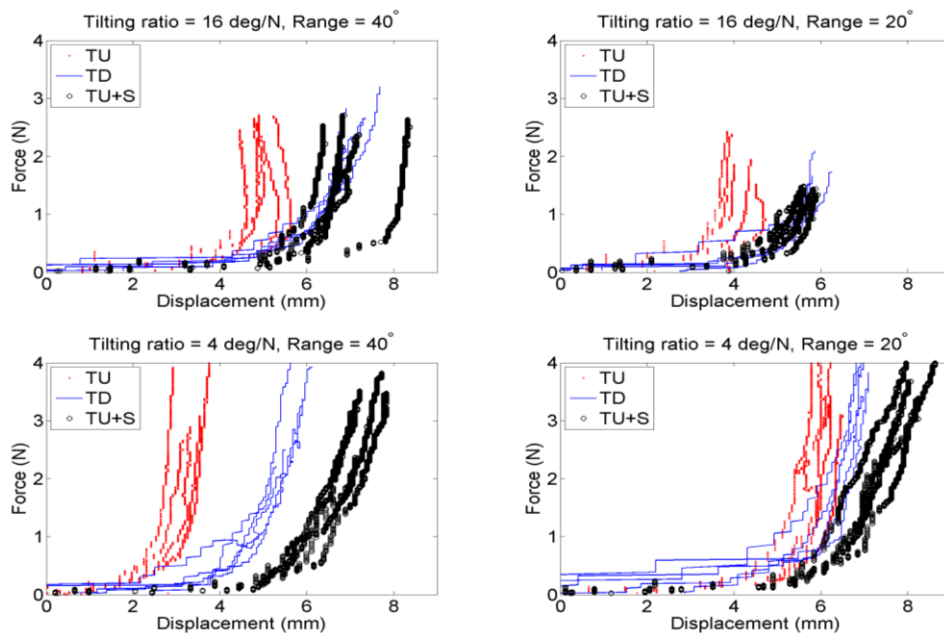


Figure 7.11. Force-displacement characteristic curves of tilt-up (TU), tilt-down (TD), and tilt-up plus 3000 N/m spring (TU+S) feedback. Adding the spring reduces the slopes of TU curves. For tilting ratio of 4 deg/N, the slopes of TU+S curves are lower than the slopes of TD curves; however, for tilting ratio of 16 deg/N, the TU+S slopes are still higher than the slope of TD curves.

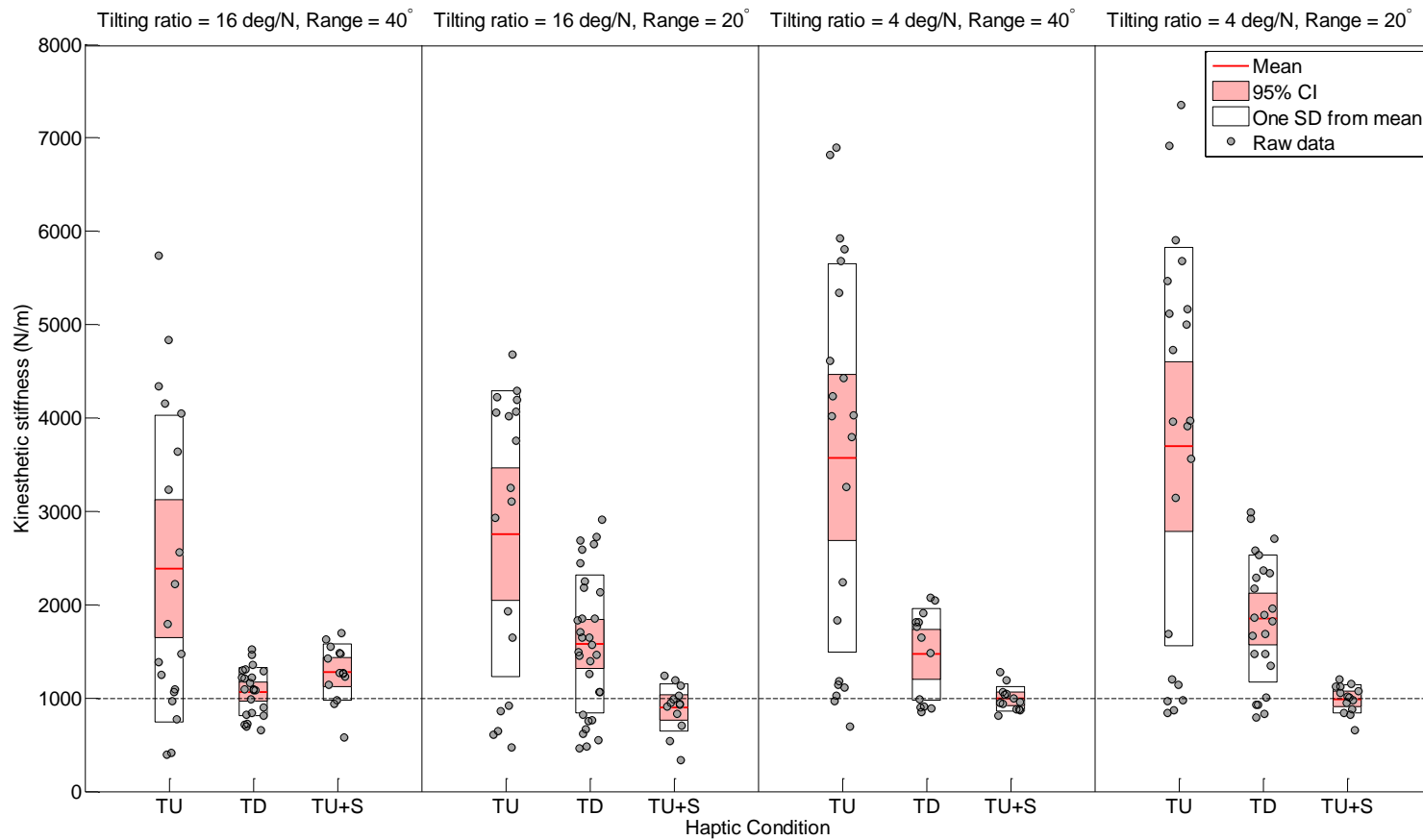


Figure 7.12. Equivalent kinesthetic stiffness of tilt-up (TU), tilt-down (TD) feedback, and tilt-up plus spring feedback with 1000 N/m stiffness (TU+S). The outliers with more than three standard deviation from mean were excluded. For TU feedback, the absolute value of the kinesthetic stiffness was used.

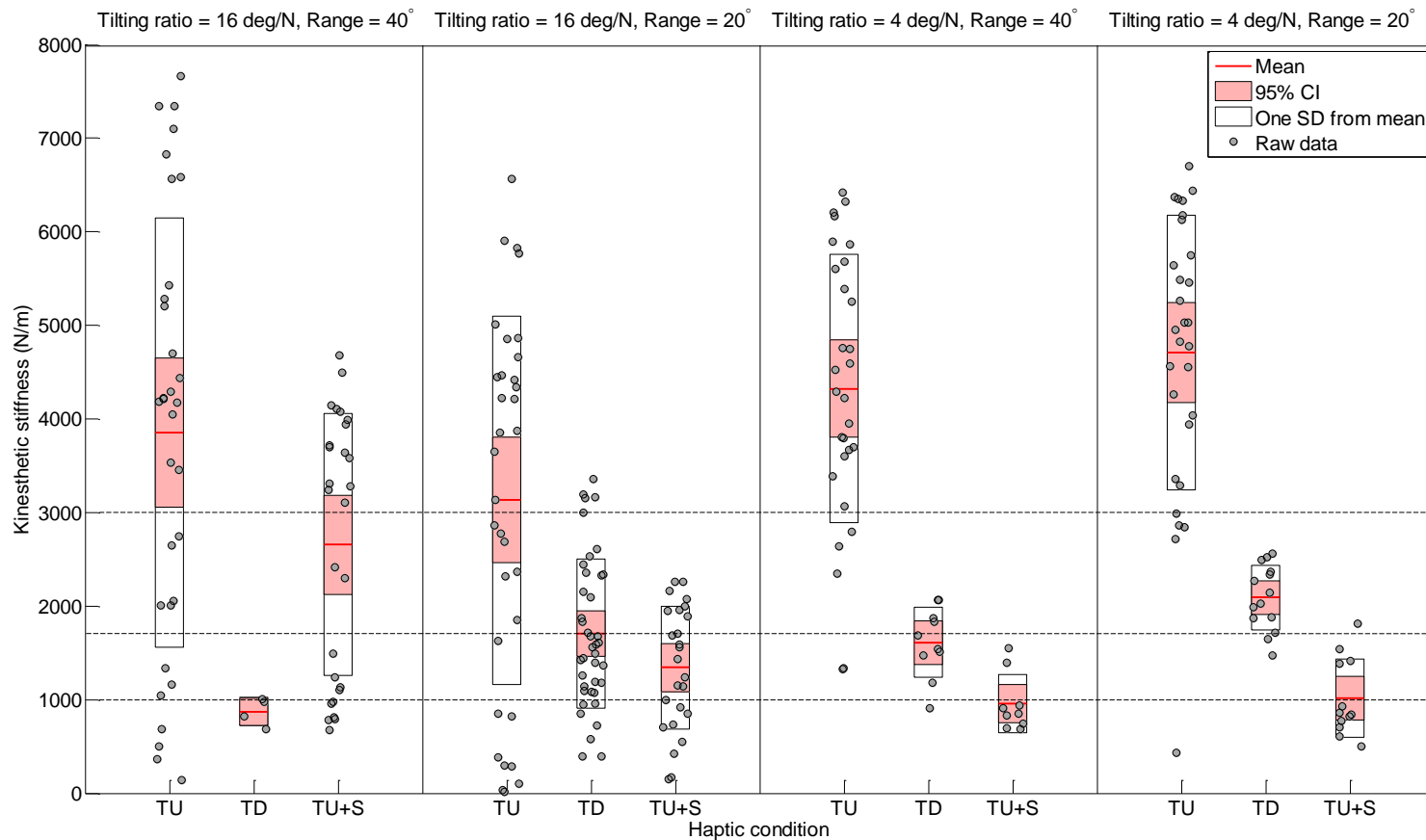


Figure 7.13. Equivalent kinesthetic stiffness of tilt-up (TU), tilt-down (TD) feedback, and tilt-up plus spring feedback with 3000 N/m stiffness (TU+S). The outliers with more than three standard deviation from mean were excluded. For TU feedback, the absolute value of the kinesthetic stiffness was used. The kinesthetic stiffness of tilt-up (or tilt-down) feedback are close to that of in Figure 7.12 since the conditions are identical.

kinesthetic stiffness of tilt-up plus spring feedback is reduced such that it is significantly lower than the kinesthetic stiffness of tilt-down feedback [t-tests $t(24) = 3.40$, $p < 0.01$]. Only for the condition with 16 deg/N tilting ratio and 40-degree tilt range, the kinesthetic stiffness of tilt-up plus spring (1279 N/m) is greater than that of tilt-down feedback (1067 N/m), but not significantly.

For the 3000 N/m spring stiffness case, no statistically significant difference was found between the kinesthetic stiffness of tilt-up plus spring feedback and tilt-down feedback. Only for the condition with tilting ratio of 16 deg/N and tilt range of 40 degrees, is the kinesthetic stiffness of tilt-up feedback plus spring feedback (2656 N/m) significantly higher than the kinesthetic stiffness of tilt-down feedback (871 N/m) [$t(29) = 2.51$, $p < 0.001$]. Thus the spring with 1000 N/m (3000 N/m) would be compliant (stiff) enough to test the hypotheses for the compliance comparison experiment in Section 7.6.

7.5.7 Experiment Conclusion

For each participant, tilting ratio or tilt range, different spring stiffness value is required to match the stiffness of tilt-up plus spring feedback with the stiffness of tilt-down feedback. Thus in an alternative approach, two physical springs with stiffness of 1000 and 3000 N/m were used to reduce the kinesthetic stiffness of tilt-up plus spring feedback, such that it is close to the kinesthetic stiffness of tilt-down feedback, but chosen to be just below and above the kinesthetic stiffness of tilt-down feedback. The force-displacement characteristic curves for tilt-down, tilt-up, and tilt-up plus spring feedback were generated and the kinesthetic stiffness values were compared quantitatively.

7.6 Experiment 7.4: Comparison between Perceived Compliance
of Tilt-up and Tilt-down Feedback after Controlling
for the Relative Kinesthetic Stiffness

In this experiment, participants compared the perceived compliance of tilt-down and tilt-up feedback after controlling for their relative kinesthetic stiffness using two physical springs (1000 and 3000 N/m) in series with tilt-up feedback. It was hypothesized that (1) tilt-up with 1000 N/m spring feedback would be perceived as more compliant than tilt-down feedback, (2) tilt-up with 3000 N/m spring feedback would be perceived as less compliant than tilt-down feedback.

7.6.1 Participants

The same participants in Section 7.5.2 took part in this experiment after they participated in Experiment 7.3 (which was used to characterize the equivalent kinesthetic stiffness when with tilt-down vs. tilt-up + spring test conditions). That is, Experiment 7.3 was the pretest of the current Experiment 7.4.

7.6.2 Device

The device used in this experiment was similar to the device described for Experiment 7.3 (Section 7.5.3). However, the finger tracking system was not used.

7.6.3 Stimuli

Reference stimuli were tilt-up plus spring feedback with two levels of spring stiffness (1000 and 3000 deg/N), four levels of tilting ratio (0, 4, 8, and 16 deg/N), and two levels of tilt range (20 and 40 degrees). Comparison stimuli were rendered by tilt-down

feedback with a tilting ratio between 0 and 20 deg/N.

7.6.4 Procedures

The participants sat in front of the tilting-plate device (Figure 7.14). Their right hands were placed on a wrist support and their index fingers were positioned above the device interface. The device and their hand were covered by a cloth to prevent any visual cues from affecting their compliance judgment. Participants wore noise cancelling headphones, which blocked background noise and played audio cues, indicating when a stimulus was ready to be examined.

Using an adaptive 1-up 1-down staircase method [Levitt 1971], the participants compared the compliance of pairs of reference-comparison stimuli under 16 different conditions (2 spring stiffness values \times 4 tilting ratios \times 2 tilt ranges). The experiment was divided into two sessions for the 1000 and 3000 N/m spring stiffness values. In each

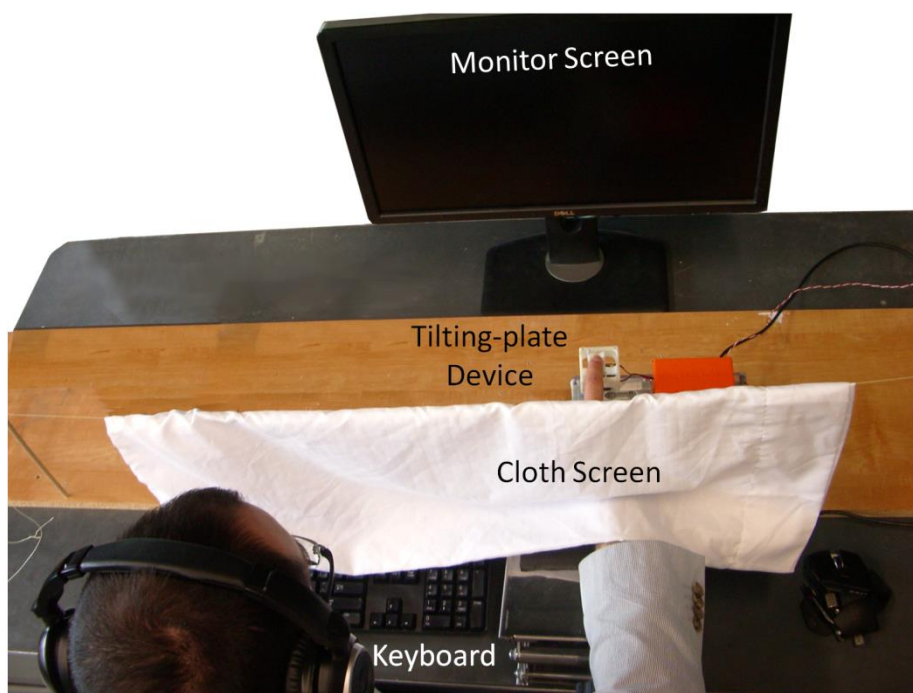


Figure 7.14. Setup of the experiment

session, an 8×8 Latin Square was used to present different conditions in different order across all participants.

Each condition was accomplished in two runs: one ascending run and one descending run. In the ascending runs, the tilting ratio of comparison stimuli was set to zero, well below estimated PSE. In the descending runs, the tilting ratio of comparison stimuli was set to a high value (i.e., 10, 10, 15, and 20 deg/N for reference stimuli with 0, 4, 8, 16 deg/N tilting ratio, respectively). The presentation order of ascending and descending runs was balanced both within and between participants.

In each trial, the participants perceived the compliance of a reference and a comparison stimulus in sequence. At the end of the trial, they indicated whether the reference or the comparison stimulus was perceived to be more compliant. If the participants selected the comparison stimulus as the more compliant (or less compliant) surface, its tilting ratio was decreased (or increased) by a specific step size to make the task more difficult for the next trial. The initial tilting ratio step size was 3 deg/N and it was reduced to 1 and then to 0.25 deg/N after the first and the fourth reversals, respectively. The experiment terminated after 10 total reversals and the PSE was computed based on the average of tilt-down tilting ratios in the 6 last reversals. There were four PSEs per condition.

Participants were asked to break contact with the device interface before proceeding to the second stimulus and when recording their responses. A minimum contact force of 0.25 N was required to ensure that participants made contact with the device interface before entering their answers. To prevent plates from complete saturation, a warning message on the screen informed participants to stop pushing when tilt angle preceded 75% of the tilt range. Prior to the actual experiment, a short practice session helped

participants become familiar with the experiment procedure.

7.6.5 Experimental Results and Discussion

The means and 95% confidence interleaves for upper and lower tilting ratio PSEs (corresponding to 1000 N/m and 3000 N/m spring stiffness values) for all participants are shown in Figure 7.15.

Under the 20-degree tilt range and 1000 N/m spring stiffness, the PSE for 16 deg/N tilt-up tilting ratio (17.52 deg/N) is higher (but not significantly) than the reference tilting ratio. However, the PSEs for 4 and 8 deg/N tilt-up tilting ratios (8.38 and 11.85 deg/N) are significantly higher than their corresponding reference tilting ratios [t-tests $t(15) = 3.55$, $p < 0.01$ and $t(15) = 2.75$, $p < 0.05$, respectively]. This implies that at the same tilting ratio, tilt-up plus 1000 N/m spring feedback is perceived as more compliant than

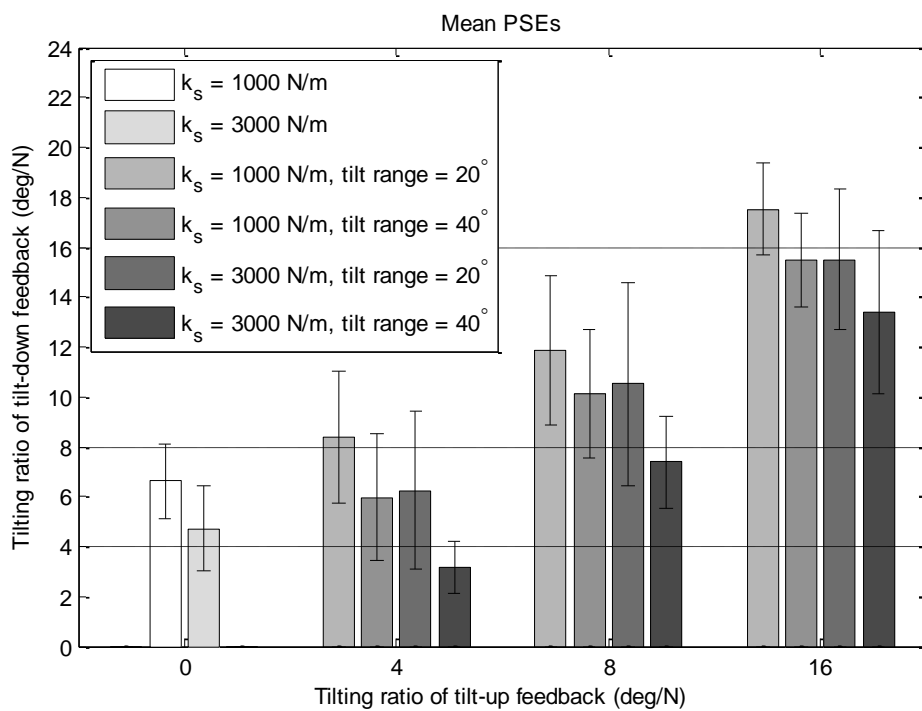


Figure 7.15. Upper and lower tilt-down PSEs vs. tilt-up tilting ratios. Error bars are 95% confidence intervals.

tilt-down feedback. However, under the 20-degree tilt range and 3000 N/m spring stiffness, the PSEs (6.24, 10.51, 15.51 deg/N) seem to be higher than their corresponding reference tilting ratios (except for 16 deg/N tilting ratio). No statistically significant difference between the PSEs and their corresponding reference tilting ratios was found for these conditions. However, the results suggest that at the same tilting ratio, tilt-up plus 3000 N/m spring feedback might be perceived as the same or less compliant than tilt-down feedback.

For the 40-degree tilt range and 1000 N/m spring stiffness, PSEs are 5.97, 10.12, and 15.46 deg/N for 4, 8, and 16 deg/N tilt-up tilting ratios, respectively. For the 40-degree tilt range and 3000 N/m spring stiffness, the PSEs are 3.18, 7.39, and 13.41 deg/N for the reference stimuli with 4, 8, and 16 deg/N tilting ratios, respectively. None of the PSEs are significantly different from their reference values. An interpolation or extrapolation between the PSE in 1000 and 3000 N/m spring stiffness cases can estimate the spring stiffness (~2800 N/m) at which the compliance of two feedback types are perceived as the same.

For zero tilting ratio (pure kinesthetic feedback) and spring stiffness of 1000 N/m, the tilt-down PSE (6.61 deg/N) is higher than the tilt-up PSE (4.3 deg/N) obtained from the results of Experiment 4.1. With the 3000 N/m spring stiffness, the PSE is 4.71 deg/N, which is slightly higher than the expected tilt-up PSE in Experiment 4.1.

There might be an effect due to tilt range regardless of tilt direction. The PSE for the 20-degree tilt range is higher than the PSE for the 40-degree tilt range for all tilting ratio levels of tilt-up feedback (Figure 7.15). Although based on obtained results, these differences are not statistically significant, but the trend indicates that at the same tilting ratio, a surface with 40-degree tilt range might be perceived as more compliant than the

surface with 20-degree tilt range.

7.6.5.1 The effect of finger size on the perceived compliance

This section investigates whether the size of index finger distal phalanx has an effect on the relative perceived compliance of tilt-down and tilt-up plus spring feedback. A series of linear regression models between the PSE (tilting ratio of tilt-down feedback) and the width, thickness, and length of the participants' fingers was conducted at each reference tilting ratio level (4, 8, and 16) and each reference spring stiffness level (1000 vs. 3000 N/m). The result of all regression analyses did not show any statistically significant effect of the finger size (width, thickness, and length) on the PSE [$R^2 < 0.75$, $F(1, 7) < 5.87$, $p > 0.07$]. However, some interesting trends were found as follows.

There appears to be an interaction effect between the finger width and the spring stiffness on the PSE. For the 1000 N/m spring, the wider the finger, the higher the PSE (Figure 7.16 a-c). The participants with wider (narrower) fingers may judge tilt-down feedback as less (more) compliant than tilt-up + 1000 N/m spring feedback with the same tilting ratio. Additionally, there is an opposite trend when the kinesthetic stiffness of tilt-down feedback is lower than that of tilt-up plus spring feedback. For the 3000 N/m spring, the participants with a wider (narrower) finger may judge tilt-down feedback as more (less) compliant than tilt-up + spring feedback (Figure 7.16 d-f). The main reason for this finger-width effect may be due to the inherent kinesthetic stiffness of tilt-up and tilt-down feedback. As shown in Figure 7.17, the distance between the pivot axis of the plates and the side of the finger is larger for a wider finger; thus, the wider fingers experience more vertical displacement (i.e., lower kinesthetic stiffness) in the presence of tilt-down feedback and tilt-up plus 3000 N/m spring feedback. However, using a

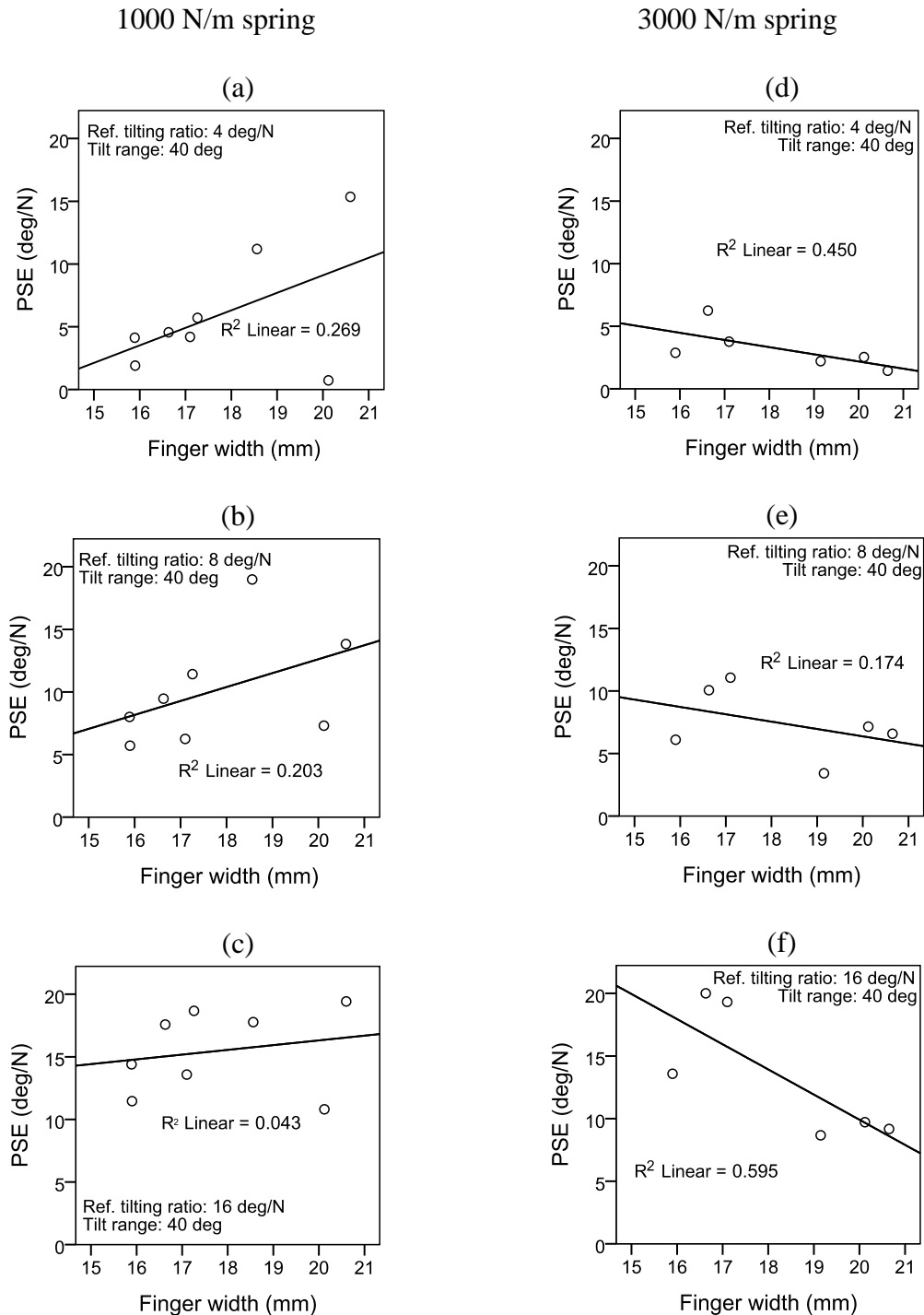


Figure 7.16. The effect of width of index finger distal phalanx on relative perceived compliance of tilt-down and tilt-up plus spring feedback. The vertical axes (PSEs) indicate the tilting ratio of tilt-down feedback. For the 1000 N/m (3000 N/m) spring, the relationship between the PSE and the finger width is positive (negative).

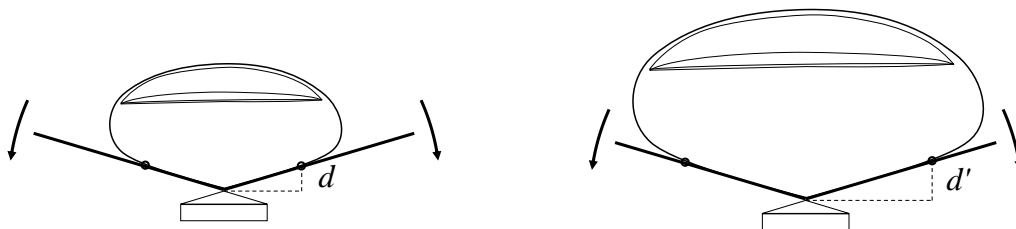


Figure 7.17. The effect of finger width on kinesthetic stiffness of tilt-down (or tilt-up) feedback. The wider the finger the longer the effective lever arm and thus the larger vertical displacement (i.e., $d' > d$).

more compliant spring (i.e., 1000 N/m) for tilt-up feedback seems to mask this effect. It is hypothesized that these trends disappear when the kinesthetic stiffness of the tilt-up plus spring and tilt-down feedback matches (using a spring with a stiffness of ~2800 N/m).

Same trends were found for the finger thickness (maximum distance between the back of the fingernail and center of the fingerpad). Further analysis revealed that there is very strong positive and significant correlation between the finger width and the finger thickness [$R^2 = 0.78$, $F(1, 8) = 21.96$, $p < 0.01$].

Additionally, the effect of the distal phalanx length on PSE was found to be always positive (but not statistically significant) regardless of the spring stiffness level. It seems that the participants with longer (shorter) fingers may judge tilt-down feedback as less (more) compliant than tilt-up plus spring feedback. It should be mentioned that this result is not conclusive since the participants could interact with the device interface at different angles.

7.6.5.2 Experiment Conclusions

Two physical springs were used to control the difference between the kinesthetic stiffness of tilt-up and tilt-down feedback. The upper and lower PSEs, equivalent tilt-

down tilting ratios, were obtained at different tilting ratio levels and tilt ranges of tilt-up feedback. The important conclusion of this experiment is summarized for the condition with 16 deg/N tilting ratio and the 40-degree tilt range. For this condition, tilt-down feedback was perceived the same as or more compliant than tilt-up plus spring feedback, even when the kinesthetic stiffness of tilt-up plus 1000 N/m spring feedback was significantly lower than the kinesthetic stiffness of tilt-down feedback. This means that the source of difference in perceived compliance between tilt-up and tilt-down feedback modes are likely due to other factors such as contact area spread ratio, which will be investigated in the next section.

7.7 Experiment 7.5: Contact Width Spread Rate of

Tilt-up and Tilt-down Feedback

Difference in perceived compliance of tilt-up and tilt-down feedback may be due to the difference in the amount of contact width (area) spread rate between the finger and the device interface for these two feedback types. It was found that the higher the contact area spread rate, the more compliant the surface [Ambrosi et al. 1999]. This section compares the contact width spread rate of tilt-up and tilt-down feedback via direct experimental measurements and a simple contact model simulation. The obtained results explain why tilt-down feedback is perceived as more compliant than tilt-up surface.

7.7.1 Participants

Two participants (one male and one female) took part in this experiment. The participants had no known abnormalities in their index fingers. Before the experiment, they were informed about the experiment procedures and signed informed consent forms

in accordance with the University of Utah's Institutional Review Board (IRB) policy.

7.7.2 Device

The device was similar to the device in Experiment 7.4. The lever arm was stationary all the time for both tilt-up and tilt-down feedback, since the kinesthetic displacement due to the physical spring did not have any effect on the result of this experiment.

7.7.3 Stimuli

Tilt-up and tilt-down feedback with tilting ratios of 4 and 16 deg/N and tilt range of 40 degrees were used for this experiment.

7.7.4 Procedures

The participants sat in front of the tilting-plate device. Their right hands were placed on a wrist support and their index fingers were positioned above the device interface. The device and their hands were covered by a cloth to prevent any visual cues. Participants wore noise cancelling headphones, which blocked background noise and played audio cues, indicating when a stimulus was ready to be examined.

For each trial, the participants rubbed their index fingers on an inkpad from side to side and then, with the help of a proctor, located their fingers above the center of the device surface. A new piece of Scotch tape was placed on the device surface to capture the fingerprint when the participants pushed against the device surface. The participants were asked to apply force at 0.05, 0.10, 0.15, 0.20, 0.25, 0.30, 0.35, 0.40, 0.45, 0.50, 1.0, 1.5, 2.0, 2.5, 3.0, 3.5, 4.0, 4.5, and 5.0 N. The level of applied force was displayed on the monitor screen to help the participant match their finger forces with the desired force

levels and also to prevent any overshooting. The pieces of tape were taken off, placed on a paper, and scanned to measure the width of contact.

7.7.5 Experimental Results and Discussion

An example of fingerprint contact areas at different contact force levels is shown in Figure 7.18. The outlines are generated by image processing using ImageJ v1.48 software. For tilt-up and tilt-down feedback, the contact area increased as the applied force became higher. For tilt-down feedback with tilting ratios of 4 and 16 deg/N, there were two contact regions if applied force was less than ~ 1.5 N and ~ 1.0 N, respectively. The regions were separated because the center of the fingerpad did not touch the center of the device surface. The net contact width is defined as the maximum distance between the left and right edges of the contact minus the gap between the separated regions (if any).

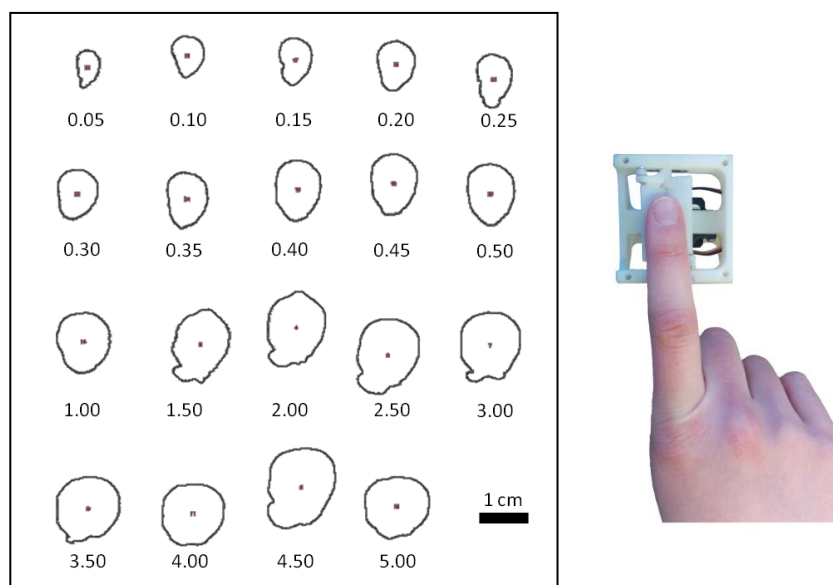


Figure 7.18. Fingerprint contact areas for different contact force levels for tilt-up feedback with 16 deg/N tilting ratio and 40-degree tilt range. The image on the right shows the orientation of the finger with respect to the contact areas.

Figure 7.19 plots the net contact width at different levels of applied force and tilt angle for tilt-up and tilt-down feedback. The net contact width for tilt-down feedback is almost always higher than the net contact width for tilt-up feedback. The initial contact-width-to-force ratio (the average slope of the curves for forces below 0.5 N) of tilt-down feedback (~ 24 mm/N) is higher than that of tilt-up feedback (~ 18 mm/N). This higher contact-width-to-force ratio of tilt-down feedback may be the main reason why the feedback is perceived as more compliant than tilt-up feedback [Ambrosi et al. 1999]. At high levels of force, the slopes of the curves reduced and the curves plateaued. For tilt-up feedback and applied forces less than ~ 2.5 N, it seems that the contact width spread rate is higher at 16 deg/N tilting ratio than 4 deg/N tilting ratio (Figure 7.19 top). This supports the previous findings that increasing the tilting ratio of tilt-up feedback increases the perceived compliance. However, for tilt-down feedback the trend is different. For forces less than ~ 1.25 N, the contact width spread rate is higher at 16 deg/N tilting ratio than 4 deg/N tilting ratio. This is likely because the center of the fingerpad touches the center of the interface more quickly at 16 deg/N tilting ratio than 4 deg/N tilting ratio. For contact forces between ~ 1.25 and ~ 2.5 N, it seems that the contact width at 4 deg/N tilting ratio is equal to or higher than that of 16 deg/N tilting ratio. The lower contact area at higher tilting ratio is more likely because of the flattening effect of the tilt-down feedback.

Regardless of tilt feedback type, the contact width is higher for 4 deg/N tilting ratio than 16 deg/N tilting ratio at the same amount of tilt (Figure 7.19 bottom). The reason for this difference is that the applied force is higher at a smaller tilting ratio, thus the contact area is lower as well. This means that the feedback type and applied force are important predictors of contact width. We also simulate a simple model to generate contact width

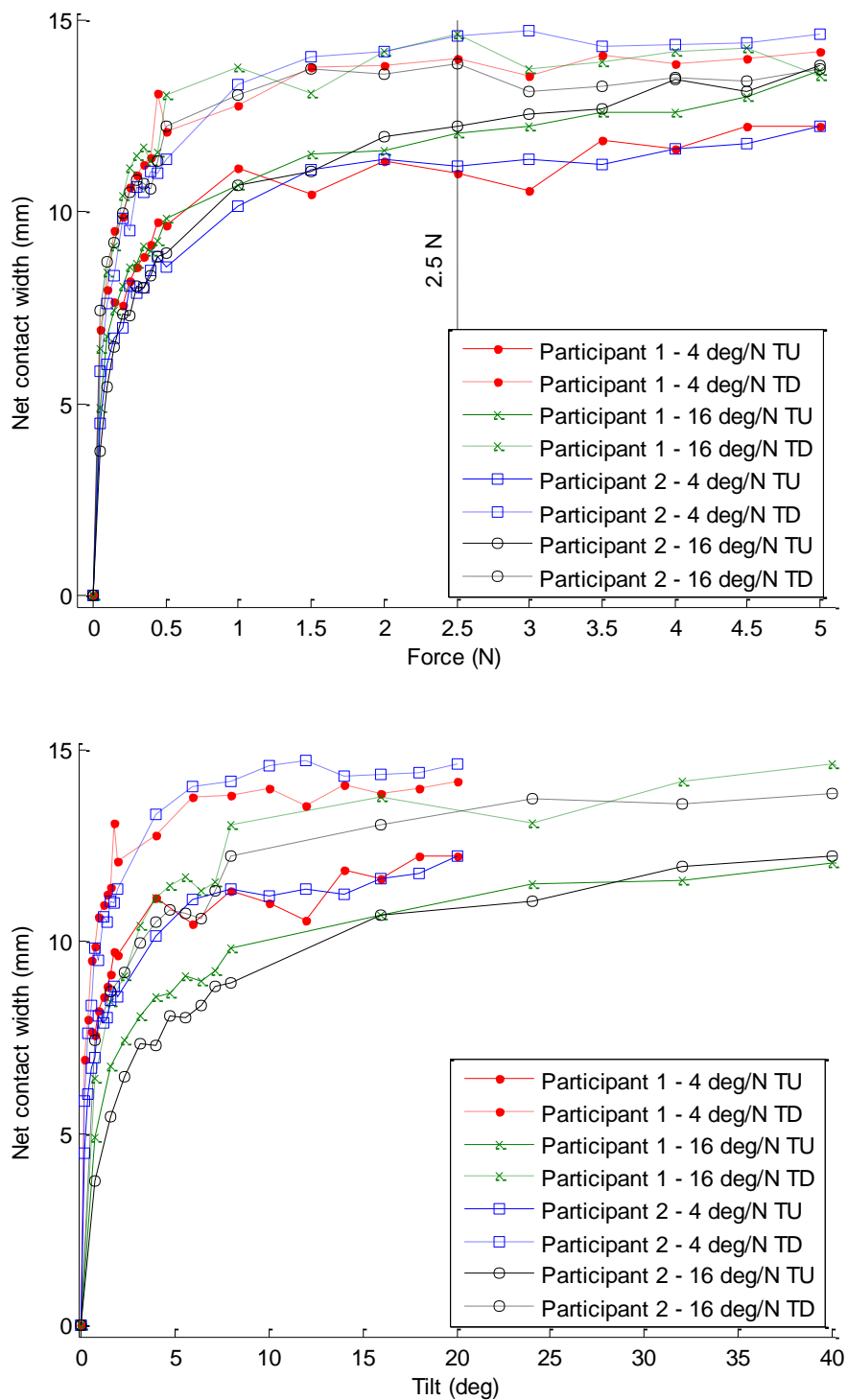


Figure 7.19. Net contact width for tilt-up (TU), which is indicated with solid lines, and tilt-down (TD) feedback, which is indicated with dotted lines, as a function of applied force (top) and tilt angle (bottom) under different conditions. For forces higher than 2.5 N (vertical dashed line), the plates stop moving at of 16 deg/N tilting ratio.

curves as function of applied force. For this model, it was assumed the finger was rigid and had a circular cross section with diameter of 13.9 mm. The relative position of the circle with respect to the plates and the tilt angle of the plates were set based on the recorded force-displacement data obtained in the previous experiment. For each time instance, the contact points between the circle and the plates were computed. The contact width was defined as the sum of the distances between the center of surface and the contact points.

Figure 7.20 shows the simulated contact width vs. applied force. Similar to the results from measurements, at the beginning of contact, the slope of tilt-down feedback is higher than the slope of tilt-up feedback. For high levels of forces, there is a similar trend for the slope of the curves as shown in Figure 7.19. However, there is a difference in the amount of contact width between simulated and measurement results. This difference might be because of the rigid finger model used in the simulation.

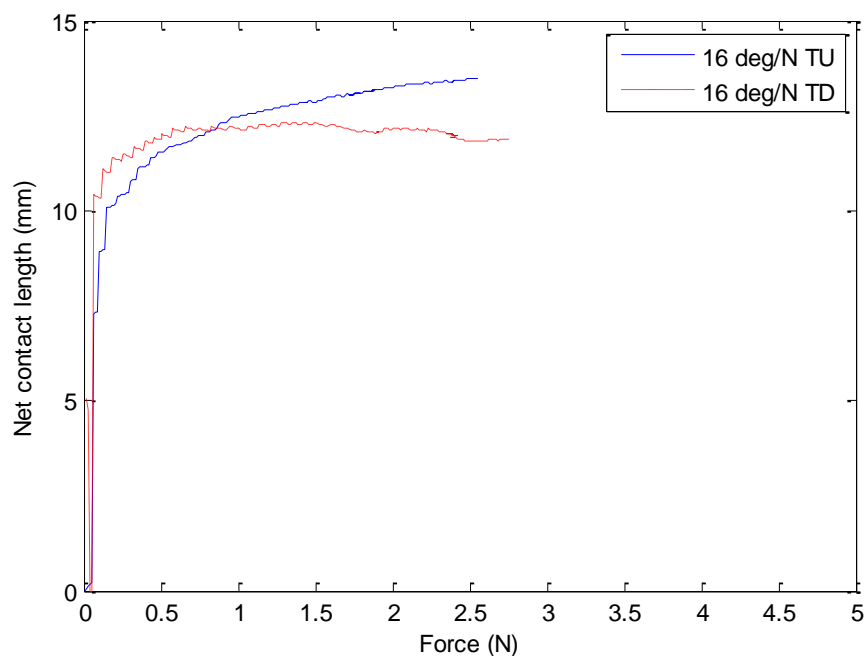


Figure 7.20. Net contact width vs. applied force generated using a rigid finger model.

7.7.6 Experiment Conclusions

The contact width between finger and tilting-plate interface was measured for both tilt-up and tilt-down feedback under applied force between 0 and 5 N. For both feedback modes, the contact width increases as the applied force increases. It was found that at the same contact force, the contact width in tilt-down mode is almost always higher than that in tilt-up mode. At the beginning of contact (< 0.5 N force), the contact width spread rates for tilt-down and tilt-up modes are ~ 24 and 18 mm/N, respectively. The higher initial contact width spread rate of tilt-down feedback might be the main reason this feedback type was perceived as more compliant than tilt-up feedback in Experiments 7.1 and 7.4. [Ambrosi et al. 1999]. In addition, the initial contact width spread rate of tilt-down feedback is higher at 16 deg/N tilting ratio than 4 deg/N tilting ratio. These two findings imply that participants likely judged the compliance of tilting-plate stimuli based on the perceived information at the beginning of contact. Lastly, a simple contact model with a rigid finger was simulated and similar initial contact area spread rate was obtained for tilt-up and tilt-down feedback.

7.8 Chapter Conclusions

The results of Experiments 7.1 and 7.4 indicate that at the same tilting ratio, a surface with tilt-down feedback is perceived as more compliant than a surface with tilt-up feedback (even after reducing the kinesthetic stiffness of tilt-up feedback in Experiment 7.4). This finding is in contrast with the initial hypothesis; i.e., tilt-down feedback may have a stiffening effect because the tilt direction is flipped. The difference in the contact area spread rate of tilt-up and tilt-down feedback was briefly investigated in Experiment 7.5. The result of the experiment showed that the tilt-down contact width not only

reduces as applied force increases, but also that its contact-width-to-force ratio is higher than that of tilt-up feedback. This higher contact width spread rate for tilt-down feedback is likely the main reason that the tilt-down feedback is perceived as more compliant than tilt-up or even tilt-up plus spring feedback.

In addition, the results obtained from Experiments 7.2 and 7.3 estimate the kinesthetic stiffness of tilt-down, tilt-up, and tilt-up plus spring feedback under different levels of tilting ratio and tilt range. The obtained kinesthetic stiffness values can be used as a starting point to match the kinesthetic stiffness of tilt-up or tilt-down feedback to the stiffness of a real or virtual object with a known stiffness.

CHAPTER 8

TILTING-PLATE FEEDBACK FOR PINCH GRASP

8.1 Overview

A pinch grasp interaction, in contrast to single-finger interaction, provides more precise information for the perception of compliance [Chen and Srinivasan 1998] since two fingers (usually index finger and thumb) are engaged to convey kinesthetic and tactile information. In daily life, we use pinch grasp to check the compliance of different objects such as estimating the pressure of a bicycle tire [Bergmann Tiest and Kappers 2009] or to select ripe fruits [Greer 2009]. The tilting-plate compliance display concept, presented in Chapter 5, can be extended to a back-to-back tilting-plate device to provide the compliance information of virtual objects experienced in a pinch grasp interaction. This back-to-back tilting-plate device is suitable for rendering intuitive pinch grasp interaction in handheld devices such as a game controller or a laparoscopy instrument.

It was hypothesized that one would have a greater sense of compliance when tilting-plate feedback was provided to one or both fingers in a pinch grasp. To test this hypothesis, a back-to-back tilting-plate compliance display device was designed and three human-subject compliance discrimination experiments were conducted (Experiments 8.1-8.3 in Sections 8.4-8.6).

8.2 Device Description

The back-to-back tilting-plate device consists of two tilting-plate units mounted on each side of a force sensor (Figure 8.1a). The amount of tilt between the plates of each unit is a function of the user's applied pinch force. To measure the net pinching force accurately, the whole device is mounted on a vertical shaft such that the entire device can rotate freely (Figure 8.1b). For detailed specifications of the main components, refer to Sections 4.2 and 5.2.

The back-to-back tilting-plate device is capable of rendering surface deformation only on index finger, only on thumb, or on both index finger and thumb (Figure 8.2).

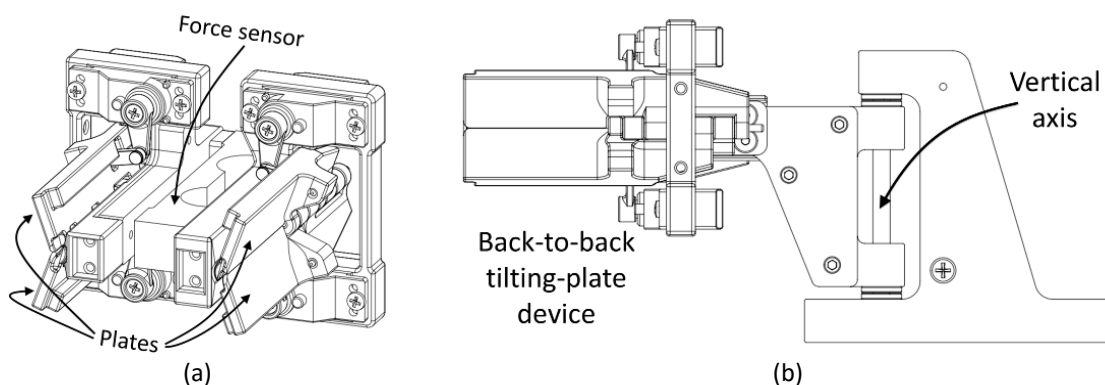


Figure 8.1. Back-to-back tilting-plate device for two-finger pinch grasp: (a) 3-D view: four servomotors actuate the plates individually based on the measured pinch force. (b) Side view: the device can rotate freely about a vertical axis, thus the force sensor accurately measures net pinching force.

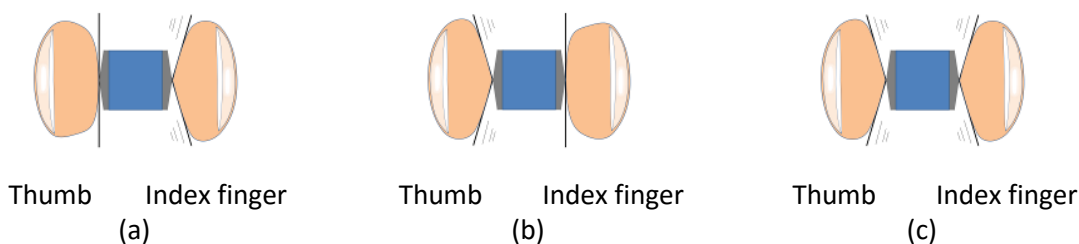


Figure 8.2. Three different operation configurations of the back-to-back tilting-plate device: surface deformation provided only on the index finger (a), only on the thumb (b), and on both thumb and index fingers (c).

8.3 General Methods

Three compliance discrimination experiments (Experiments 8.1-8.3) were conducted to investigate the effect of tilting-plate feedback in pinch grasp. The following sections present the general conditions, which were the same among all three experiments.

8.3.1 Participants

A total of 10 participants (3 females, 2 left-handed) aged 20 to 33 years (mean 24 years old) were recruited for the experiments. All participants conducted all three experiments on different days. The participants had no known abnormalities in their index fingers. Before the experiment, they were informed about the experiment procedures and signed informed consent forms in accordance with the University of Utah's Institutional Review Board (IRB) policy.

8.3.2 General Experimental Setup

During the experiments, the entire test apparatus and the participants' hands were covered by a cloth to prevent any visual cues from affecting their compliance judgment. Participants wore noise cancelling headphones, which blocked background noise and played audio cues indicating when a stimulus was ready to be examined.

Before rendering a stimulus, participants were required to break contact with the device interface(s) to prevent them from perceiving changes in haptic condition. A minimum contact force of 0.25 N was required to ensure that participants made contact with the device interfaces before responding with their answers. To prevent plates from complete saturation, a warning message on the screen informed participants to stop pushing when tilt angle proceeded 75% of the tilt range. Prior to the actual experiment, a

short practice session helped participants become familiar with the experiment procedure.

For the experiments, the tilting-plate device only rendered symmetrical surface deformation with linear force-tilt relationship (see Equation (4.1)). In addition, participants were informed not to rotate the device quickly, otherwise the inertia of the device could affect the measured force, thus displaying false tactile information.

8.4 Experiment 8.1: Index-finger-display Pinch Feedback vs.

Index-finger-display Push Feedback

This experiment investigates the effect of providing a support surface for the thumb (Figure 8.2a) on perception of compliance. We hypothesized that the tilting-plate feedback would have larger softening effect in the pinch grasp mode than in the single-finger pushing mode.

8.4.1 Stimuli

Reference stimuli were rendered by the single-finger, single-display, tilting-plate device (Figure 5.1) at four different tilting ratio levels (2, 4, 6, and 8 deg/N). Comparison stimuli were rendered by the dual-finger, single-display, tilting-plate device (Figure 8.2a) with a tilting ratio between zero and 12 deg/N. For both stimuli types, the tilting-plate feedback was only provided to the index finger. For the comparison stimuli, no surface deformation information was provided to the user's thumb (i.e., zero tilting ratio).

8.4.2 Procedures

The experiment started with a training session using two foam blocks. The two foam blocks were identical, except for a rigid plate attached on the thumb side of one of the

blocks. The participants were asked to push against one of the blocks and pinch the other with their contralateral hand and compare the perceived compliance of the two blocks based only on haptic information on their index fingers. No correct feedback was provided on their responses.

The experiment was split into two sessions, each with different hand-device configuration and conducted on a different day. The participants sat in front of the test apparatus (Figure 8.3). Their right and left hands were placed on two adjustable wrist supports. Their right index fingers were positioned above the single-finger, single-display, interface and their left hands were placed on the dual-finger, single-display, tilting-plate device. To eliminate the effect of handedness, the position of the devices was swapped for the second session.

Using an adaptive 1-up 1-down staircase method [Levitt 1971], the participants compared the compliance of pairs of reference-comparison stimuli. The experiment was

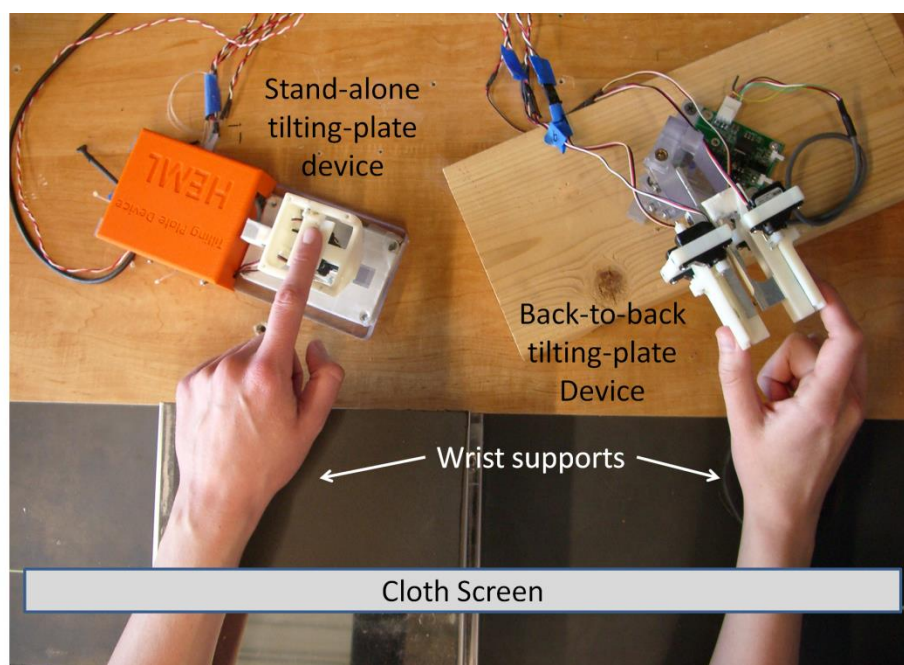


Figure 8.3. The experimental setup

divided into four sessions, each presenting a different reference stimulus. A 4×4 Latin Square was used to present different reference stimuli in different orders across all participants. Each session was accomplished in two runs: one ascending run and one descending run. In the ascending runs, the tilting ratio of comparison stimuli was set to zero, well below estimated PSE. In the descending runs, the tilting ratio of comparison stimuli was set to a high value (i.e., 5, 10, 10, and 10 deg/N for reference stimuli with 2, 4, 6, 8 deg/N tilting ratio, respectively). The presentation order of ascending and descending runs was balanced both within and between participants. In each trial, a reference and a comparison stimulus were presented to the participants at the same time. Participants perceived the compliance of both stimuli. Using two foot pedals, they responded whether the left or right stimulus was perceived to be more compliant. If the participants selected the comparison stimulus as the more compliant (or less compliant) surface, its tilting ratio was decreased (or increased) by a specific step size to make the task more difficult for the next trial. The initial tilting ratio step size was 0.5 deg/N and was reduced to 0.25 and then to 0.125 deg/N after the first and the fourth reversals.

The experiment was terminated after 10 total reversals. The arithmetic mean of comparison tilting ratios in the last six reversals of each run was considered as the PSE of that run. The overall PSE was estimated based on the average of the PSEs for all four runs (2 ascending and descending runs \times 2 hand-device configurations).

8.4.3 Experimental Results and Discussion

Figure 8.4 shows the mean PSEs for all participants. For the reference stimuli with tilting ratios of 2, 4, 6, and 8 deg/N, the mean PSEs are 1.75, 3.53, 4.89, 6.66 deg/N,

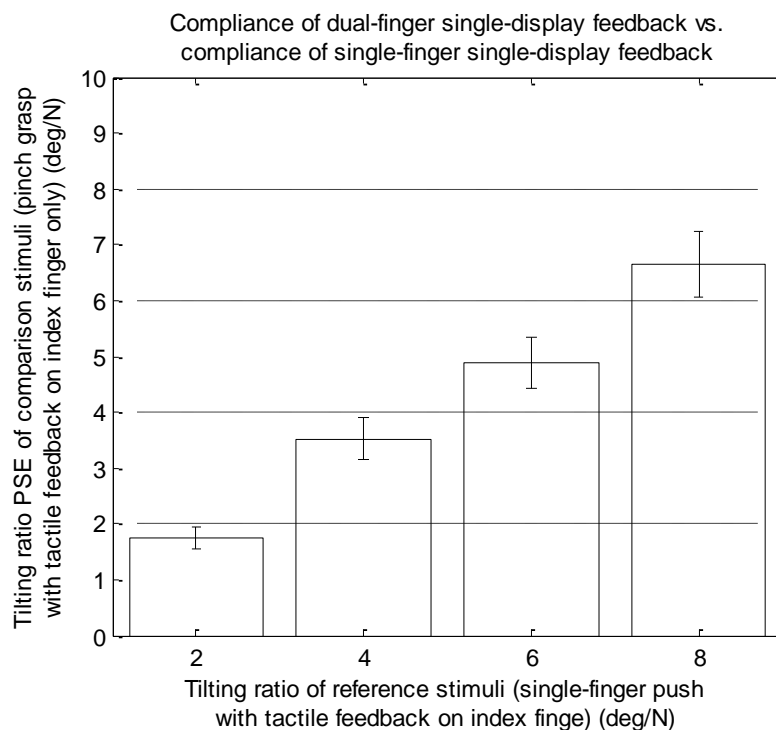


Figure 8.4. Means and 95% confidence intervals of tilting ratio PSEs of the index-finger-display pinch (comparison) stimuli at different tilting ratio levels of the index-finger-display push (reference) stimuli. All PSEs are significantly lower than the tilting ratio of their corresponding reference stimuli; i.e., at the same tilting ratio, an object in pinch mode is perceived as more compliant than an object in push mode.

respectively. The results of series t-tests indicate that all PSEs are statistically lower than the tilting ratio of their corresponding reference stimuli [$t(43) > 2.55$, $p < 0.012$]. This implies that at the same tilting ratio, an object in pinch grasp mode with tilting-plate feedback on the index finger is perceived to be more compliant than a surface in pushing mode with tilting-plate feedback on the index finger. This difference may be due to humans' greater ability in controlling finger force and displacement in a pinch grasp than in a single-finger integration.

There is a very strong and significant correlation between PSE and tilting ratio [Pearson $R^2 = 0.626$, $F(1, 174) = 290.75$, $p < 0.01$]. The regression line fit is shown in Figure 8.5. The PSE can be estimated by regression model in Equation (8.1).

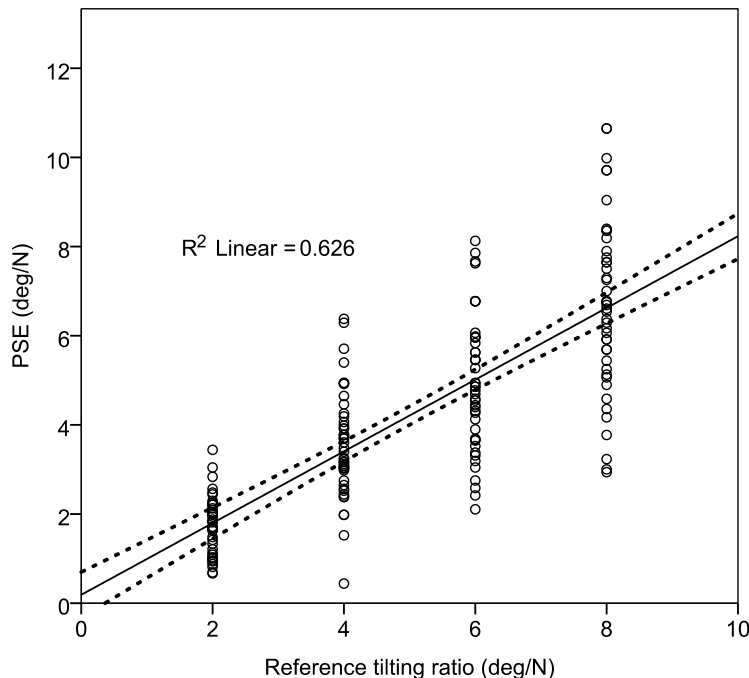


Figure 8.5. Very strong correlation between tilting ratios of tilting index-finger-display pinch stimuli (compassion PSE) and index-finger push (reference) stimuli.

$$\widehat{SE} = 0.80 R_{push} + 0.19 \quad (8.1)$$

The model suggests that the perceived compliance change due to 0.80 deg/N change in the tilting ratio of the back-to-back tilting-plate device is equivalent to the perceived compliance change due to 1.00 deg/N change in the tilting ratio of the standalone tilting-plate device when pressed upon by one's index finger. Combining this correlation with the relationship between the compliance of tilting-plate feedback and pure kinesthetic feedback (Equation (5.2) in Section 5.4), one can estimate the perceived compliance of index-finger-display pinch tilting-plate feedback in terms of pure kinesthetic stiffness feedback (Equation (8.2)); i.e., a unit change in the tilting ratio of the single-display pinch feedback is roughly equivalent to 178 N/m reduction in perceived kinesthetic stiffness. This connection enables use of the tilting-plate device for scenarios such as pinching a

virtual spring or a virtual syringe.

$$K \approx -178 R_{index-finger\ pinch} + 1895 \quad (8.2)$$

Figure 8.6 shows the average of maximum applied force on the reference and comparison stimuli across all participants. Similar to the computation of the PSEs, the maximum applied force was based on the average of applied force in the last six reversals. A regression analysis revealed that the reference tilting ratio and touch mode (pinch vs. push) have a statistically significant effect on the maximum applied force [$F(2, 349) = 18.94, p < 0.01$]. The participants applied higher force in the pinching mode (4.86 N) compared to the pushing mode (4.41 N) [$F(1, 344) = 17.23, p < 0.01$]. It should be mentioned that the opposite trend was found for mean applied force. The higher

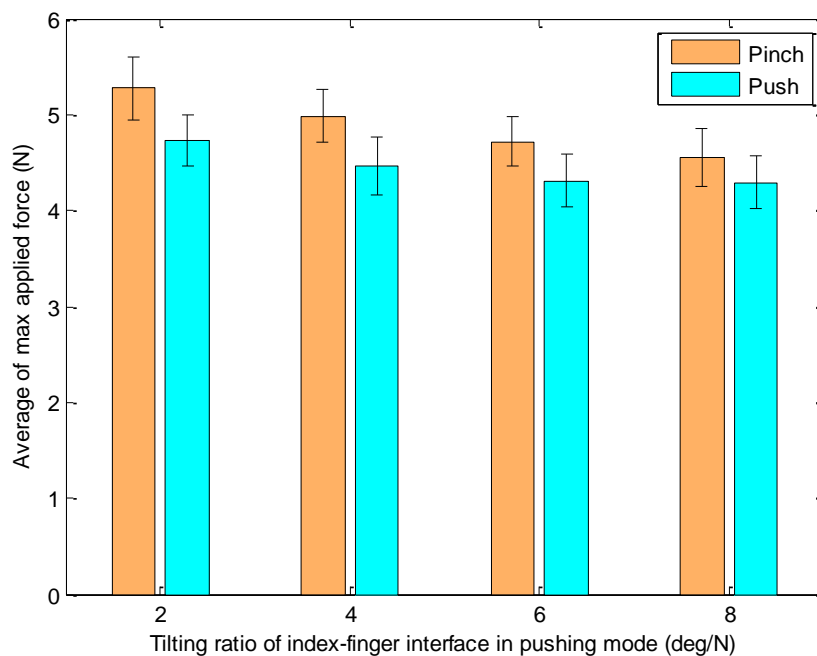


Figure 8.6. Average of maximum applied force on reference and comparison stimuli for all participants. Error bars are 95% confidence intervals. Participants applied significantly less maximum force in push mode than pinch mode.

maximum applied force in pinch mode might be due to slight bending of the index finger in pinch mode. The applied force on both surfaces was significantly higher for lower tilting ratio of the reference stimuli. This is in agreement with the results of Section 6.6; i.e., the participants tended to apply more force on stiffer objects. The reason that the participants applied less ‘mean force’ in pinch mode than push mode might be because of the fact that they perceived the index-finger-display pinch stimuli as more compliant than the index-finger-display push stimuli. No significant interaction between the reference tilting ratio and touch mode was found.

8.5 Experiment 8.2: Dual-display Pinch Feedback vs. Single-display Pinch Feedback

The second experiment investigates the effect of presenting tilting-plate feedback on the thumb in addition to the index finger on perceived compliance. We hypothesized that providing additional tilting-plate feedback on the thumb would increase the perceived compliance of virtual objects. The result of this experiment would indicate if there is any benefit to using two tilting-plate displays instead of one display for practical application, such as in game controllers or laparoscopy tools.

8.5.1 Stimuli

Reference stimuli were rendered by the dual-finger tilting-plate display at only a single-finger with four different tilting ratios (2, 4, 6, and 8 deg/N). The tilting-plate feedback was only provided to the index finger (Figure 8.2a). Comparison stimuli were rendered at both the index finger and thumb by the dual-finger, dual-display, tilting-plate device (Figure 8.2c) with tilting ratios between zero and 12 deg/N. The identical tilting-

plate feedback was provided to both index finger and thumb.

8.5.2 Procedures

The experiment started with a training session using two foam blocks, which were identical except for a rigid plate attached on the thumb side on one of the blocks. The participants were instructed to pinch the two blocks using their right hands and compare the overall perceived compliance of the two blocks based on combined tactile feedback on their thumbs and index fingers. No correct feedback was provided on their responses.

The participants sat in front of the test apparatus. Their right hands were placed on an adjustable wrist support. Their right index fingers and thumbs were positioned on each side of the back-to-back tilting-plate device.

The experiment was divided into four sessions, each presenting a different reference stimulus. A 4×4 Latin Square was used to present different reference stimuli in different orders across all participants. Each session was accomplished in two runs: one ascending run and one descending run. In the ascending runs, the tilting ratio of comparison stimuli was set to zero, well below estimated PSE. In the descending runs, the tilting ratio of comparison stimuli was set to a high value (i.e., 6, 8, 10, and 12 deg/N for reference stimuli with 2, 4, 6, 8 deg/N tilting ratio, respectively). The presentation order of ascending and descending runs was balanced both within and between participants. In each trial, a reference and a comparison stimulus were presented to the participants in sequence. The order of presentation for the reference and comparison stimuli was random but balanced.

Participants perceived the compliance of both stimuli. Using a keyboard, they indicated whether the first or the second stimulus was perceived to be more compliant. If

the participants selected the comparison stimulus as the more compliant (or less compliant) surface, its tilting ratio was decreased (or increased) by a specific step size to make the task more difficult for the next trial. The initial tilting ratio step sizes for the reference stimuli with tilting ratios of 2, 4, 6, and 8 deg/N were 0.5, 0.5, 1, and 1 deg/N, respectively. The step size was decreased by half after the first and the fourth reversals.

The experiment was terminated after 10 total reversals. The arithmetic mean of comparison tilting ratios in the last six reversals of each run was considered as the PSE of that run. The overall PSE was estimated based on the mean of the PSEs of both runs.

8.5.3 Experimental Results and Discussion

The mean tilting ratio PSEs across all participants are shown in Figure 8.7. The mean PSEs at 2, 4, 6, and 8 deg/N reference tilting ratios are 1.34, 2.60, 3.98, and 5.26, respectively. The results of t-tests shows that all tilting ratio PSEs are significantly lower than the tilting ratio of the corresponding reference stimuli [$t(15) > 7.55$, $p < 0.01$]. This means that at the same tilting ratio, an object in pinch mode with tilting-plate feedback on both thumb and index finger is perceived to be more compliant than an object in pinch mode with tilting-plate feedback provided only on index finger. The Weber fractions [Gescheider 1997] for the 2, 4, 6, and 8 deg/N reference tilting ratios are 0.33, 0.35, 0.34, and 0.34, respectively. This relatively constant Weber fraction over a wide range of the reference tilting ratio levels indicates that the amount of reduction in perceived compliance in the dual-display pinch grasp is proportional to the tilting ratio of the reference stimuli (i.e., the single-display pinch grasp).

The linear regression model between the tilting ratios of reference and comparison stimuli is given in Equation (8.3). There is very strong and significant linear correlation

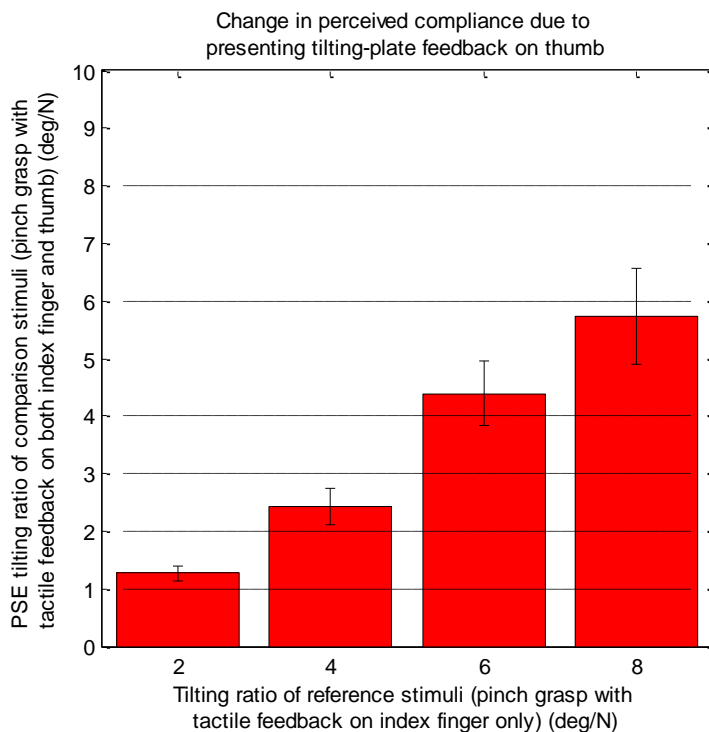


Figure 8.7. PSE tilting ratios of dual-finger, dual-display, (comparison) stimuli at different tilting ratios of dual-finger, single-display, (reference) stimuli. Error bars are 95% confidence intervals. All PSEs are significantly lower than the tilting ratio of their corresponding reference stimuli. This means a dual-display pinch stimulus is perceived more compliant than a single-display pinch stimulus.

between tilting ratio of dual-display pinch stimuli and single-display pinch stimuli [$R^2 = 0.72$, $F(1, 62) = 161.15$, $p < 0.01$]. The model suggests that the change in perceived compliance due to 0.66 deg/N change in the tilting ratio of dual-display pinch feedback is equivalent to the perceived compliance change due to 1.00 deg/N change in the tilting ratio of single-display feedback.

$$\widehat{PSE} = 0.66 R_{single-disply\ pinch} + 0.01 \quad (8.3)$$

Using Equations (8.1) and (8.2), the compliance of dual-display pinch feedback can be related to the tilting ratio of index-finger-display push feedback and to the kinesthetic

stiffness of a nondeformable surface, respectively.

$$R_{single\text{-}display\text{ push}} \approx 1.89 R_{dual\text{-}display\text{ pinch}} - 0.24 \quad (8.4)$$

$$K \approx -270 R_{dual\text{-}display\text{ pinch}} + 1895 \quad (8.5)$$

Equation (8.4) indicates that the tilting ratio of the single-finger, single-display, tilting-plate device needs to be about twice the tilting ratio of the dual-finger, dual-display, tilting-plate device to render the same level of perceived compliance. Additionally, Equation (8.5) indicates that there is ~270 N/m reduction in perceived kinesthetic stiffness per unit change in the tilting ratio of dual-finger, dual-display, feedback.

8.6 Experiment 8.3: Thumb-display Pinch Feedback vs.

Index-finger-display Pinch Feedback

The third experiment investigates the difference in perceived compliance of thumb-display pinch feedback vs. index-finger-display pinch feedback. We hypothesized that providing the same tilting-plate feedback either on the thumb or index finger results in the same level of perceived compliance.

8.6.1 Stimuli

Reference stimuli were rendered by the dual-finger, single-display, tilting-plate device with four different tilting ratios (2, 4, 6, and 8 deg/N); the tilting-plate feedback

was only provided to the index finger (Figure 8.2a). Comparison stimuli were rendered by the dual-finger, single-display, tilting-plate device with tilting ratios between zero and 12 deg/N; the tilting-plate feedback was only provided to the thumb (Figure 8.2b).

8.6.2 Procedures

The experiment started with a training session using a foam block with a rigid plate attached to one side. The participants were instructed to pinch the block using their right hands once with the rigid plate on their thumbs and once with it on their index fingers. They were asked to compare the perceived compliance of the two blocks based only on compliance information perceived on the deformable side.

The participants sat in front of the test apparatus. Their right hands were placed on an adjustable wrist support. Their right index fingers and thumbs were positioned on each side of the back-to-back tilting-plate device.

The experiment was divided into four sessions, each presenting a different reference stimulus. A 4×4 Latin Square was used to present different reference stimuli in different orders across all participants. Each session was accomplished in two runs: one ascending run and one descending run. In the ascending runs, the tilting ratios of comparison stimuli were set to zero, well below estimated PSEs. In the descending runs, the tilting ratios of comparison stimuli were set to a high value (i.e., 6, 8, 10, and 12 deg/N for reference stimuli with 2, 4, 6, 8 deg/N tilting ratio, respectively). The presentation order of ascending and descending runs was balanced both within and between participants. In each trial, a reference and a comparison stimulus were presented to the participants in sequence. The order of presenting reference or comparison stimuli was random but balanced. Participants perceived the compliance of both stimuli. Using a keyboard, they

indicated whether the first or the second stimulus was perceived to be more compliant. If the participants selected the comparison stimulus as the more compliant (or less compliant) surface, its tilting ratio was decreased (or increased) by a specific step size to make the task more difficult for the next trial. The initial tilting ratio step sizes for the reference stimuli with tilting ratios of 2, 4, 6, and 8 deg/N were 0.5, 0.5, 1, and 1 deg/N, respectively. The step size was decreased by half after the first and the fourth reversals.

The experiment was terminated after 10 total reversals. The arithmetic mean of comparison tilting ratios in the last six reversals of each run was considered as the PSE of that run. The overall PSE was estimated based on the mean of the PSEs of both runs.

8.6.3 Experimental Results and Discussion

The mean PSE tilting ratios across all participants are shown in Figure 8.8. The mean PSEs at 2, 4, 6, and 8 deg/N reference tilting ratios are 2.04, 4.29, 6.51, and 7.68, respectively. No statistically significant difference between PSEs and the tilting ratios of their corresponding reference stimuli was found [t-tests $p > 0.05$]. This means that at the same tilting ratio, an object in pinch mode with tilting-plate feedback on the thumb is likely perceived to be as compliant as an object in pinch mode with tilting-plate feedback provided on the index finger.

A supporting reason for this equality might be because one usually uses the thumb and index finger at the same time to judge the compliance of an object, and thus it is likely that one's brain registers the perceived compliance for both fingers regardless of the differences in shape and size of thumb and index fingers.

A regression analysis shows a very strong and linear correlation between the tilting ratio of index-finger-display pinch and thumb-display pinch feedback [Pearson $R^2 = 0.75$,

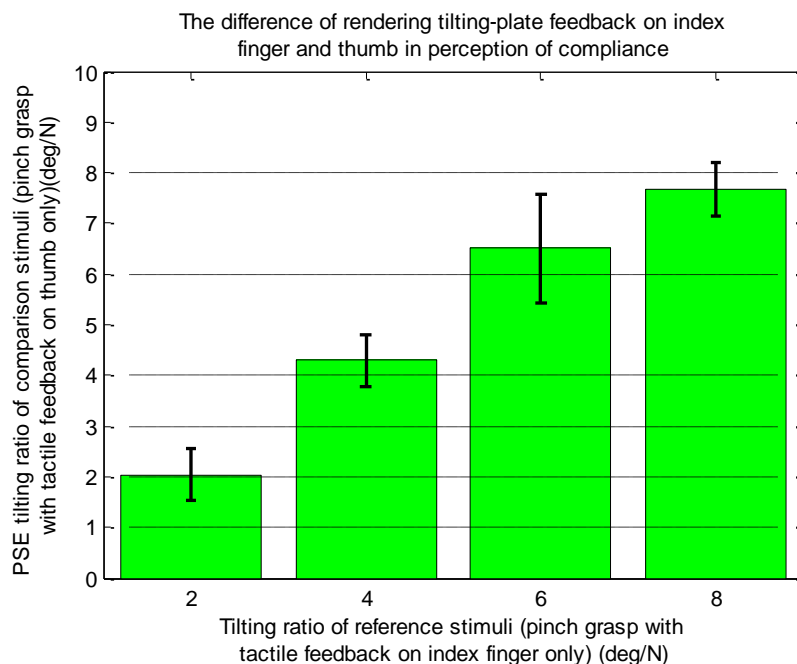


Figure 8.8. The mean tilting ratio PSEs of thumb-display pinch (comparison) stimuli at different tilting ratios of index-finger-display pinch (reference) stimuli across all participants. Error bars are 95% confidence intervals. None of the PSEs are significantly different from the corresponding reference tilting ratios. This means that at the same tilting ratio, the perceived compliance of both stimuli is likely the same.

$F(1, 57) = 167.35, p < 0.01]$. The regression model is presented in Equation (8.6). This model suggests that the compliance change due to one unit change in the tilting ratio of the index-finger-display pinch feedback is the same as the compliance change due to 0.96 unit change in the tilting ratio of the thumb-display pinch feedback.

$$\widehat{PSE} = 0.96 R_{index-finger-disply\ pinch} + 0.33 \quad (8.6)$$

8.7 Chapter Conclusions

To extend the functionality of the tilting-plate compliance display concept, a back-to-back tilting-plate device was designed, fabricated, and evaluated. This device enables perceiving the compliance of a virtual object in an intuitive interaction mode: pinch

grasp. Different interaction modes, including providing tilting-plate feedback only on the index finger, only on the thumb, and on both fingers, were considered. Three psychophysical experiments were conducted to correlate the perceived compliance of each interaction mode to the others as well as to the perceived compliance of single-finger, single-display, tilting-plate feedback described in Chapter 5.

The results show that at the same tilting ratio, single-display pinch feedback is perceived as more compliant than single-finger push feedback. In other words, to render the same perceived compliance level, the tilting ratio of single-display pinch feedback must be ~20% lower than that of single-display push feedback. Furthermore, the result of the second experiment suggests that providing tilting-plate feedback to the thumb in addition to the index finger increases the perceived compliance as well. To render the same perceived compliance level, the tilting ratio of dual-display pinch feedback must be ~48% lower than that of single-display push feedback. Combining these results with the results of Chapter 5, it was found that there is ~270 N/m reduction in perceived kinesthetic stiffness per unit change in the tilting ratio of dual-finger, dual-display, feedback

Additionally, in the third experiment, it was found that the perceived compliance of thumb-display pinch feedback and index-finger-display pinch feedback are almost the same. These findings suggest that the difference in shape and size of thumb and index finger does not have a significant effect on the perceived compliance of tilting-plate feedback.

From the system design point of view, the single-display pinch-grasp may have some advantages over the dual-display pinch-grasp mode: a simpler and more compact design. These features are beneficial for handheld devices with limited space. However, the

single-display pinch-grasp mode may provide less realistic and less intuitive compliance sensation compared to the dual-display pinch-grasp mode, since one of the interfaces always renders a nondeformable surface. In pilot studies, the participants' feedback indicated that without proper instructions (e.g., the training procedure in Section 8.5.2), they could confuse whether to judge the compliance based on the nondeformable or deformable surfaces. For practical use of the single-display pinch-grasp mode, it is suggested to instruct the users to judge the compliance based on the perceived compliance of the deformable surface (either on thumb or index finger).

CHAPTER 9

CONCLUSION

Two different types of tactile display interfaces were developed and evaluated in this study for improving haptic interaction with virtual environments: (1) a two-degree-of-freedom contact location display (2-DOF CLD) device, which provides local contact geometry information, and (2) different versions of tilting-plate compliance display devices for reproducing compliance information of deformable and nondeformable compliant objects in a virtual environment. The main goal of this study was to develop compact haptic devices that display simplified tactile information, which can be integrated with kinesthetic force-feedback or mobile devices.

9.1 Two-degree-of-freedom Contact Location Display Device

The developed 2-DOF CLD device is a finger-mounted tactile display device, which renders the location of contact between a 3-D virtual object and a user's fingerpad through a small spherical contactor. To reduce the size and mass of the device on the user's finger, the contactor was actuated remotely through two push-pull wires. The compact size and low effective mass of the device enabled the integration of it with a kinesthetic force-feedback. The integrated system provides both tactile and kinesthetic-force feedback for interactive exploration and manipulation of 3-D virtual objects.

Compared to the previous 1-DOF CLD device [Provancher et al. 2005], the 2-DOF CLD device provides consistent tactile information for interacting with three-dimensional virtual objects through positioning the contactor in both proximal-distal and ulnar-radial directions. Additionally, equipped with a custom 3-DOF gimbal, the current device enables unrestricted finger motions when exploring or manipulating three-dimensional (3-D) virtual objects.

A ball manipulation experiment was conducted to assess the performance of the 2-DOF CLD device under five different tactile rendering conditions. No statistically significant benefit of the 2-DOF CLD feedback was found based on speed and accuracy performance; however, the participants had a better ability to locate the ball using a 30 mm hybrid prepositioning condition, compared to a pure kinesthetic-force-feedback condition. Moreover, the result of a subjective survey revealed that the contact location plus kinesthetic feedback conditions were judged to be the more realistic and more preferred conditions compared to pure kinesthetic feedback.

9.1.1 Future Work Regarding Contact Location Display

The performance of the current 2-DOF contact location display device can be improved by adding making-and-breaking-contact functionality as well as reducing mechanical backlash. This was achieved and presented at the end of Chapter 3, but this revised system has not been evaluated. The thimble unit also needs to be revisited to reduce the packaging size and mass further. Once this modified 2-DOF CLD is achieved, one can investigate whether the hybrid positioning condition (C4) is preferred over a making-and-breaking-contact condition for dexterous manipulation of virtual objects.

9.2 Tilting-plate Tactile Compliance Display Device

The tilting-plate tactile compliance display device reproduces simplified surface deformation of a virtual object through two small tilting plates. The plates tilt as a linear function of applied finger force and form a small V-shaped groove underneath the user's fingerpad. The most important feature of this study is that the tilting-plate device can render a wide range of kinesthetic stiffness levels (from ~120 N/m to about infinity) in a compact package. In this study, different versions of tilting-plate devices were developed to investigate the effect of tilting-plate feedback on the perception of compliance for different haptic interaction configurations, including push and pinch interaction modes.

Initially, the compact tilting-plate device was mounted on a force-feedback device (Haptic Paddle) to render both kinesthetic and tactile feedback simultaneously (Chapter 4). Conducting a compliance discrimination experiment, it was found that presenting tilting-plate feedback increases the perceived compliance of kinesthetically rendered surfaces. This effect is larger at higher tilting ratio or reference kinesthetic stiffness levels. At 60, 400, and 1600 N/m reference kinesthetic stiffness, there are ~0.53, 7.87, and 38.94 N/m reductions in the perceived stiffness per unit change in tilting ratio.

In another study, the tilting-plate interface was mounted on a force sensor to investigate the capability of the standalone tilting-plate device in replicating compliance information of kinesthetically rendered surfaces. The results of a human-subject experiment show that the standalone tilting plate feedback with tilting ratios of 3 and 18 deg/N are correlated to kinesthetic compliance levels of ~1600 and ~200 deg/N, respectively.

In Chapter 6, the capability of the standalone tilting-plate device in rendering the compliance of real materials was investigated. Three different silicone rubber materials

with wide a range of compliance levels (equivalent kinesthetic stiffness of 450, 940, and 1514 N/m, respectively) were cast and selected as reference stimuli. The tilting ratio PSEs, at which the compliance of tilting-plate surface matches with the compliance of each silicone rubber specimen, were obtained (5.87, 3.06, and 1.28 deg/N, respectively). It seems that the PSE for tilting-plate feedback on the right index finger is consistently lower than the PSEs for tilting-plate feedback on left index finger. All the participants were right-handed. This implies that tilting-plate feedback on the right index finger is likely perceived as more compliant than the same tilting-plate feedback on the left index finger. Additionally, it was found that there is a significant effect of the hand-device configuration on the difference of applied force on both tilting-plate and silicone rubber specimen. The participants almost always applied more force using their left index fingers than their right index fingers. This difference might be due to (1) better force and/or motion control of right index finger compared to left index finger, or (2) richer compliance information provided by mechanoreceptors of the right index finger. More investigation is required to explain the main reason behind the effect of the hand-device configuration. In the literature, different findings were reported for the relative tactile acuity of the left hand vs. the right hand [Jones and Lederman 2006]. For example, Vega-Bermudez and Johnson 2001 could not find a significant difference in tactile acuity between the left and right hands of right-handed participants [Vega-Bermudez and Johnson 2001]. On the contrary, other researchers found that the nondominant hand of right-handed participants has better spatial sensitivity compared to their dominant hand [Duncan and Boynton 2007]. However, this effect was marginally significant and the authors hesitated to draw a strong conclusion based on their experimental results. In another study, Elbert et al. [1995] found that the cortical representation of the fingers of

the left hand is higher for string players. This suggests that the lower tactile acuity of the left index finger reported in this dissertation might be because of the fact that the right-handed participants mostly use their dominant hands when judging compliance.

In Chapter 7, the difference between the perceived compliance of tilt-up and tilt-down feedback was investigated. In tilt-up feedback, the interface of the tilting-plate device wraps around the finger, thus the contact area between the finger and the device interface increases. It was hypothesized that providing tilt-down feedback would increase the perceived stiffness of a kinesthetically rendered surface because of the negative tilting ratio in tilt-down feedback. To test this hypothesis, a series of measurements and psychophysical experiments were conducted. The results of Experiment 7.4 indicate that even after reducing the kinesthetic stiffness of tilt-up, a surface with tilt-down feedback is perceived as more compliant than a surface with tilt-up feedback with the same tilting ratio. This finding was in contrast with our hypothesis. In Experiment 7.5, the difference in the contact area of tilt-up and tilt-down feedback was investigated. The result of the experiment showed that the tilt-down contact width not only reduces as applied force increases, but also that its contact-width-to-force ratio is higher than that of tilt-up feedback. This higher contact width spread rate for tilt-down feedback is likely the main reason that the tilt-down feedback is perceived as more compliant than tilt-up plus spring feedback.

In Chapter 8, the effect of tilting-plate feedback in a pinch grasp configuration was studied. Pinch grasp provides more intuitive interaction for checking compliance (e.g., selecting fruit or checking the pressure of a bicycle tire) than a single-finger interaction. Participants compared the perceived compliance of index-finger-display pinch feedback against the perceived compliance of index-display push feedback. The results of the

experiment showed that index-display push feedback with tilting ratios of 2, 4, 6, and 8 deg/N are perceived to be as compliant as index-finger-display pinch feedback with the mean tilting ratio PSEs of 1.75, 3.53, 4.89, 6.66 deg/N, respectively. This means that at the same tilting ratio, an object in pinch mode with tilting-plate feedback on the index finger is perceived to be more compliant than a surface in pushing mode with tilting-plate feedback on the index finger. This difference may be due to humans' better ability in controlling finger force and displacement in a pinch grasp than in a single-finger integration. Further, it was found that providing additional tilting-plate feedback on the thumb increases the perceived compliance of the virtual object. The sum of these results suggests that for rendering the same level of compliance, the tilting ratio of single-finger, single-display, feedback must be almost twice (1.96 times) the tilting ratio of dual-finger, dual-display, feedback. Thus a simpler device with only one tilting-plate interface may be used over the dual-display display for rendering low levels of compliance. Finally, using the results obtained in Chapter 5, the tilting ratio of the back-to-back tilting-plate device was mapped to pure kinesthetic stiffness. One unit increase in the tilting ratio (1 deg/N) of dual-display pinch feedback; single-finger pinch feedback; and single-finger, single-display, push feedback are equivalent to 270, 178, and 142 N/m reduction, respectively, in the perceived compliance of pure kinesthetic feedback. The mapping between the tilting ratio and the pure kinesthetic stiffness enables the tilting-plate device to directly communicate with current physics engines, wherein the compliance is usually modeled based on simple rigid displacement information rather than surface deformation information.

In summary, the tilting-plate device is capable of rendering the compliance information of virtual objects. Its simple, low-cost, and light-weight design makes it a

suitable to be integrated with a wide range of human interfaces for applications such as laparoscopic surgery, video games, cell phones, or virtual reality.

9.2.1 Future Work Regarding Tilting-plate

Compliance Display Device

The current tilting-plate tactile compliance device can improve haptic interaction in many different applications. However, to assess its performance for rendering compliance of specific materials, further studies are required. For example, investigating the effect of tilting-plate feedback with nonlinear or time-dependent force-tilt relationships can provide more insight for displaying proper surface deformation of biological tissue with nonlinear properties. The effect of providing asymmetric tilting-plate feedback may be investigated for rendering the compliance of inhomogeneous materials (e.g., for finding a tumor beneath a compliant medium using palpation).

It would also be interesting to investigate whether sequential presentation of tilt-up and tilt-down feedback has any beneficial effect on rendering compliance. From the system design point of view, rendering both tilt-up and tilt-down feedback may provide a wider range of compliance levels, increase device configuration space to operate the device (providing greater flexibility to control the device), and may reduce the power consumption of the overall system. For example, the compliance of a virtual surface can be rendered via regular tilt-up feedback, but when the user decides to break contact with the surface, the tilting plates need not return back to the flat configuration. Therefore, for the next fresh contact, the compliance can be rendered by tilt-down feedback (if the tilt-range for tilt-up feedback is close to saturation; i.e., 40 degrees). Therefore, this combination of tilt-up and tilt-down feedback in temporal fashion could expand the

configuration space of the device.

One of the limitations of the current tilting-plate device is that the user is required to hold the interface in a specific orientation. This problem may be solved by using a higher number of plates in circular pattern, providing more uniform surface deformations. These investigations can extend the capability of the tilting-plate device for telerobotic surgery procedures or medical training applications.

APPENDIX

Table A.1. List of possible compliance perception tests using the tilting-plate device.

Test	Reference Stimuli	Comparison Stimuli	Comment	Section
1	KF* +TP* + Push	KF + Push	- Quantifying the effect of tilting-plate feedback in increasing the perceived compliance of kinesthetically rendered surfaces.	4.4
2	KF + Push	TP + Push	- Can tilting-plate feedback substitute for pure kinesthetic compliance information?	5.3
3	Real object + Push	TP + Push	- Can tilting-plate feedback replicate the compliance of real materials (e.g., biological tissues)?	6.5
4	TP + Push	TP + Index-finger-display pinch	- Effect of adding thumb as an anchor finger. - Using both hands is suggested.	8.4
5	TP + Push	TP + Thumb-display pinch	- This test along with test 4 provides an indirect comparison between the effect of thumb and index finger on compliance in pinch mode. - Using both hands is suggested.	--
6	TP + Index-finger-display pinch	TP + Thumb-display pinch	- Direct comparison between presenting tilting-plate feedback on index-finger and thumb in a pinch grasp. - Using only one hand is suggested.	8.6

Table A.1. Continued

Test	Reference Stimuli	Comparison Stimuli	Comment	Section
7	TP + Index-finger-display pinch	TP + Dual-display pinch	<ul style="list-style-type: none"> - Direct effect of adding tilting-plate feedback to thumb, in addition to index finger, on perceived compliance of an object in a pinch grasp mode. - Using only one hand is suggested. 	8.5
8	KF + Push	TP + Index-finger-display pinch	<ul style="list-style-type: none"> - Using the same reference stimuli in Test 2, one can investigate the effect of thumb as an anchor finger in pinch grasp. - An alternative option to Test 4. 	--
9	KF + Push	TP + Dual-display pinch	<ul style="list-style-type: none"> - Using the results of Test 8, this test can describe the effect of providing additional tactile feedback to thumb on perceived compliance? This is an alternative option to Test 7, and enables a direct comparison with the result of Test 2. 	--
10	KF + Pinch	TP + Dual-display pinch	<ul style="list-style-type: none"> - Test investigates whether the back-to-back tilting-plate device can substitute for the back-to-back kinesthetic display devices. - Physical spring between two rigid surfaces can be used to render pure kinesthetic information. 	--
11	Real object + Pinch	TP + Dual-display Pinch	<ul style="list-style-type: none"> - Similar to Test 3 — i.e., tilting-plate feedback replicates the compliance information of real materials. 	--

REFERENCES

- Ambrosi, G., A. Bicchi, D. De Rossi, and E. Scilingo. 1999. The role of contact area spread rate in haptic discrimination of softness. *Proceedings of IEEE International Conference on Robotics and Automation*: 305–310.
- Barton, M., R. Harris, and S. Fletcher. 1999. Does this patient have breast cancer? *JAMA: The Journal of the American Medical Association* 282, no. 13: 1270–1280.
- Becker, J. 2012. Ranked likert-scale visualization. <http://blog.jasonpbecker.com/2012/07/10/ranked-likert-scale-visualization> (accessed December 15, 2012).
- Bergmann Tiest, W., and A. Kappers. 2008. Kinaesthetic and cutaneous contributions to the perception of compressibility. *Haptics: Perception, Devices and Scenarios*: 255–264.
- Bergmann Tiest, W., and A. Kappers. 2009. Cues for haptic perception of compliance. *IEEE Transactions on Haptics* 2, no. 4: 189–99.
- Bianchi, M., A. Serio, E. Scilingo, and A. Bicchi. 2010. A new fabric-based softness display. *IEEE Haptics Symposium*: 105–112.
- Bicchi, A., G. Canepa, D. De Rossi, P. Iacconi, and E. Scilingo. 1996. A sensor-based minimally invasive surgery tool for detecting tissue elastic properties. *Proceedings of the IEEE International Conference on Robotics and Automation* 1: 884–888.
- Bicchi, A., E. Scilingo, and D. De Rossi. 2000. Haptic discrimination of softness in teleoperation: the role of the contact area spread rate. *IEEE Transactions on Robotics and Automation* 16, no. 5: 496–504.
- Chinello, F., M. Malvezzi, C. Pacchierotti, and D. Prattichizzo. 2012. A three DOFs wearable tactile display for exploration and manipulation of virtual objects. *IEEE Haptics Symposium*: 71–76.
- Culmer, P., J. Barrie, R. Hewson, M. Levesley, M. Mon-Williams, D. Jayne, and A. Neville. 2012. Reviewing the technological challenges associated with the development of a laparoscopic palpation device. *The International Journal of Medical Robotics and Computer Assisted Surgery* 8, no. 2: 146–159.

- Duncan R., Boynton G. 2007. Tactile hyperacuity thresholds correlate with finger maps in primary somatosensory cortex (S1). *Cereb Cortex* 17: 2878–2891.
- Dostmohamed, H., and V. Hayward. 2005. Trajectory of contact region on the fingerpad gives the illusion of haptic shape. *Experimental Brain Research* 164, no. 3: 387–394.
- Doxon, A., D. Johnson, H. Tan, and W. Provancher. 2013. Human detection and discrimination of tactile repeatability, mechanical backlash, and temporal delay in a combined tactile-kinesthetic haptic display system. *IEEE Transactions on Haptics* 6, no. 4: 453–463.
- Doxon, A., D. Johnson, H. Tan, and W. Provancher. 2011. Force and contact location shading methods for use within two- and three-dimensional polygonal environments. *Presence: Teleoperators and Virtual Environments* 20, no. 6: 505–528.
- Doxon, A., D. Johnson, H. Tan, and W. Provancher. 2010. Force and contact location shading thresholds for smoothly rendering polygonal models. *IEEE Haptics Symposium*: 183–190.
- Elbert, T., C. Pantev, C. Wienbruch, B. Rockstroh, E. Taub. 1995. Increased cortical representation of the fingers of the left hand in string players. *Science* 13: 305–307.
- Frisoli, A., M. Solazzi, F. Salsedo, and M. Bergamasco. 2008. A fingertip haptic display for improving curvature discrimination. *Presence: Teleoperators and Virtual Environments* 17, no. 6: 550–561.
- Fujita, K., and H. Ohmori. 2001. A new softness display interface by dynamic fingertip contact area control. *5th World Multiconference on Systemics, Cybernetics and Informatics*: 78–82.
- Gescheider, G. 1997. *Psychophysics: The fundamentals*. London: Lawrence Erlbaum.
- Greer, B.. 2009. *A guide to buying fresh fruit and vegetables*. Tennessee: The University of Tennessee Institute of Agriculture.
- Gurari, N., K. Kuchenbecker, and A. Okamura. 2009. Stiffness discrimination with visual and proprioceptive cues. *IEEE Third Joint EuroHaptics Conference and Symposium on Haptic Interfaces for Virtual Environment and Teleoperator Systems*: 121–126.
- Han, H., and S. Kawamura. 1999. Analysis of stiffness of human fingertip and comparison with artificial fingers. *Proceedings of IEEE International Conference on Systems, Man, and Cybernetics*, 800–805.
- Haveran, L., Y. Novitsky, D. Czerniach, G. Kaban, M. Taylor, K. Gallagher-Dorval, R. Schmidt, J. Kelly, and D. Litwin. 2007. Optimizing laparoscopic task efficiency: The role of camera and monitor positions. *Surgical Endoscopy and Other Interventional Techniques* 21, no. 6: 980–984.

- Howe, R. 2004. The shape of things to come: pin-based tactile shape displays. *Proceedings of the 4th International Conference Eurohaptics*: 2–11.
- Johnson, K. 1985. *Contact mechanics*. Cambridge, U.K.: Cambridge University Press.
- Jones, L., and S. Lederman. 2006. *Human Hand Function*. New York, Oxford University Press.
- Kimura, F., A. Yamamoto, and T. Higuchi. 2009. Development of a contact width sensor for tactile tele-presentation of softness. *The 18th IEEE International Symposium on Robot and Human Interactive Communication*: 34–39.
- Kimura, F., A. Yamamoto, T. Higuchi. 2010. Development of a 2-DOF softness feeling display for tactile tele-presentation of deformable surfaces. *IEEE International Conference on Robotics and Automation*: 1822–1827.
- Klaesner, J., M. Hastings, D. Zou, C. Lewis, and M. Mueller. 2002. Plantar tissue stiffness in patients with diabetes mellitus and peripheral neuropathy. *Archives of Physical Medicine and Rehabilitation* 83, no. 12: 1796–1801.
- Klatzky, R., S. Lederman, and D. Matula. 1993. Haptic exploration in the presence of vision. *Journal of Experimental Psychology: Human Perception and Performance* 19, no. 4: 726–743.
- Klatzky, R., and S. Lederman. 2002. Touch: In *Handbook of Psychology: Experimental psychology*, eds. Healy, Proctor, and Weiner, 4: 147-176. New York: Wiley.
- Kuchenbecker, K., D. Ferguson, M. Kutzer, M. Moses, and A. Okamura. 2008. The touch thimble: Providing fingertip contact feedback during point-force haptic interaction. *Haptic Interfaces for Virtual Environment and Teleoperator Systems, Symposium on Haptics*: 239–246.
- Kuchenbecker, K., W. Provancher, G. Niemeyer, and M. Cutkosky. 2004. Haptic display of contact location. *Proceedings of the 12th International Symposium on Haptic Interfaces for Virtual Environment and Teleoperator Systems (HAPTICS'04)*: 40–47.
- Kuebler, B., U. Seibold, and G. Hirzinger. 2005. Development of actuated and sensor integrated forceps for minimally invasive robotic surgery. *The International Journal of Medical Robotics and Computer Assisted Surgery* 1, no. 3: 96–107.
- Langley, R. 1970. *Practical statistics simply explained*. New York: Dover.
- Lederman, Susan J, and Roberta L Klatzky. 1999. Sensing and displaying spatially distributed fingertip forces in haptic interfaces for teleoperator and virtual environment systems. *Presence: Teleoperators and Virtual Environments* 8, no. 1: 86–103.

- Lederman, S., and R. Klatzky. 1990. Haptic exploration and object representation. In *Vision and action: The control of grasping*, ed. M. Goodale. New Jersey: Ablex.
- Levitt, H. 1971. Transformed up-down methods in psychoacoustics. *Journal of the Acoustical Society of America*, 49: 467–477.
- Linville, J., and J. Bliss. 1966. A direct translation reading aid for the blind. *Proceedings of the IEEE* 54, no. 1: 40–51.
- Moy, G., U. Singh, E. Tan, and R. Fearing. 2000. Human psychophysics for teletaction system design. *Haptics-E* 1, no. 3.
- Okamura, A. 2009. Haptic feedback in robot-assisted minimally invasive surgery. *Current Opinion in Urology* 19, no. 1: 102–107.
- Pacchierotti, C., F. Chinello, M. Malvezzi, L. Meli, and D. Prattichizzo. 2012. Two finger grasping simulation with cutaneous and kinesthetic force feedback. *Haptics: Perception, Devices, Mobility, and Communication* 7282: 373–382.
- Park, J., A. Doxon, W. Provancher, D. Johnson, and H. Tan. 2012. Haptic edge sharpness perception with a contact location display. *IEEE Transactions on Haptics* 5, no. 4: 323–331.
- Pawluk, D., and R. Howe. 1999. Dynamic lumped element response of the human fingerpad. *Journal of Biomechanical Engineering, ASME* 121, no. 2: 178–183.
- Porquis, L., D. Maemori, N. Nagaya, M. Konyo, and S. Tadokoro. 2014. Presenting virtual stiffness by modulating the perceived force profile with suction pressure. *IEEE Haptics Symposium*: 289–294.
- Prattichizzo, D., C. Pacchierotti, and G. Rosati. 2012. Cutaneous force feedback as a sensory subtraction technique in haptics. *IEEE Transactions on Haptics* 5, no. 4: 289–300.
- Provancher, W., M. Cutkosky, K. Kuchenbecker, and G. Niemeyer. 2005. Contact location display for haptic perception of curvature and object motion. *The International Journal of Robotics Research* 24, no. 9: 691–702.
- Provancher, W., and A. Doxon. 2009. Assembly instructions for the Utah haptic paddle. <http://elecansisms.olin.edu/projects/utahhapticpaddle.pdf> (accessed November, 2011).
- Provancher, W. 2003. *On tactile sensing and display*. Dissertation, Stanford University.
- Sarakoglou, I., N. Garcia-Hernandez, N. Tsagarakis, and D. Caldwell. 2012. A high performance tactile feedback display and its integration in teleoperation. *IEEE Transactions on Haptics* 5, no. 3: 252–263.

- Schostek, S., M. Schurr, and G. Buess. 2009. Review on aspects of artificial tactile feedback in laparoscopic surgery. *Medical Engineering & Physics* 31, no. 8: 887–898.
- Scilingo, E., M. Bianchi, G. Grioli, and A. Bicchi. 2010. Rendering softness: integration of kinesthetic and cutaneous information in a haptic device. *IEEE Transactions on Haptics* 3, no. 2: 109–118.
- Srinivasan, M., and R. LaMotte. 1995. Tactual discrimination of softness. *Journal of Neurophysiology* 73, no. 1: 88–101.
- Tal, J. 1999. Two feedback loops are better than one. *Machine Design* 71, no. 7: 85–87.
- Tavakoli, M., A. Aziminejad, R. Patel, and M. Moallem. 2006. Methods and mechanisms for contact feedback in a robot-assisted minimally invasive environment. *Surgical Endoscopy And Other Interventional Techniques* 20, no. 10: 1570–1579.
- Tholey, G., J. Desai, and A. Castellanos. 2005. Force feedback plays a significant role in minimally. *Annals of Surgery* 241, no. 1: 102–109.
- Vega-Bermudez, F., and K. Johnson. 2001. Differences in spatial acuity between digits. *Journal of Neurology*. 56, no. 10: 1389–1391.
- Wagner, C., S. Lederman, and R. Howe. 2004. Design and performance of a tactile shape display using rc servomotors. *Haptics-E* 3, no. 4: 1–6.
- Wellman, P., W. Peine, G. Favalora, and R. Howe. 1998. Mechanical design and control of a high-bandwidth shape memory alloy tactile display. In *Lecture notes in control and information sciences; Experimental robotics*, eds. A. Casals and A. Almeida, 56-66.
- Yazdian, S., A. Doxon, D. Johnson, H. Tan, and W. Provancher. 2013. 2-DOF contact location display for manipulating virtual objects. *World Haptics Conference*: 443–48.
- Yazdian, S., A. Doxon, D. Johnson, H. Tan, and W. Provancher. 2014. Compliance display using a tilting-plate tactile feedback device. *IEEE Haptics Symposium*: 13–18.
- Yoshikawa, T., and A. Nagura. 1999. A three-dimensional touch/force display system for haptic interface. *Proceedings of IEEE International Conference on Robotics and Automation*, 4: 2943–51.